SECONDARY STAR SURFACE MAGNETIC ACTIVITY AND MASS TRANSFER IN CATACLYSMIC VARIABLES

By

Edward Jurua

B.Sc. Hons

This dissertation is submitted in accordance with the requirement for the

Degree of Master of Science

in the

Faculty of Natural and Agricultural Sciences

Department of Physics

at the University of the Free State

South Africa.

Supervisor: **Prof. P.J. Meintjes**

May 30, 2005

To Nathan Bright Yikki

Acknowledgement

I wish to extend my sincere gratitude and deepest appreciation to my supervisor Prof. P.J. Meintjes for his great ideas and from whom I have learnt so much.

I am also grateful to the NASSP[1]/Ford Foundation, for the scholarship and other financial support, without which I wouldn't have done this study.

I also extend my sincere gratitude and appreciation to Mbarara University of Science and Technology, University of Cape Town and the Department of Physics, University of the Free State for their financial and moral support.

I would also like to thank the following for their valuable inputs into this study:

Prof. Peter Dunsby, the NASSP coordinator, for his advice and encouragement.

Simon Anguma Katrini, for his support and encouragement.

All my friends, for their moral support.

I also extend my heartfelt respect and deepest love to my family for their continued support and encouragement throughout my studies.

Above all, I must thank the Almighty God for blessing me abundantly and providing me with everything I needed throughout my studies. "How we praise God, the Father of our Lord Jesus Christ, who has blessed us with every blessing in heaven because we belong to Christ" (Ephesians 1:3).

[1] National Astrophysics and Space Science Programme.

Abstract

In this study it is shown that secondary star magnetic fields influence the mass transfer process in close interacting binaries, especially cataclysmic variables (CVs) and thus play a fundamental role in the whole mass transfer process, and evolution of these systems.

The Mestel and Spruit (1987) stellar wind theory is used to model the surface magnetic field of the secondary star in CVs, particularly the intermediate polars, constraining the angular momentum that is required to drive the observed mass transfer rate through Roche lobe overflow. This in turn allows solving for the mass transfer rates, via magnetic braking, and the surface polar magnetic field of these stars. These field strengths are used to study and constrain magnetic advection from the secondary star to the primary star, and its effect on the mass flow in the funnel in magnetic CVs. This has important consequences for the so-called magnetic viscosity in the accretion discs of disc accreting magnetic cataclysmic variables, which are fed by these magnetic secondary stars.

It is shown that the mass transfer rates in these systems vary with orbital period, with lower mass transfer rates in more compact systems than in the wider systems. It is also shown that advection of magnetic flux into the funnel results in severe magnetic viscosity at the L_1 region. The advected magnetic field into the funnel flow results in a magnetized flow and enhanced magnetic pressure in the L_1 region. Since the magnetic pressure in the L_1 region exceeds the flow ram pressure, continuous flow of material through the L_1 region is prevented. It is shown that matter can easily cross the funnel if pressure builds up behind the barrier. This therefore implies that the mass transfer in these systems is not continuous but fragmented in the form of blobs.

Key words: Cataclysmic variables, Mass transfer, Angular momentum, Surface polar magnetic field, Magnetic advection and Magnetic viscosity,

Contents

Chapter One

Chapter Two: Stellar wind theory

Chapter One

1.1 Introduction

The aim of this study is an in-depth investigation of the influence of the secondary star magnetic field on the mass transfer process in close interacting binaries, especially the cataclysmic variable stars. Since the secondary star magnetic field plays a fundamental role in the whole mass transfer process (magnetic braking), which will be discussed in detail later, as well as the evolution of these systems as a whole, a detailed investigation is certainly appropriate. Of particular interest is the process of magnetic transport from the secondary star to the accretion disc of the primary star, which may have important consequences towards the so-called magnetic viscosity facilitating rapid accretion in some of these systems. To put everything in context, the general properties of close binaries, in particular cataclysmic variables, will be reviewed briefly.

1.2 Cataclysmic variables

Cataclysmic variables (CVs) are binary systems that come in many flavors. It sometimes seems that each cataclysmic variable defines its own class, but the underlying structure remains similar for most of them, namely a binary system comprising of a cool late-type main-sequence star (the secondary star) orbiting a compact white dwarf (the primary star). They are typically small; a typical binary system is roughly the size of the earth-moon system, with orbital periods of 1 – 10 hours (e.g. Warner 1995, p.29).

Due to the proximity of the two stars, the secondary star is distorted into a tear-shape, as a result of the strong gravitational pull of the compact white dwarf on the secondary star. This usually results in the tenuous gas being brought into contact with a region of zero

gravity between the two stars, resulting in thermal motions carrying the material into the gravitational potential well of the white dwarf. Depending on the physical size of the white dwarf's magnetosphere, this transferred material can either interact directly with the magnetosphere, e.g. in AM Her stars, or result in the formation of an accretion disc, e.g. in intermediate polars. The accretion disc can be thought of as a machine, facilitating the extraction of angular momentum from the material, allowing it to accrete onto the white dwarf where gravitational potential energy of the gas is released as heat and radiation resulting in interesting observational properties of these systems (outbursts and brightening). Based upon the observational properties of these systems, cataclysmic variables can be grouped into several categories (see e.g. Warner 1995, p.27 - 28 for an extensive review) e.g. classical novae, dwarf novae, recurrent novae, nova-like variables and Magnetic Cataclysmic Variables (MCVs).

Since the secondary star magnetic field plays an intimate role in the mass transfer process in the broad class of the MCVs, they form the basis of our theoretical investigation, and therefore their properties will be reviewed in more detail later.

1.2.1 Formation of cataclysmic variables

Stars are born from gravitationally collapsing molecular and interstellar dust clouds. The collapse is induced through an instability in the cloud which could be due to shock waves from a nearby supernova. A star develops when the core of the contracting protostar reaches temperatures for ignition of nuclear fusion reactions. Less massive clouds require high densities to collapse while more massive clouds require lower densities to collapse (Kippenhahn & Weigert 1990). Thus more massive clouds collapse first. As the density of the gas cloud increases, small parts of the cloud would collapse independently. Ultimately the cloud would fragment into many parts forming a whole cluster of stars. Stars therefore form in clusters finding themselves gravitationally bound in binaries, triples, pairs of binaries or similar combinations.

Stars destined to become CVs begin as binaries separated by a few hundred solar radii, orbiting each other approximately every ten years (e.g. Hellier 2001, p.45). One of the stars must be less than a solar mass and the other more massive. The more massive star evolves more rapidly, since the greater weight on its core ensures a higher pressure and temperature, and therefore a more vigorous nuclear burning rate. The more massive star eventually expands and becomes a red giant (e.g. Hellier 2001, p.45). At this stage it overflows its Roche lobe, and transfers its outer layers to the less massive companion.

The more massive star is closer to the centre-of-mass (CM) of the binary, and material transferred to the less massive companion star therefore moves further from the CM. This results in increase of angular momentum of the material being transferred. Conserving the overall binary angular momentum will result in a decrease in the binary separation if the mass transfer is conservative (e.g. Frank, King & Raine 1992, p.52). This decrease in binary separation decreases the Roche lobe size. The more massive star then finds itself overfilling its Roche lobe, yet more material is being transferred. This results in a run-away feedback as the whole envelope of the red giant is dumped onto the companion star, limited only by the speed at which the material can flow (e.g. Frank, King & Raine 1992, p.53; Hellier 2001, p.45 - 46). This dynamical mass transfer to the companion star will have dramatic consequences that will sculpture the further evolution of this system.

This influx of material cannot be assimilated by the companion star, and the material overfills both Roche lobes forming a cloud surrounding the two stars. This is the "common envelope" phase in which the pre-cataclysmic variable is effectively orbiting within a massive red giant. The drag on the stars as they orbit drain their orbital energy causing them to spiral inwards, reducing their separation from about one hundred solar radii to about one solar radius in approximately one thousand years (e.g. Hellier 2001, p.46). This results in a tidal back reaction on the envelope, propelling it outwards into interstellar space, forming a planetary nebula. The new-naked binary is either a cataclysmic binary, or if the separation is still too large for mass transfer, a detached binary (e.g. Hellier 2001, p.46).

1.2.2 Roche lobe geometry

Most stars are spherical, pulled by gravity into the most compact configuration. Stars in wide binary systems where the separation is much greater than their sizes are also spherical. In CVs the white dwarf, with a radius of about 0.02 of the binary separation, is compact and spherical while the less dense red dwarf is greatly distorted by the gravity of the compact white dwarf which acts on the secondary star (e.g. Frank, King & Raine 1992, p.50; Warner 1995, p.30).

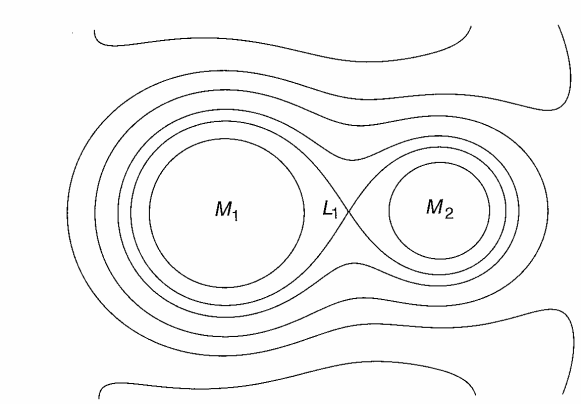

Figure 1. Contours of equal gravitation potential drawn for a binary system (Adopted from Hellier 2001, p.20).

If the two stars move closer, the secondary star becomes increasingly distorted since the material nearest the primary experiences a greater gravitational attraction towards the compact object than the material at the back of this star. Stellar material would then flow from the secondary star, a characteristic of cataclysmic variables. The outline of a star at the critical point when it is just possible to transfer mass to the companion star is called the Roche lobe. The apex of the Roche lobe, called the inner Lagrangian point (L_1 point), is the easiest path by which material can be transferred between the two stars (see Figure 1). The inner Lagrangian point basically constitutes a region of zero effective gravity, allowing thermal motions to carry the gas from the outer envelope of the secondary star across L_1 towards the gravitational potential well of the white dwarf. This will be discussed briefly in the next section.

The immediate consequence of binary motion on a red dwarf star filling its Roche lobe is that tidal locking ensures that its spin period is equal to the orbital period. Otherwise there would be continuous tidal flow of material into and out of the bulge of the Roche lobe dissipating an enormous amount of energy. The star therefore quickly adjusts its spin period so that the same material remains in the bulge. The distorted Roche lobe of the red dwarf is often detected directly in the light curve of cataclysmic variables.

1.2.3 Mass transfer

For a stable long-lived mass transfer, the secondary star must fill its Roche lobe. There are two ways in which the secondary star can fill its Roche lobe (King 1988; e.g. Frank, King & Raine 1992, p.46):

(i) The star expanding i.e. $R_2 \rightarrow R_L$.

(ii) The Roche lobe shrinking i.e. $R_L \rightarrow R_2$,

where R_2 is the radius of the secondary star and R_L the Roche lobe radius. The first case occurs in any reasonably close binary once one star evolves off the main sequence and climbs the giant branch. To reach this stage within the life time of the Galaxy requires a mass greater or equal to one solar mass for this star at the onset of mass transfer. This mechanism cannot be invoked for compact binary stars as the masses of the secondaries are too low for them to have evolved off the main sequence (King 1988). The alternative process of shrinking R_L must therefore occur in compact binary stars.

If the secondary star fills its Roche lobe, stellar material will be in contact with the L_1 point. This is pushed from behind by the pressure of the stellar atmosphere and it finds itself in the empty space of the Roche lobe of the primary star. Thermal motions allow particles to cross over the L_1 point with a velocity of the order of sound speed in gas (c_s ~10 km s^{-1}, i.e. sound speed in an astrophysical environment at a temperature of the order of 10^3 K), falling into the potential well of the primary in form of a narrow stream and subsequently accelerated by the effective gravitational field of the binary system. In the

Roche lobe of the primary, the dominant contribution towards the effective gravity is the compact white dwarf.

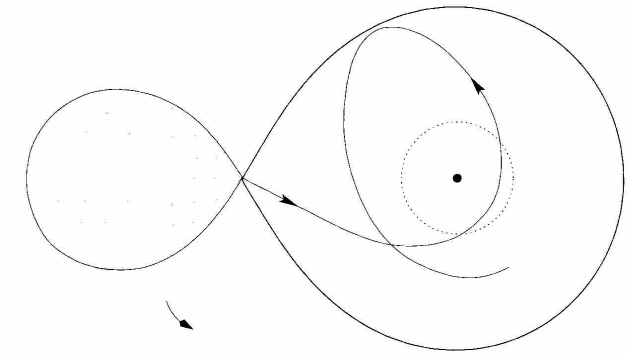

Figure 2. Plane view of the trajectory of a gas stream emanating from the secondary star (left) (Adopted from e.g. Hellier, 2001, p.25). The dotted ring forms the circularization radius.

The L_1 point itself is orbiting perpendicular to this motion at a speed more than ~ 1000 km s^{-1} (e.g. Frank, King & Raine 1992, p.81). Injected with this orbital motion, the stream swings into an orbit around the compact star rather than flowing directly towards it due to the conservation of angular momentum in conjunction with the coriolis force (e.g. Frank, King & Raine 1992, p.54). The stream then follows a trajectory determined by the injection velocity and gravity of the primary star and sweeps past a radius of closest approach with respect to the white dwarf, looping around to cross its earlier path (see Figure 2) (Lubow & Shu 1975). A continuous stream following this orbit will therefore intersect itself, resulting in dissipation of energy via shocks (e.g. Frank, King & Raine 1992, p.57). On the other hand, the stream has little opportunity to rid itself of the angular momentum it had on leaving the L_1 point and will tend to settle into the orbit of lowest energy for a given angular momentum, i.e. a circular orbit (see Figure 2) (e.g. Frank, King & Raine 1992, p.55). The stream will therefore settle in an orbit at a radius conserving its initial angular momentum at the L_1 point, the so-called circularization radius (R_{circ}) (e.g. Frank, King & Raine 1992, p55 - 56). The physical size of the orbit at R_{circ} is determined by the intrinsic specific angular momentum of the material leaving the L_1 region.

1.2.4 Accretion Disc formation

The circularization radius is always smaller than the Roche lobe radius of the primary star ($R_{L,1}$), typically a factor of 2-3 smaller, except for very small mass ratio, e.g. $M_2/M_1 \leq$ 0.005 (e.g. Frank, King & Raine 1992, p.56). The captured material would therefore orbit the primary well inside its Roche lobe (see Figure 2). This would be prevented however, if the primary star, or its magnetosphere had already occupied this space (i.e. if $R_1 > R_{circ}$; $R_{mag} > R_{circ}$), where R_1 and R_{mag} are the radii of the primary star and the magnetosphere respectively. However for CVs, where the compact object is a white dwarf, $R_1 << R_{circ}$.

Within the ring of material orbiting at the circularization radius, blobs of material closer to the primary star will orbit faster (Kepler's law) causing friction as they slide past blobs further out. Within such a ring there are dissipative processes, e.g. collisions between gas elements, shocks, viscous dissipation etc, which convert some of the energy of the ordered bulk orbital motion about the primary into thermal energy (heat energy), being radiated away (e.g. Frank, King & Raine 1992, p57). The gas can only meet this drain of energy by moving deeper into the gravitational potential of the primary star; and some of the material would move into smaller orbits in the process. The spiralling-in process entails a loss of angular momentum, being transferred outwards by internal torques (e.g. Frank, King & Raine 1992, p.57; Hellier 2001, p.25). The ring thus spreads out into a thin disc which continues spreading until the inner edge meets the compact star; or in the case of a magnetized primary, the radius where the disc ram pressure balances the magnetospheric pressure. This defines the so called magnetospheric radius of the white dwarf.

The interaction of the disc with the primary star may lead to a spin-up or spin-down torque that affects the rotating compact star (Wang 1987). Angular momentum flowing outwards through the disc enables the inward flow of material thereby releasing energy. At the outer edge of the disc tidal interactions with the secondary star soak up the angular

momentum and return it to the orbit of the secondary; limiting the outward spread of the disc (e.g. Hellier 2001, p25). This is replenished by the mass transfer from the secondary star. Material will continue to flow inwards towards the white dwarf (e.g. Frank, King & Raine 1992, p.57) if:

(i) Material in the disc loses angular momentum.

(ii) The primary star rotates slow enough allowing inflow of material instead of expelling it centrifugally.

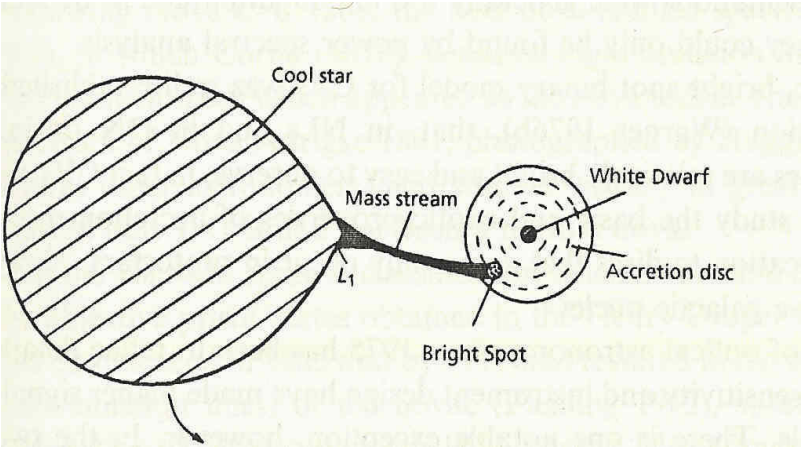

Figure 3. Schematic view of cataclysmic variables viewed from the pole of the orbit (Adopted from e.g. Warner 1995, p.11).

When a disc has been formed, the stream of material from the secondary star hits the edge of the disc, forming a "bright spot" (see Figure 3). At this spot, the stream of material falling radially, encounters material moving across its path in a circular orbit. Not much is understood about the turbulent encounter, however, computer simulations suggest that the dense core of the stream punches a hole in the disc and is gradually assimilated into the circular flow (e.g. Hellier 2001, p.27).

The stream is slightly wider than the disc edge and some of the material flows over the disc continuing onto the original trajectory. Kinetic energy of the stream is converted to heat and radiated away during the encounter. In some CVs this region emits about 30% of the total light of the system (King & Losata 1979; Lamb & Masters 1979, King & Watson 1987; e.g. Warner 1995, p.38). This is known through the observation of orbital

humps (e.g. Warner 1995, p.10), that are caused by the additional light seen when the bright spot is on the side facing the observer (e.g. Hellier 2001, p.27).

This study investigates the influence of the secondary star magnetic activity on the mass transfer in CVs, i.e. those systems where mass transfer is driven by magnetic braking of the secondary star. This includes the majority of the MCVs with orbital period $P_{orb} > 3$ hours, i.e. the so called intermediate polars and DQ Her systems. Therefore their properties will be reviewed.

1.3 Magnetic Cataclysmic Variables (MCVs)

1.3.1 Magnetic accretion

In MCVs the white dwarf usually has a substantial magnetic field that can either intercept the mass flow from the secondary, preventing the formation of an accretion disc, or disrupting the disc if present, preventing it from reaching down to the surface of the white dwarf. The magnetospheric field also facilitates the mass inflow onto the surface of the compact white dwarf, a process called magnetic accretion. This is the direct result of the complex interaction of ionized (or partially ionized) gas with the magnetic field. Two of the most important fluid-field interactions responsible for dynamical effects resulting in interesting observational consequences are:

(i) In most astrophysical environments of interest the field is frozen into the plasma (e.g. Jackson 1975, p.473). The thermal charged particles in plasma are tied to the field via the Lorentz force ($\vec{v} \times \vec{B}$), resulting in particles not being able to cross the field readily. However, they can migrate along the field lines following a helical path.

(ii) Effective motion of the gas across the field results in a viscous drag, and under certain conditions magnetic field may also be advected with the flow (e.g. Jackson 1975, p.478)

These processes both have far reaching consequences. The motion of trapped thermal plasma in a magnetic field allows determining the field strength through the emission of cyclotron emission. The frequency with which the electrons orbit the field, i.e. the Larmor frequency (e.g. Frank, King & Raine 1992, p.130) implies that most of the radiation is emitted as a spectral line centered on the fundamental frequency

$$\nu_{cyc} = \frac{eB}{2\pi m_e c} = 2.8 \times 10^{13} \left(\frac{B}{10^7\ Gauss} \right) \text{ Hz.} \qquad (1.1)$$

The second process, i.e. viscous drag, is the process leading to the loss of orbital angular momentum of orbiting satellites as they cross the earth's magnetic field lines. In astrophysical environments this process is almost a neglected process which has a very important effect on the flow dynamics of material from the secondary star, if it is magnetic, as well as in the accretion process of accreting compact objects. This may be the origin of the mysterious anomalous disc viscosity which is orders of magnitude higher than the kinematic viscosity.

The scale of the magnetosphere of the compact accreting object is usually expressed by the dipole moment

$$\mu \sim B_* R_*^3 \text{ (Gauss cm}^3\text{)}, \qquad (1.2)$$

where B_* and R_* represent the surface field and white dwarf radius respectively. Some of the properties of MCVs will be reviewed briefly.

1.3.2 Polars

Polars or AM Hercules (AM Her) stars are MCVs in which the white dwarfs have very strong magnetic field strengths (Schmidt 1999) which are confirmed by the Zeeman splitting and polarization measurements, revealing magnetic field strengths that are between 15 and 56 MG. Zeeman splitting is the broadening or splitting of spectral lines into several components when the source is in a strong magnetic field. The amount of Zeeman splitting and polarization depends on the magnetic field strength, and this effect therefore provides a powerful tool for investigating magnetic field strengths (e.g. Hellier

2001, p.118). The strong magnetic field of the white dwarf has the following important implications:

(i) Polars are synchronously rotating systems ($P_{rot} = P_{orb}$), with orbital periods lying between ~ 81 and 222 minutes (e.g. Chanmugam & Ray 1984). The phase locked interaction is caused by the strong magnetic interaction between the white dwarf and the low mass magnetic secondary star.

(ii) The formation of the disc is prevented (i.e. discless accretion) since the small orbital period ($P \leq 3$ hours), implies small binary separation and an extended magnetosphere, resulting in the mass transfer stream to ram directly into the magnetosphere of the white dwarf. The stream punches through the magnetosphere until the magnetospheric pressure starts to dominate, from where the flow is channeled along the field lines onto one or both poles of the white dwarf.

Evolutionary models (see e.g. Warner & Wickramasinge (1991) for a discussion) describe the condition for synchronization and discless accretion which are set by the ratio of the magnetic moment of the white dwarf to the mass accretion rate onto the white dwarf. For discless accretion to occur the following precondition must be satisfied:

$$0.4\left(\frac{P_{orb}}{4h}\right)^{7/6} M_1^{5/6} < \frac{\mu_{34}}{\sqrt{\dot{M}_{18}(\max)}} < 7\left(\frac{P_{orb}}{4h}\right)^{7/6}\left(\frac{M_1}{M_\Theta}\right)^{5/6} \qquad (1.3)$$

where M_1 is the mass of the white dwarf, M_Θ the solar mass, μ_{34} the magnetic moment of the white dwarf in units of 10^{34} Gauss cm^3 and $\dot{M}_{18}(\max)$ is the maximum mass accretion rate in units of 10^{18} g s^{-1}, for a discless accretion to occur. For orbital periods ≤ 4 hours and mass accretion rates $\leq 10^{18}$ g s^{-1}, synchronism can be achieved if $0.4 \leq \mu_{34} \leq 7$, which is in fact observed from most polars. This range of magnetic moments determines synchronization timescales which are short compared to the spin-up timescale. For effective synchronism and discless accretion the ratio of the synchronization timescale to the spin-up timescale must be

$$\frac{t_{syn}}{t_{spin-up}} \leq 1. \qquad (1.4)$$

Close to the white dwarf surface, matter falling in with supersonic velocities is decelerated and heated to approximately 10^8 K in a stand-off shock (e.g. Warner 1995; Boris 1998) resulting in a release of kinetic energy as flux distribution from the accretion column (Kuijper & Pringle 1982; Done, Osborne, Beardmore 1995; Beardmore, Done, Osborne, Ishida 1995; Gansicke, Beuermann, de Martino 1995) (see Figure 4). These are characterized by

(i) Strong polarized emission at optical/IR wavelengths.

(ii) Intense soft and in some cases hard X-ray emission.

(iii) An emission line spectrum of excitation which reflects the large streaming motion of accreted matter in the magnetosphere of the white dwarf (see e.g. Beuerman 1988).

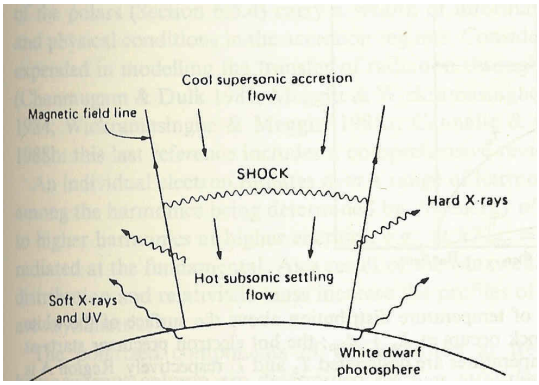

Figure 4. Schematic picture of a standard accretion column geometry for a magnetized white dwarf (Adopted from e.g. Frank, King & Raine, 1992, p.137).

1.3.3 Intermediate Polars

In intermediate polars the white dwarfs rotate asynchronously ($P_{rot} \neq P_{orb}$) (Chanmugam & Frank 1987), with rotation periods $P_{rot} >>$ 100 s and orbital periods > 3 hours (e.g. Warner 1983; Chanmugam & Ray 1984), except for EX Hya which has $P_{orb} < 2$ hours (e.g. Warner 1995, p.370) The white dwarfs in these systems have magnetic field strengths B ≤ 10 MG (i.e. $\mu_{34} \leq 0.4$). In terms of evolutionary models (e.g. Warner & Wickramasinghe 1991) they may oscillate between disced and discless states since

variations in the mass accretion rate from the secondary star influences the distance scale over which mass and angular momentum can be transferred to the white dwarf. Two scenarios are applicable for these systems (see e.g. Warner & Wickramasinghe 1991 for detailed discussion)

$$\frac{\mu_{34}}{\sqrt{\dot{M}_{18}(\max)}} < 0.4\left(\frac{P_{orb}}{4h}\right)^{7/6}\left(\frac{M_1}{M_\Theta}\right)^{5/6} \tag{1.5}$$

and

$$\frac{\mu_{34}}{\sqrt{\dot{M}_{16}(\min)}} > 0.4\left(\frac{P_{orb}}{4h}\right)^{7/6}\left(\frac{M_1}{M_\Theta}\right)^{5/6} \tag{1.6}$$

where $\dot{M}_{16}(\min)$ is the minimum mass accretion rate in units of 10^{16} g s^{-1}, for a disc accretion to occur. This limit is only valid if the variation in $\dot{M}$ exceeds a factor of 100, which is observed from those systems with orbital periods ≤ 6 hours. A high accretion rate $\dot{M}_{18}(\max) \sim 1$ causes a decrease in the magnetospheric radius of the white dwarf to a value which is small enough to allow matter to form a disc around the white dwarf. A significant decrease by a factor ~100 in $\dot{M}$ will lead to an increasing magnetospheric radius which will capture the accretion stream from the companion star and no disc can develop in this case.

The spin periods of the white dwarfs are usually prominent in hard X-rays (E_x > 4 KeV). Hard X-ray emitters may be discless systems accreting matter directly onto restricted regions of the white dwarf. Some evolutionary models (e.g. Norton & Watson 1988) suggest that polars and intermediate polars are similar systems observed during different stages of their evolution. These models imply that in some stage of the life cycle of disc accreting intermediate polars, the system may loose angular momentum due to magnetic braking and gravitational radiation of the secondary star, causing the binary separation to shrink. For white dwarf magnetic fields $B_* \geq 3\times10^6$ Gauss, a point in orbital evolution will be reached when the magnetospheric radius of the white dwarf will extend to the

companion causing synchronism over some timescale (e.g. Chanmugam & Ray 1984) depending on the magnetic field strength.

1.3.4 DQ Hercules (DQ Her) stars

DQ Her stars constitute a subset of intermediate polars. The observed rotational period of white dwarfs in these systems are shorter ($P_{rot} < 100\,\mathrm{s}$) than the period of intermediate polars, with orbital period lying in the range between 4.65 hours and 9.88 hours (e.g. Chanmugam & Ray 1984). The large orbital periods of these systems imply a wide binary separation which improves the chance for the formation of an accretion disc (Harmeury, King & Lasota 1986). These conditions are summarized (e.g. Warner & Wickramasinghe 1991)

$$\frac{\mu_{34}}{\sqrt{\dot{M}_{18}(\max)}} < 0.4\left(\frac{P_{orb}}{4h}\right)^{7/6}\left(\frac{M_1}{M_\Theta}\right)^{5/6} \quad \text{(Equation 1.5)}$$

and

$$\frac{\mu_{34}}{\sqrt{\dot{M}_{16}(\min)}} < 0.4\left(\frac{P_{orb}}{4h}\right)^{7/6}\left(\frac{M_1}{M_\Theta}\right)^{5/6} \qquad (1.7)$$

implying that permanent discs may develop due to the wide separation between the white dwarf and the secondary star providing a mechanism for reducing the angular momentum of the accretion from the secondary star before it accretes onto the white dwarf. The evolution of these systems (see e.g. Warner & Wickramasinghe 1991) is described in terms of large initial accretion rates ($\dot{M}_1(\max) \sim 10^{18}\, g\, s^{-1}$) from the companion star. Under these conditions, the disc which lies close to the white dwarf exerts a torque on the white dwarf causing a spin-up over timescales of

$$t_{spin-up} \sim 4.5\times10^5\, \mu_{33}^{-8/7}\, \dot{M}_{17}^{\,-3/7}\; yr \qquad (1.8)$$

By fitting the best parameter for DQ Her systems which are $\mu_{33} = 0.16$ and $\dot{M}_{17} = 10$

(e.g. Warner &Wickramasinghe 1991), a spin-up timescale of $t_{spin-up} \sim 1.4 \times 10^6$ yr is estimated. Hameury, King & Lasota (1989) found that the variations in $\dot{M}$ over timescales similar to the spin-up timescale can be as large as

$$\alpha \sim \frac{\dot{M}_{\min}}{\dot{M}_{\max}} \geq 10^{-5} \tag{1.9}$$

and will influence any further evolution of the system. A significant drop in the mass transfer rate from the secondary star after the white dwarf has been spun-up will cause the disc inner edge to be pushed out by the magnetic pressure of the rotating white dwarf. If the disc is pushed out to regions outside the corotation radius, the disc torque on the faster rotating white dwarf will gradually spin the white dwarf down. This will cause the white dwarf to enter the propeller phase. If the inner disc edge radius $r_i \leq r_{cor}$ (where r_{cor} is the corotation radius), the white dwarf and the disc torque will be balanced, and the system will be in equilibrium. In the Warner & Wickramasinghe (1991) discussion of the period evolution of these systems, the most prominent parameter influencing the evolution of the period of the white dwarf is the mass transfer rate from the secondary star, implying that stellar evolution of the secondary star will determine whether the white dwarf will spin-up, spin in equilibrium or spin-down.

1.4 Objectives of the study

Magnetic activity among rotating stars with convective envelopes is widespread and this includes the secondary stars in CVs (Collier 2002). The importance of dynamo-generated magnetic fields on the secondary stars has long been recognized, and their effects have played an important role in the development of theories for both long-term evolution of CVs and the short-term variations in mass transfer rate through the L_1 point (Collier, 2002). However, little has been known about the magnetic activity on the secondary stars from direct observation (Collier, 2002). This could be because most CVs are considerably fainter than the nearby stars on which most magnetic-field studies have been performed, and partly because the spectrum of the secondary star is strongly

diluted by the accretion driven radiation emanating from other parts of the system (Collier 2002).

Ritter (1988) showed that the surface magnetic field of a secondary star in cataclysmic variables has a significant influence on the mass transfer variations if the average field strength near the L_1 region exceeds the equipartition value, i.e. when the magnetic pressure exceeds the gas pressure in that region. Meintjes (2004) showed that the surface magnetic field of the secondary star in AE Aquarii, which applies to all cataclysmic variables in general, influences the mass transfer; supporting the idea that magnetic field variation across the surface of the star can have a dramatic effect on the mass transfer from the secondary star to the white dwarf primary star. Meintjes (2004) further showed that if the surface magnetic field of the secondary star in cataclysmic variables is below a critical value near the L_1 region, the magnetic field can be advected with the flow of material into the funnel (towards the white dwarf). This process of magnetic advection from the secondary star into the funnel acts as a mechanism of magnetizing the mass transfer through the funnel. Magnetic flux advection is effective if the surface magnetic field of the secondary star is such that the ratio of the magnetic Reynolds number to the Hartmann number of the flow is greater than one (e.g. Jackson 1975, p.478). This means that the flow viscosity in the funnel exceeds the magnetic viscosity, i.e. implying that the flow ram pressure significantly exceeds the magnetic pressure, as expected.

The surface magnetic field of secondary stars can be modelled using the Mestel and Spruit stellar wind theory (1987) and estimating the amount of angular momentum required to drive the observed mass accretion rate through Roche lobe overflow, and solving for the surface polar magnetic field. This modelling allows for a search for systematic trends in the surface polar field strength of mass transferring secondary stars in CVs. Magnetic braking of the secondary star (e.g. Campbell 1997, p.268 - 278) can also be used to constrain the surface magnetic field of the secondary star. This can then be compared with typical fields needed for effective magnetic advection in the flow from the secondary star.

Therefore, the main objectives of this study are:

(i) The systematic modelling of the mass transfer in intermediate Polars that is driven by magnetic braking and calculating the surface polar magnetic field strength of the secondary stars. This will be used to search for possible relationships between surface polar magnetic field and orbital period for different dynamo laws.

(ii) To investigate the effect of advected magnetic field on the mass flow in the funnel in some intermediate polars. This can be generalized to other MCVs.

1.5 The outline

This dissertation consists of four chapters.

Chapter two briefly presents the stellar wind theory. In this chapter orbital angular momentum losses are reviewed and their influence on secular evolution and mass transfer from the secondary star is discussed. Mass transfer and angular momentum losses by stellar winds for the inferred dynamo laws are also presented here.

In chapter three the models for determining the surface polar magnetic fields of mass transferring secondary stars are developed using the stellar wind theory and this is used to calculate the surface polar magnetic field of some intermediate polars with known orbital periods. The influence of the secondary star magnetic field on mass transfer in intermediate polars is also investigated in this chapter.

The conclusions will be presented in chapter four.

Chapter Two

Stellar wind theory

2.1 Introduction

One of the characteristics of CVs is the mass transfer from the secondary star to the white dwarf primary star. For a continuous and stable mass transfer through the L_1 region, the Roche lobe of the secondary star must shrink at least as fast as the stellar surface; which is achieved through loss of angular momentum via a suitable mechanism. Short-period ($P_{orb} < 3$ hours) binary systems generate gravitational waves which remove orbital angular momentum (Kraft, Mathews, Grennstein 1962; Paczyñski 1967). Observations of binary systems with orbital periods > 3 hours often suggest higher mass transfer rates than that determined by gravitational radiation (Verbunt & Zwaan 1981). Mestel (1968) pointed out that a main-sequence secondary star in a binary system would have a wind flow from its surface similar to that of a single star. The presence of a magnetic field would result in channelling the flow, with a consequent braking torque on the star (Weber & Davis 1967). In binary systems, however, tidal torques keep the secondary star rotation close to orbital synchronism. This magnetic braking torque removes orbital angular momentum from the star, thus driving it towards an under-synchronous state. Tidal coupling to the orbit replaces this loss in keeping the star near corotation. This results in a continuous removal of orbital angular momentum. A detailed review of orbital angular momentum losses, and their influence on the secular evolution and mass transfer from the secondary star, will therefore be presented.

2.1.1 Angular momentum loss

In the most simple scenario consider a body of mass m moving with velocity v in a circular orbit of radius a around a mass M at the centre. The centripetal force on m directed towards the centre is given by

$$F = \frac{mv^2}{a}. \tag{2.1}$$

This centripetal force is supplied by the gravitational attraction between the two masses given by

$$F = \frac{GMm}{a^2}, \tag{2.2}$$

where G is the gravitational constant. Equating equations (2.1) and (2.2) gives

$$v = \left(\frac{GM}{a}\right)^{1/2}, \tag{2.3}$$

where v is the Keplerian velocity. The orbital period is given by

$$P_{orb} = \frac{2\pi a}{v}, \tag{2.4}$$

where $2\pi a$ is the circumference of the orbit. Substituting equation (2.3) into (2.4) gives

$$P_{orb}^2 = \frac{4\pi^2 a^3}{GM}. \tag{2.5}$$

The same principle can be applied to describe binary motion:

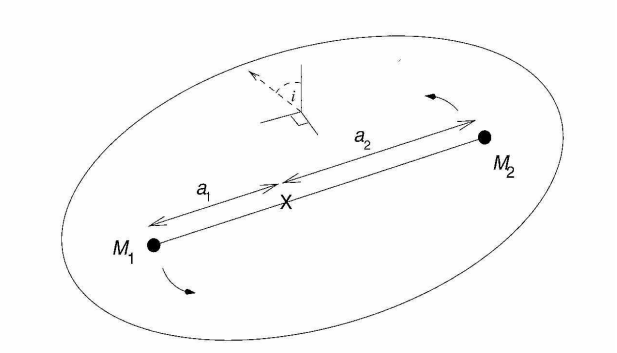

Figure 5. Two stars of masses M_1 and M_2 orbiting in a plane about the centre-of-mass X (Adopted from Hellier 2001, p.189).

Consider two stars of masses M_1 (primary) and M_2 (secondary) separated by a distance a, and let $M = M_1 + M_2$. Equation (2.5) can then be written as

$$4\pi^2 a^3 = G(M_1 + M_2)P_{orb}^2 . \tag{2.6}$$

Equation (2.6) is referred to as Kepler's law (the third law). If the distances of M_1 and M_2 from the centre-of-mass (CM) are a_1 and a_2 respectively (see Figure 5), where $a_1 + a_2 = a$; then from the definition of angular momentum, $J = mav$, the total orbital angular momentum of the system can be expressed as

$$J_{orb} = M_1 a_1 v_1 + M_2 a_2 v_2 . \tag{2.7}$$

From equation (2.4), the orbital velocity can be expressed in terms of

$$v_i = \frac{2\pi a_i}{P_{orb}},$$

and substituting this in equation (2.7) gives

$$J_{orb} = M_1 a_1 \frac{2\pi a_1}{P_{orb}} + M_2 a_2 \frac{2\pi a_2}{P_{orb}} . \tag{2.8}$$

From equation (2.6), the orbital period can be presented as

$$P_{orb} = 2\pi a\left(\frac{a}{GM}\right)^{1/2} .$$

Substituting for P_{orb} in equation (2.8) gives

$$J_{orb} = \left(\frac{GM}{a}\right)^{1/2} \frac{1}{a}\left(M_1 a_1^2 + M_2 a_2^2\right). \tag{2.9}$$

For a binary system $a_1 + a_2 = a$ and $M_1 a_1 = M_2 a_2$, and a_1 can be expressed in the form

$$a_1 = \frac{M_2 a}{(M_1 + M_2)} \tag{2.10}$$

and equation (2.9) can then be expressed as

$$J_{orb} = \left(\frac{GM}{a}\right)^{1/2} \frac{1}{a}\left[(M_1 a_1)a_1 + (M_2 a_2)a_2\right]$$

$$J_{orb} = \left(\frac{GM}{a}\right)^{1/2} \frac{1}{a}(M_1 a_1)\left[a_1 + a_2\right]$$

$$\Rightarrow \quad J_{orb} = \left(\frac{GM}{a}\right)^{1/2} M_1 a_1 . \tag{2.11}$$

Substituting equation (2.10) into equation (2.11) gives

$$J_{orb} = M_1 M_2 \left(\frac{Ga}{M}\right)^{1/2} . \tag{2.12}$$

Equation (2.12) gives the total orbital angular momentum of the binary system. From equations (2.3) and (2.12) it is noted that there are three concepts involved:

(i) Material in smaller orbits move faster (Kepler's law).

(ii) Material in smaller orbits have lower angular momentum (increase in speed is not enough to offset the decrease in radius).

(iii) By transferring into smaller orbit material liberates gravitational energy.

Logarithmic differentiation of equation (2.12) gives

$$\frac{\dot{J}_{orb}}{J_{orb}} = \frac{\dot{M}_1}{M_1} + \frac{\dot{M}_2}{M_2} + \frac{1}{2}\left(\frac{\dot{a}}{a} - \frac{\dot{M}}{M}\right). \tag{2.13}$$

If it is assumed that all the mass lost by the secondary star is accreted by the primary star, i.e. $\dot{M}_1 = -\dot{M}_2$ and $\dot{M} = 0$, then equation (2.13) can be expressed as

$$\frac{\dot{a}}{a} = 2\frac{\dot{J}_{orb}}{J_{orb}} + 2\frac{(-\dot{M}_2)}{M_2}\left(1 - \frac{M_2}{M_1}\right). \tag{2.14}$$

In the equation above the meaning of the various terms are:

$\dot{a}/a$ is the rate of change of the binary separation.

$\dot{J}_{orb}/J_{orb}$ is the rate of change of orbital angular momentum (note $\dot{J}_{orb} < 0$).

$-\dot{M}_2/M_2$ is the rate of mass transfer from the secondary star.

Therefore, if angular momentum is also conserved, i.e. conservative mass transfer ($\dot{M} = 0$ and $\dot{J}_{orb} = 0$), mass transfer from the secondary star $(-\dot{M}_2 > 0)$ results in an increase in a ($\dot{a} > 0$) provided that $M_2 < M_1$. In cataclysmic variables, material is transferred from a low mass secondary star to a more massive white dwarf. Assuming a

conservative mass transfer, more material is placed near the centre-of-mass and the remaining mass M_2 must move to a wider orbit in order to conserve the total angular momentum. In the opposite case where mass is transferred from the more massive star to the less massive star, the centre-of-mass is losing mass, transferring the remaining mass to a smaller orbit to conserve the total angular momentum (e.g. Frank, King & Raine 1992, p.52).

For a mass ratio in the range $0.1 \le M_2/M_1 \le 0.8$, the mean radius of the secondary star's Roche lobe obeys the equation (e.g. Frank, King & Raine 1992, p.51; Campbell 1997, p.269)

$$\frac{M}{M_2}\left(\frac{R_{L,2}}{a}\right)^3 \approx 0.1, \tag{2.15}$$

where $R_{L,2}$ is the Roche lobe radius of the secondary star. Logarithmic differentiation of equation (2.15) gives

$$\frac{\dot{R}_{L,2}}{R_{L,2}} = \frac{\dot{a}}{a} + \frac{1}{3}\left(\frac{\dot{M}_2}{M_2} - \frac{\dot{M}}{M}\right). \tag{2.16}$$

For a conservative mass transfer, i.e. $\dot{M} = 0$, equation (2.16) becomes

$$\frac{\dot{R}_{L,2}}{R_{L,2}} = \frac{\dot{a}}{a} + \frac{1}{3}\frac{\dot{M}_2}{M_2}. \tag{2.17}$$

Substituting for $\dot{a}/a$ from equation (2.14) into (2.17) gives

$$\frac{\dot{R}_{L,2}}{R_{L,2}} = 2\frac{\dot{J}_{orb}}{J_{orb}} + 2\frac{(-\dot{M}_2)}{M_2}\left(1 - \frac{M_2}{M_1}\right) + \frac{1}{3}\frac{\dot{M}_2}{M_2}$$

$$\Rightarrow \quad \frac{\dot{R}_{L,2}}{R_{L,2}} = 2\frac{\dot{J}_{orb}}{J_{orb}} + 2\frac{(-\dot{M}_2)}{M_2}\left(\frac{5}{6} - \frac{M_2}{M_1}\right). \tag{2.18}$$

For conserved angular momentum ($\dot{J}_{orb} = 0$), mass transfer from the secondary star causes the Roche lobe of the secondary star to expand ($\dot{R}_{L,2} > 0$) provided

$M_2/M_1 < 5/6$, effectively increasing the binary separation causing the secondary to detach itself from the Roche lobe, inhibiting further mass transfer (King 1988; e.g. Frank, King & Raine 1992, p.53). Sustained and stable mass transfer requires a gradual loss of angular momentum from the binary system, grinding down the orbit and hence the secondary star's Roche lobe, re-establishing Roche lobe contact, enabling further transfer of material. The ultimate driving mechanism for mass transfer in compact binaries is therefore the angular momentum loss process of the binary system. Given such a process, it can be assumed $R_2 = R_{L,2}$ at least in a long-term average sense (R_2 is the radius of the secondary star). If mass loss is sufficiently gentle the star will stay close to thermal equilibrium, allowing the secondary star remain on the main sequence, i.e. obeying the inferred main-sequence mass-radius relation $R_2 \propto M_2$ (King 1988; e.g. Frank, King & Raine 1992, p.54). Therefore the relationship

$$\frac{\dot{R}_2}{R_2} = \frac{\dot{M}_2}{M_2} \tag{2.19}$$

holds. Substituting equation (2.19) into (2.18) for a lobe filling secondary star (i.e. $R_{L,2} = R_2$), it can be shown that

$$\frac{-\dot{M}_2}{M_2} = \frac{-\dot{J}_{orb}/J_{orb}}{4/3 - M_2/M_1}. \tag{2.20}$$

Logarithmic differentiation of equation (2.6) gives

$$\frac{\dot{a}}{a} = \frac{2\dot{P}_{orb}}{3P_{orb}}. \tag{2.21}$$

From equations (2.20) and (2.14) it can be shown that

$$\frac{\dot{a}}{a} = 2\frac{\dot{J}_{orb}}{J_{orb}} + 2\frac{-\dot{J}_{orb}/J_{orb}}{4/3 - M_2/M_1}\left(1 - \frac{M_2}{M_1}\right)$$

$$\Rightarrow \quad \frac{\dot{a}}{a} = \frac{2}{3}\left(\frac{\dot{J}_{orb}/J_{orb}}{4/3 - M_2/M_1}\right).$$

Using equation (2.21), it can be shown that an evolution equation is given by

$$\frac{\dot{a}}{a} = \frac{2}{3}\frac{\dot{P}_{orb}}{P_{orb}} = \frac{2}{3}\left(\frac{\dot{J}_{orb}/J_{orb}}{4/3 - M_2/M_1}\right). \tag{2.22}$$

This results in a converging binary evolution with time for all $M_2/M_1 < 4/3$, since mass transfer and orbital evolution are driven by angular momentum loss ($\dot{J}_{orb} < 0$) on a characteristic timescale determined by specific angular momentum loss mechanisms (Meintjes 2002a).

From equation (2.14), for $M_2/M_1 < 1$, it is clear that binary systems experiencing quasi-conservative evolution where mass transfer dominates angular momentum loss ($-\dot{M}_2/M_2 >> \dot{J}_{orb}/J_{orb}$) will likely evolve according to $\dot{a}/a > 0$ (diverging binary) (Meintjes 2002b). The binary will shrink (converging binary) if $M_2/M_1 < 1$ and $-\dot{M}_2/M_2 << \dot{J}_{orb}/J_{orb}$ (Meintjes 2002b). From equation (2.18), for $M_2/M_1 \leq 5/6$, the effective mass transfer between a main sequence secondary star and a white dwarf is only driven effectively if $-\dot{J}_{orb}/J_{orb} > 0$. This causes the binary to evolve such that $\dot{a}/a < 0$ for all $M_2/M_1 < 4/3$ (converging binary). In the absence of angular momentum losses, mass transfer can only be driven by an evolving secondary star (King 1988; e.g. Frank, King & Raine 1992, p.53 - 54). In this scenario, the binary will expand ($\dot{a}/a > 0$) for all $M_2/M_1 < 5/6$. The timescale for this to occur, especially in CVs where the secondary is a low mass star ($M_2 < M_\Theta$ where M_Θ is the solar mass), is billions of years, resulting in this mode of mass transfer to be insignificant.

Mass transfer flow from the secondary star to the primary star in intermediate polars and polars may be clumpy or blob-like (King & Lasota 1991; King 1993; Wynn & King 1995). It was shown (King 1993) that the rotating magnetosphere of an intermediate polar accretes blobs with mechanical energies less than a certain critical value depending on its spin rate, and expels blobs with higher mechanical energy. In this blob accretion model

orbital angular momentum is carried away by any blob expelled from the system; and this may result in a dynamically unstable mass transfer process if the Roche lobe of the secondary star shrinks down into the surface layers of the secondary star, causing a run-away mass transfer (Wynn & King 1995). A discussion of the condition for stable mass transfer in terms of the Roche lobe behavior will now be presented.

2.1.2 Stable mass transfer

The equation of state of a star with a fully convective envelope is (King 1988):

$$P = K\rho^{5/3}, \tag{2.23}$$

where P is the gas pressure and ρ the density. The condition for hydrostatic equilibrium for such a star is given by the familiar mass-radius relation applicable to ordinary main-sequence stars (King 1988)

$$R_2 = \left(\frac{K}{G}\right) M_2^{-1/3}. \tag{2.24}$$

Logarithmic differentiation of equation (2.24) gives

$$\frac{\dot{R}_2}{R_2} = -\frac{1}{3}\left(\frac{\dot{M}_2}{M_2}\right). \tag{2.25}$$

To avoid a run-away mass transfer, the Roche lobe of the secondary star must grow faster than the star, i.e. $\dot{R}_{L,2} > \dot{R}_2$ for $R_2 = R_{L,2}$; and therefore

$$\frac{\dot{R}_{L,2}}{R_{L,2}} - \frac{\dot{R}_2}{R_2} > 0. \tag{2.26}$$

Equation (2.13) relates the orbital evolution ($\dot{a}/a$) with mass transfer ($\dot{M}_2/M_2$), mass accretion ($\dot{M}_1/M_1$) and angular momentum loss from the system. By combining it with equation (2.16), i.e.

$$\frac{\dot{a}}{a} = \frac{\dot{R}_{L,2}}{R_{L,2}} - \frac{1}{3}\left(\frac{\dot{M}_2}{M_2} - \frac{\dot{M}}{M}\right),$$

it can be shown that an expression relating the mass transfer ($\dot{M}_2 / M_2$) and mass accretion ($\dot{M}_1 / M_1$) to the orbital angular momentum evolution of the system is given by

$$\frac{\dot{J}_{orb}}{J_{orb}} = \frac{\dot{M}_1}{M_1} + \frac{\dot{M}_2}{M_2} + \frac{1}{2}\left(\frac{\dot{R}_{L,2}}{R_{L,2}} - \frac{1}{3}\frac{\dot{M}_2}{M_2} + \frac{1}{3}\frac{\dot{M}}{M}\right).$$

Re-arranging terms and grouping together similar terms results in

$$\frac{\dot{J}_{orb}}{J_{orb}} = \frac{\dot{M}_1}{M_1} + \frac{5}{6}\frac{\dot{M}_2}{M_2} + \frac{1}{2}\frac{\dot{R}_{L,2}}{R_{L,2}} - \frac{1}{3}\frac{\dot{M}}{M},$$

which can be written as follows

$$\frac{\dot{R}_{L,2}}{R_{L,2}} = 2\frac{\dot{J}_{orb}}{J_{orb}} - 2\frac{\dot{M}_1}{M_1} - \frac{5}{3}\frac{\dot{M}_2}{M_2} + \frac{2}{3}\frac{\dot{M}}{M}. \qquad (2.27)$$

Equation (2.27) is independent of the nature of angular momentum mechanism, but expresses the influence of angular momentum evolution ($\dot{J}_{orb} / J_{orb}$), mass transfer ($\dot{M}_2 / M_2$) and mass accretion ($\dot{M}_1 / M_1$) on the Roche lobe evolution, which in turn facilitates the mass transfer from the secondary star over a long timescale.

From equation (2.27) it is clear that the total binary angular momentum ($\dot{J}_{orb} / J_{orb}$) evolution, among other parameters, has a direct influence on the Roche lobe dynamics ($\dot{R}_{L,2} / R_{L,2}$) of the secondary star, which in turn facilitates the long term mass transfer from the secondary to the primary. A significant contribution towards the angular momentum evolution is the mass-loss of the secondary star through the L_1 point, resulting in a drain of angular momentum of the secondary star. This, in turn, feeds back to the dynamics of the Roche lobe of the secondary which has to stay in close contact with the stellar photosphere to secure stable mass transfer. Since the mass loss of the secondary

star provides the dominant contribution towards the angular momentum drain in the system, a brief discussion towards its quantification will be presented.

The Roche lobe overflow from the surface of the secondary star through the L_1 region results in a drain of angular momentum

$$\dot{J}_{ov} \approx \dot{M}_2 \, b_1^2 \, \Omega_{orb}, \tag{2.28}$$

where b_1 represents the distance of L_1 point from the centre of the primary star. Since the material at the L_1 region has the same specific angular momentum as the material orbiting at the so-called circularization radius, defined earlier (p.6), it allows the quantification of b_1, which is

$$b_1^2 \, \Omega_{orb} = R_{circ} v_K(circ)$$

$$\Rightarrow \; b_1^2 = \frac{\left(GM_1 R_{circ}\right)^{1/2}}{\Omega_{orb}}. \tag{2.29}$$

In this expression $v_K(circ) = \left(GM_1 / R_{circ}\right)^{1/2}$ is the Keplerian velocity at the circularization radius. Therefore the angular momentum loss as a result of material lost by the secondary star via Roche lobe overflow, $\dot{J}_{ov}$, results in loss of angular momentum at the rate

$$\dot{J}_{ov} = \dot{M}_2 \left(GM_1 R_{circ}\right)^{1/2}.$$

Assuming that the binary as a whole loses a fraction, η, of this angular momentum, we get

$$\frac{\dot{J}_{orb}}{J_{orb}} = \eta \frac{\dot{J}_{ov}}{J_{orb}}$$

$$\Rightarrow \; \frac{\dot{J}_{orb}}{J_{orb}} = \eta \frac{\dot{M}_2 \left(GM_1 R_{circ}\right)^{1/2}}{J_{orb}}. \tag{2.30}$$

Some of the mass lost by the secondary star will be accreted by the primary star and the rest lost from the system. In this case the rate of mass-loss of the secondary star is given by

$$-\dot{M}_2 = \dot{M}_1 - \dot{M} .$$

If a fraction, β, of this mass is lost from the system, then

$$\dot{M} = \beta \dot{M}_2 \text{ and } -\dot{M}_2 = \dot{M}_1 - \beta \dot{M}_2 \text{ ; therefore}$$

$$\Rightarrow \dot{M}_1 = -(1-\beta)\dot{M}_2 . \tag{2.31}$$

Substituting equations (2.30) and (2.31) into equation (2.27) gives

$$\frac{\dot{R}_{L,2}}{R_{L,2}} = 2\left[\eta \frac{\dot{M}_2 (GM_1 R_{circ})^{1/2}}{J_{orb}}\right] + 2(1-\beta)\frac{\dot{M}_2}{M_1} - \frac{5\dot{M}_2}{3M_2} - \frac{2\beta\dot{M}_2}{3M}$$

$$\Rightarrow \frac{\dot{R}_{L,2}}{R_{L,2}} = -\frac{\dot{M}_2}{M_2}\left[\frac{5}{3} - 2(1-\beta)\frac{M_2}{M_1} - 2\eta\frac{(GM_1 R_{circ})^{1/2} M_2}{J_{orb}} - \frac{2}{3}\frac{\beta M_2}{M}\right]. \tag{2.32}$$

Comparing the expression above with the reaction of the secondary star's envelope, i.e. equation (2.25), if its equilibrium has been distorted, i.e. equation (2.26), can reveal the condition for stable mass transfer. Substituting equations (2.25) and (2.32) into the condition for stable mass transfer, i.e. equation (2.26), it can be shown that

$$-\frac{\dot{M}_2}{M_2}\left[\frac{5}{3} - 2(1-\beta)\frac{M_2}{M_1} - 2\eta\frac{(GM_1 R_{circ})^{1/2} M_2}{J_{orb}} - \frac{2}{3}\frac{\beta M_2}{M}\right] + \frac{1}{3}\frac{\dot{M}_2}{M_2} > 0$$

$$-\frac{\dot{M}_2}{M_2}\left[\frac{4}{3} - 2(1-\beta)\frac{M_2}{M_1} - 2\eta\frac{(GM_1 R_{circ})^{1/2} M_2}{J_{orb}} - \frac{2}{3}\frac{\beta M_2}{M}\right] > 0$$

$$\Rightarrow \left[\frac{4}{3} - 2(1-\beta)\frac{M_2}{M_1} - 2\eta\frac{(GM_1 R_{circ})^{1/2} M_2}{J_{orb}} - \frac{2}{3}\frac{\beta M_2}{M}\right] > 0 . \tag{2.33}$$

From Kepler's law, equation (2.6), it can be shown that

$$a^3 = GM\left(\frac{P_{orb}}{2\pi}\right)^2$$

$$a^3 = GM\left(\frac{1}{\Omega_{orb}}\right)^2$$

$$\Rightarrow \Omega_{orb}^2 = \frac{GM}{a^3} .$$

Substituting for Ω_{orb}^2 in equation (2.29) gives

$$R_{circ} = \frac{b_1^4 \Omega_{orb}^2}{GM_1}$$

$$R_{circ} = \frac{b_1^4}{GM_1}\left[\frac{GM}{a^3}\right]$$

$$\Rightarrow\ R_{circ} = \left(\frac{b_1}{a}\right)^3 b_1\left(1+\frac{M_2}{M_1}\right). \tag{2.34}$$

Using equations (2.12) and (2.34) in equation (2.33) gives

$$\frac{4}{3} - 2(1-\beta)\frac{M_2}{M_1} - \frac{2}{3}\beta\frac{M_2}{M} - 2\eta\frac{\left\{GM_1(b_1/a)^3 b_1(1+M_2/M_1)\right\}^{1/2} M_2}{M_1 M_2 (Ga/M)^{1/2}} > 0$$

$$\frac{2}{3} - (1-\beta)\frac{M_2}{M_1} - \frac{1}{3}\beta\frac{M_2}{M} - \eta\left(1+\frac{M_2}{M_1}\right)\left(\frac{b_1}{a}\right)^2 > 0$$

$$\Rightarrow\quad (1-\beta)\frac{M_2}{M_1} + \frac{1}{3}\beta\frac{M_2}{M} + \eta\left(1+\frac{M_2}{M_1}\right)\left(\frac{b_1}{a}\right)^2 < \frac{2}{3}. \tag{2.35}$$

The quantity (b_1/a) can also be expressed as a function of mass ratio (M_2/M_1), which is (e.g. Warner 1995, p.33)

$$\frac{b_1}{a} = 0.5 - 0.227\log_{10}\left(\frac{M_2}{M_1}\right). \tag{2.36}$$

Equation (2.35) gives the condition for stable mass transfer; and can be used to evaluate the stability of mass transfer during different phases of evolution.

If the binary evolution conserves mass, i.e. ($\dot{M} = 0$) the white dwarf will accrete all the gas that is crossing the L_1 region (Wynn & King 1995). This is only possible if the circularization radius, where material initially settles, is inside the so-called corotation radius of the magnetized white dwarf, i.e. in regions where the Keplerian motion exceeds the angular velocity of the white dwarf. This results in the orbiting material being able to attach to the field lines, resulting in effective accretion onto the white dwarf. In this case the white dwarf is acting as a sink (e.g. drain) for the angular momentum lost by the secondary star. This results in a conservative evolution of the system ($\beta = 0; \eta = 1$). The opposite scenario, i.e. the circularization radius being outside the corotation radius,

results in a spectacular propelling of the material from the system, leading to a non-conservative evolution ($\beta = 1; \eta = 1$). The condition for conservative ($\beta = 0; \eta = 1$) and non-conservative ($\beta = 1; \eta = 1$) evolution can be summarized as follows:

$$\frac{M_2}{M_1} + \left(1 + \frac{M_2}{M_1}\right)\left(\frac{b_1}{a}\right)^2 < \frac{2}{3} \qquad [\beta = 0; \eta = 1]$$

$$\frac{1}{3}\frac{M_2}{M} + \left(1 + \frac{M_2}{M_1}\right)\left(\frac{b_1}{a}\right)^2 < \frac{2}{3} \qquad [\beta = 1; \eta = 1]$$

These equations can be used to evaluate the stability of mass transfer in different phases of the spin history of the white dwarf.

In reality the orbital evolution of the binary system is not only sculptured by the angular momentum loss from the secondary star through the L_1 region, but magnetic braking of the secondary results in mass and angular momentum loss from the rotating binary system as a whole, while gravitational radiation is also in some cases an effective drain of orbital angular momentum. Gravitational radiation is predominantly effective in short period systems ($P_{orb} < 3$ hours) and falls outside the scope of this study. Since this study is focusing on the influence of the secondary star's magnetic field on the mass transfer in the system, the focus will be mainly on the other dominant drain of orbital angular momentum, i.e. magnetic braking. Before the mechanism itself is going to be discussed, the combined effect of magnetic braking and Roche lobe overflow will be investigated. This will be used to obtain an equation relating the orbital evolution ($\dot{a}/a$), mass transfer ($\dot{M}_2/M_2$) and mass accretion ($\dot{M}_1/M_1$) to the total angular momentum lost from the binary. By quantifying the magnetic braking of the secondary star through a suitable model, the magnetic profile of the secondary star and its influence on mass transfer can be constrained. Mestel & Spruit (1987) developed a magnetohydrodynamic model quantifying the angular momentum losses from a rotating magnetized main-sequence star, which will be discussed in detail in the following section. However, to allow the investigation of magnetic braking on the binary evolution ($\dot{a}/a$), mass transfer ($\dot{M}_2/M_2$)

and mass accretion ($\dot{M}_1 / M_1$), the equation has to be modified somewhat. The effect of magnetic braking and Roche lobe overflow will now be considered, i.e.

$$\frac{\dot{J}_{orb}}{J_{orb}} = \frac{\dot{J}_{mb}}{J_{orb}} + \frac{\dot{J}_{ov}}{J_{orb}}.$$

From equations (2.12) and (2.30), the rate of loss of angular momentum of the secondary star as a result of Roche lobe overflow can be expressed as

$$\frac{\dot{J}_{ov}}{J_{orb}} = \eta \frac{\dot{M}_2 (G M_1 R_{circ})^{1/2}}{M_1 M_2 \left(\frac{Ga}{M}\right)^{1/2}}$$

$$\Rightarrow \frac{\dot{J}_{ov}}{J_{orb}} = \eta \left(\frac{M}{M_1}\right)^{1/2} \left(\frac{R_{circ}}{a}\right)^{1/2} \left(\frac{\dot{M}_2}{M_2}\right).$$

Therefore, the total angular momentum loss of the system is given by

$$\frac{\dot{J}_{orb}}{J_{orb}} = \frac{\dot{J}_{mb}}{J_{orb}} + \eta \left(\frac{M}{M_1}\right)^{1/2} \left(\frac{R_{circ}}{a}\right)^{1/2} \left(\frac{\dot{M}_2}{M_2}\right). \qquad (2.37)$$

From equations (2.13) and (2.37) it can be shown that

$$\frac{\dot{J}_{mb}}{J_{orb}} + \eta \left(\frac{M}{M_1}\right)^{1/2} \left(\frac{R_{circ}}{a}\right)^{1/2} \left(\frac{\dot{M}_2}{M_2}\right) = \frac{\dot{M}_1}{M_1} + \frac{\dot{M}_2}{M_2} + \frac{1}{2}\left(\frac{\dot{a}}{a} - \frac{\dot{M}}{M}\right)$$

$$\Rightarrow 2\frac{\dot{J}_{mb}}{J_{orb}} + 2\eta \left(\frac{M}{M_1}\right)^{1/2} \left(\frac{R_{circ}}{a}\right)^{1/2} \left(\frac{\dot{M}_2}{M_2}\right) - 2\frac{\dot{M}_1}{M_1} - 2\frac{\dot{M}_2}{M_2} + \frac{\dot{M}}{M} = \frac{\dot{a}}{a}.$$

For the case where $\dot{a}/a \geq 0$ gives

$$\frac{\dot{J}_{mb}}{J_{orb}} + \eta \left(\frac{M}{M_1}\right)^{1/2} \left(\frac{R_{circ}}{a}\right)^{1/2} \left(\frac{\dot{M}_2}{M_2}\right) - \frac{\dot{M}_1}{M_1} - \frac{\dot{M}_2}{M_2} + \frac{1}{2}\frac{\dot{M}}{M} \geq 0. \qquad (2.38)$$

Substituting for $\dot{M}_1$ from equation (2.31), equation (2.38) can be expressed as

$$\frac{\dot{J}_{mb}}{J_{orb}} - \eta \left(\frac{M}{M_1}\right)^{1/2} \left(\frac{R_{circ}}{a}\right)^{1/2} \left(\frac{-\dot{M}_2}{M}\right) - \frac{(1-\beta)\dot{M}_2}{M_1} - \frac{\dot{M}_2}{M_2} + \frac{1}{2}\frac{\beta \dot{M}_2}{M} \geq 0$$

$$-\frac{\dot{J}_{mb}}{J_{orb}} \le \left(\frac{-\dot{M}_2}{M_2}\right)\left[1-(1-\beta)\frac{M_2}{M_1}-\frac{\beta}{2}\left(\frac{M_2}{M}\right)-\eta\left(\frac{M}{M_1}\right)^{1/2}\left(\frac{R_{circ}}{a}\right)^{1/2}\right]$$

$$\Rightarrow\ -\frac{\dot{M}_2}{M_2} \ge \frac{-\dot{J}_{mb}/J_{orb}}{\left[1-(1-\beta)\frac{M_2}{M_1}-\frac{\beta}{2}\left(\frac{M_2}{M}\right)-\eta\left(\frac{M}{M_1}\right)^{1/2}\left(\frac{R_{circ}}{a}\right)^{1/2}\right]}. \qquad (2.39)$$

This equation allows constraining the mass transfer from the secondary star driven by magnetic braking of the secondary star; and also the evaluation of the conditions for stable mass transfer for various scenarios in a binary system. The condition for stable mass transfer in converging ($\dot{a}/a < 0$) and diverging ($\dot{a}/a > 0$) binaries can be determined for systems following a conservative and non-conservative evolution. In the case of binaries following a conservative evolution, i.e. white dwarf accreting all the mass and angular momentum fed to it from the secondary, i.e. $\beta = 0; \eta = 1$, the condition for stable mass transfer for a converging and diverging evolutions are respectively

$$\frac{\dot{a}}{a} < 0\ \Rightarrow\ -\frac{\dot{M}_2}{M_2} \le \frac{-\dot{J}_{mb}/J_{orb}}{\left[1-\frac{M_2}{M_1}-\left(\frac{M}{M_1}\right)^{1/2}\left(\frac{R_{circ}}{a}\right)^{1/2}\right]} \qquad (2.40a)$$

$$\frac{\dot{a}}{a} > 0\ \Rightarrow -\frac{\dot{M}_2}{M_2} \ge \frac{-\dot{J}_{mb}/J_{orb}}{\left[1-\frac{M_2}{M_1}-\left(\frac{M}{M_1}\right)^{1/2}\left(\frac{R_{circ}}{a}\right)^{1/2}\right]} \qquad (2.40b)$$

A typical example of a non-conservative evolution is a system in a propeller phase of its evolution. An example is the nova-like variable AE Aquarii (AE Aqr) which is propelling the full load of mass transfer and angular momentum from the binary, i.e. $\beta = 1; \eta = 1$. The condition for stable mass transfer in this case requires

$$\frac{\dot{a}}{a} < 0\ \Rightarrow\ -\frac{\dot{M}_2}{M_2} \le \frac{-\dot{J}_{mb}/J_{orb}}{\left[1-\frac{1}{2}\frac{M_2}{M}-\left(\frac{M}{M_1}\right)^{1/2}\left(\frac{R_{circ}}{a}\right)^{1/2}\right]} \qquad (2.41a)$$

$$\frac{\dot{a}}{a} > 0 \Rightarrow -\frac{\dot{M}_2}{M_2} \geq \frac{-\dot{J}_{mb}/J_{orb}}{\left[1-\frac{1}{2}\frac{M_2}{M}-\left(\frac{M}{M_1}\right)^{1/2}\left(\frac{R_{circ}}{a}\right)^{1/2}\right]}. \qquad (2.41b)$$

For the sake of comparison the nova-like variable AE Aqr has been selected to illustrate the condition for stable mass transfer for a source that is currently in the propeller phase, i.e. $\beta = \eta = 1$ (Meintjes & Venter 2003);

$$M_1 \cong 0.9M_\Theta, \quad M_2 \cong 0.6M_\Theta, \quad \frac{M_2}{M_1} = 0.6667, \quad P_{orb} = 9.88h$$

The binary separation a can then be expressed in the form (e.g. Frank, King & Raine 1992, p.47)

$$a = 1.845\times10^{11}\left(\frac{M_1}{0.9M_\Theta}\right)^{1/3}\left(\frac{P_{orb}}{9.88h}\right)^{2/3} \text{ cm.}$$

Substituting for a in equation (2.36) gives

$$b_1 = 9.962\times10^{10}\left(\frac{M_1}{0.9M_\Theta}\right)^{1/3}\left(\frac{P_{orb}}{9.88h}\right)^{2/3} \text{ cm.}$$

Substituting for b_1 and a in equation (2.34) gives

$$R_{circ} = (1+0.6667)\left(\frac{9.962\times10^{10}}{1.845\times10^{11}}\right)^3\left(9.962\times10^{10}\right) \text{ cm}$$

$$\Rightarrow \quad R_{circ} = 2.61\times10^{10} \text{ cm.}$$

Therefore $$\frac{R_{circ}}{a} = \frac{2.61\times10^{10}}{1.845\times10^{11}} = 0.1415.$$

For the propeller source, i.e. $\beta = \eta = 1$, and the parameters applicable to AE Aqr gives

$$\frac{\dot{J}_{mb}}{J_{orb}} > \left[1-\frac{1}{2}\left(\frac{M_2}{M_1}\right)-\left(\frac{M}{M_1}\right)^{1/2}\left(\frac{R_{circ}}{a}\right)^{1/2}\right]\left(\frac{\dot{M}_2}{M_2}\right)$$

$$\frac{\dot{J}_{mb}}{J_{orb}} > \frac{0.3144\left(2\times10^{18}\right)}{0.6\times2\times10^{33}}\left(\frac{\dot{M}_2}{2\times10^{18}}\right)\left(\frac{M_2}{0.6M_\Theta}\right) \text{ s}^{-1}$$

$$\Rightarrow \frac{\dot{J}_{mb}}{J_{orb}} > 5.24\times10^{-16}\left(\frac{\dot{M}_2}{2\times10^{18}}\right)\left(\frac{M_2}{0.6M_\Theta}\right)\ \text{s}^{-1}. \qquad (2.42)$$

Equation (2.42) gives the required rate of angular momentum drain through magnetic braking that will drive a stable mass transfer in a propeller source like AE Aqr. In a similar fashion, equations (2.40a), (2.40b) and (2.41a), (2.41b) can be applied to constrain the required magnetic braking able to drive stable mass transfer for all systems, i.e. conservative and non-conservative. Most of the review in the rest of this chapter is taken from Campbell (1997)

2.2 Stellar wind

This discussion has been aimed at providing a theoretical framework used to constrain the angular momentum drained from a system through magnetic braking that will enable a stable mass transfer from the secondary to the primary. Since the main focus of this study is the investigation of magnetic profile of the secondary star on mass transfer and secular evolution, magnetic braking from the magnetic wind of a secondary star will be implemented to constrain the angular momentum under consideration and hence the required surface field for stable mass transfer. Therefore a detailed discussion of the process of magnetic braking through a magnetized stellar wind will now be presented.

Parker (1963) formulated the basic wind theory for single stars. A hot stellar corona cannot be contained by the pressure of the surrounding interstellar medium, and thus flows away from the star. This leads to mass loss driven by a thermal pressure gradient and centrifugal acceleration (e.g. Campbell 1997, p.251). A small coronal mass flux and a moderate magnetic field result in the highly conducting material being channelled along field lines which are slightly distorted by the flow near the star. When the kinetic energy density of the outflowing material becomes comparable to the poloidal magnetic energy density, the distortion of the field becomes large (e.g. Campbell 1997, p.251). Equipartition of magnetic and fluid energy density occurs at the Alfvén surface (see Figure 6) where the wind speed approaches the so-called Alfvén speed, i.e.

$$v_A = \left(\frac{B_p^2}{\mu_0 \rho} \right)^{1/2} .$$

Here B_p represents the poloidal magnetic field, μ_0 the permeability and ρ the plasma density. If the wind speed becomes a significant fraction of v_A before a magnetic coronal loop starts to close, the field is dragged out with the flow and these open fields form the so-called "wind zone". The closed coronal loops near the stellar surface trap hot gas, which is not able to overcome the magnetic pressure, constituting the so-called "dead zone" (Mestel & Spruit 1987; e.g. Campbell 1997, p.260). A strong stellar magnetic field keeps a wind corotating with the star through magnetic torques out to large distances, carrying away more angular momentum per unit mass than in a non magnetic wind, in which the gas conserves its angular momentum (Schatzman 1962). This occurs in the wind zone.

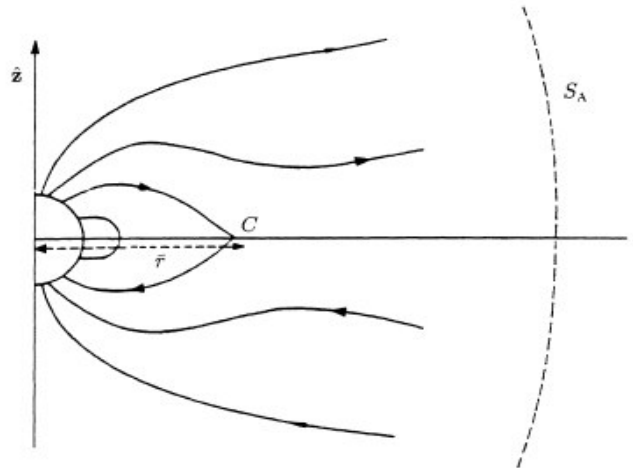

Figure 6. Schematic magnetic field model. (Adopted from e.g. Campbell 1997, p.260). In this figure $\bar{r}$ represents the equatorial boundary of the dead zone, C the cusp and S_A the Alfvén surface.

The structure of a magnetically channelled wind in a single star may not be the same as that in a binary star. In the case of a binary system, the presence of a primary star would mean that even if the secondary star had a magnetic field symmetric about its rotation axis, the wind would not be axisymmetric due to the azimuthal dependence of the total gravitational field. Despite this, the fundamental effect of a magnetically influenced wind

from a binary star and a single star is the removal of stellar angular momentum (e.g. Campbell 1997, p.268). The secondary star in a binary system is kept close to synchronism by tidal torques, which result in a continuous removal of orbital angular momentum with consequent mass transfer; which has to be discussed in more detail.

2.2.1 Mass transfer and angular momentum loss by stellar wind

The focus of this study is primarily on the evolution of CVs where the binary mass remains constant, i.e. conserving binary mass ($\dot{M} = 0$). This is to avoid having to deal with guessing the amount of angular momentum drained from the system as a result of propeller induced mass loss. To restrict the number of "unknowns" to a minimum, only conservative systems are considered. However, since most of the MCVs are disc accretors, for which $\beta \approx 0$ applies to a large extend, this selection is appropriate.

For a conservative evolution, the total binary mass remains constant and the rate of change of the Roche lobe radius of the secondary star is given by equation (2.18) where ($-\dot{M}_2$) is the mass loss rate of the secondary star due to Roche lobe overflow. The orbital evolution timescale, given by

$$\tau_{ev} = \frac{J_{orb}}{\dot{J}_{orb}}, \tag{2.43}$$

is comparable to the mass transfer timescale, given by

$$\tau_{\dot{M}_2} = \frac{M_2}{\left|\dot{M}_2\right|}. \tag{2.44}$$

For typical mass transfer rate and secondary star mass (e.g. $\dot{M}_2 \sim 10^{17}$ g s^{-1}, $M_2 \sim 0.6 M_\odot$), $\tau_{\dot{M}_2} \sim 10^{16}$ s. For a constant $M = M_1 + M_2$ over the binary life time

$$\left|\dot{M}_w\right| << \left|\dot{M}_2\right|, \tag{2.45}$$

where $\dot{M}_w$ is the wind mass loss rate. A lower main sequence secondary star, in thermal equilibrium, satisfies

$$\frac{R_2}{R_\Theta} = q\left(\frac{M_2}{M_\Theta}\right), \tag{2.46}$$

with q = 1.1 (e.g. Campbell 1997, p.269) where R_Θ represents the solar radius. For the secondary star to continuously transfer mass to the primary star, $R_{L,2}$ must shrink as fast as R_2 to keep matter in contact with the L_1 region (e.g. Frank, King & Raine 1992). From equation (2.18) it is noted that

$$\frac{\dot{R}_{L,2}}{R_{L,2}} < 0 \text{ if } \frac{5}{6} - \frac{M_2}{M_1} \geq 0 \text{ and } \frac{\dot{J}_{orb}}{J_{orb}} < 0 .$$

It is required that $|\dot{J}_{orb}|/J_{orb}$ be sufficiently large to yield $\dot{R}_{L,2}/R_{L,2} < 0$ and $|\dot{R}_{L,2}| \geq |\dot{R}_2|$. The secondary star will remain in thermal equilibrium as long as $\tau_{\dot{M}_2} >> \tau_{th}$, where τ_{th} is the thermal adjustment timescale.

Loss of orbital angular momentum is caused by magnetic braking in conjunction with strong tidal coupling and gravitational radiation. In long period binaries, gravitational radiation will not be a dominant mechanism (e.g. Campbell 1997, p.270). Magnetic braking theory can be used to obtain expressions for $\dot{M}_2$ (L_1 overflow) and the rate of loss of stellar angular momentum (e.g. Campbell 1997, p.268 - 278). This will be discussed briefly in the following discussion.

For a secondary star being kept close to orbital corotation by tidal forces, the stellar angular velocity Ω_2 is essentially the same as Ω_{orb} (orbital angular velocity). Therefore

$$\Omega_2^2 = \Omega_{orb}^2 = \frac{GM}{a^3} . \tag{2.47}$$

It can be shown (Mestel & Spruit 1987; e.g. Campbell 1997, p.270) that the stellar angular momentum loss rate is given by

$$-\dot{J}_{mb} = \frac{\Phi^2 \Omega_2}{6\pi\mu_0 v_A}, \tag{2.48}$$

where $\Phi = 4\pi \bar{r}^2 \bar{B}$ represents the magnetic flux cutting through a surface of radius $\bar{r}$. It can also be shown (Mestel & Spruit 1987; e.g. Campbell 1997, p.270) that the magnetic flux cutting through the stellar surface in the wind zone (see Figure 6) can be expressed as

$$\Phi = 2\pi R_2^2 \left(\frac{R_2}{\bar{r}} \right) B_0 . \tag{2.49}$$

In this expression the magnetic field is assumed to be dipolar, i.e. $\bar{B} = (B_0/2)(R_2/\bar{r})^3$ were $\bar{r}$ represents the radius which corresponds to the equatorial boundary of the dead zone (Figure 6). The Alfvén surface occurs in the radial field region of radius r_A, and therefore the magnitude of the wind mass loss rate is given by

$$\left| \dot{M}_w \right| = 4\pi r_A^2 \rho_A v_A , \tag{2.50}$$

where ρ_A is the wind density within the Alfvén surface. Over the Alfvén surface bounding the wind zone, it can be shown (e.g. Campbell 1997, p.264) that

$$-\dot{J}_{mb} = \frac{2}{3} \left(4\pi \rho_A v_A r_A^2 \right) \Omega_2 r_A^2 . \tag{2.51}$$

Substituting equation (2.50) into (2.51) gives

$$-\dot{J}_{mb} = \frac{2}{3} \left| \dot{M}_w \right| \Omega_2 r_A^2 . \tag{2.52}$$

From equations (2.48) and (2.52) it can be shown that the Alfvén surface is given by

$$\frac{2}{3} | \dot{M}_w | \Omega_2 r_A^2 = \frac{\Phi^2 \Omega_2}{6\pi\mu_0 v_A}$$

$$\Rightarrow \quad r_A^2 = \frac{\Phi^2}{4\pi\mu_0 \left| \dot{M}_w \right| v_A} . \tag{2.53}$$

In the fast rotator limit, applicable to most short period binaries (e.g. Campbell 1997, p.270) the Alfvén speed can be approximated by

$$v_A \approx \frac{1}{2} r_A \Omega_2 . \tag{2.54}$$

Substituting equation (2.54) in equation (2.53) gives

$$r_A^2 = \frac{\Phi^2}{4\pi\mu_0 \left|\dot{M}_w\right| (1/2) r_A \Omega_2}$$

$$\Rightarrow \quad r_A^2 = \frac{\Phi^{4/3}}{(2\pi\mu_0)^{2/3} \left|\dot{M}_w\right|^{2/3} \Omega_2^{2/3}}. \tag{2.55}$$

Substituting for r_A from equation (2.55) into equation (2.52) gives

$$\dot{J}_{mb} = -\frac{2}{3}\left|\dot{M}_w\right| \Omega_2 \frac{\Phi^{4/3}}{(2\pi\mu_0)^{2/3} \left|\dot{M}_w\right|^{2/3} \Omega_2^{2/3}}$$

$$\Rightarrow \quad \dot{J}_{mb} = -\frac{2}{3}\frac{1}{(2\pi\mu_0)^{2/3}} \left|\dot{M}_w\right|^{1/3} \Omega_2^{1/3} \Phi^{4/3}. \tag{2.56}$$

Substituting for Φ from equation (2.49) into equation (2.56), it can be shown that

$$\dot{J}_{mb} = -\frac{2}{3}\frac{1}{(2\pi\mu_0)^{2/3}} \dot{M}_w^{1/3} \Omega_2^{1/3} \left(2\pi R_2^2\right)^{4/3} \left(\frac{R_2}{\bar{r}}\right)^{4/3} B_0^{4/3}$$

$$\Rightarrow \quad \dot{J}_{mb} = -\frac{2}{3}\left(\frac{2\pi}{\mu_0}\right)^{2/3} B_\Theta^{4/3} \dot{M}_\Theta^{1/3} \left(\frac{\dot{M}_w}{\dot{M}_\Theta}\right)^{1/3} \left(\frac{B_0}{B_\Theta}\right)^{4/3} \left(\frac{R_2}{\bar{r}}\right)^{4/3} \Omega_2^{1/3} R_2^{8/3}, \tag{2.57}$$

where B_Θ is the coronal base value of the sun's magnetic field and $\dot{M}_\Theta$ the solar wind mass loss rate. For a more complicated field than dipolar, B_Θ and B_0 would essentially be mean surface values.

The rate of angular momentum loss ($\dot{J}_{mb}/J_{orb}$) can be derived by evaluating the orbital angular momentum of a lobe-filling secondary star. Substituting for the binary separation a from equation (2.47) into equation (2.15) gives

$$\frac{M}{M_2}\left(\frac{R_{L,2}^3}{GM/\Omega_2^2}\right) = 0.1$$

$$\Rightarrow\ R_{L,2}^2\Omega_2^2 = 0.1G\left(\frac{M_2}{R_{L,2}}\right). \tag{2.58}$$

A lobe-filling secondary star has $R_2 = R_{L,2}$ and therefore equation (2.46) can be re-arranged in the form,

$$\frac{M_2}{R_{L,2}} = \frac{1}{q}\left(\frac{M_\Theta}{R_\Theta}\right) = \text{constant}. \tag{2.59}$$

From equation (2.58), $R_{L,2}^2\Omega_2^2$ is also a constant as the orbit evolves. Substituting for $R_{L,2}$ from equation (2.59) into equation (2.15) gives

$$\frac{M}{M_2}\left(\frac{R_\Theta q}{a}\frac{M_2}{M_\Theta}\right)^3 = 0.1$$

and

$$a = 10^{1/3}\left(\frac{M}{M_2}\right)^{1/3}\left(\frac{M_2}{M_\Theta}\right)R_\Theta q\,.$$

Substituting for a in equation (2.12) the expression for orbital angular momentum can be obtained as

$$J_{orb} = M_1M_2\left[\frac{G}{M}10^{1/3}\left(\frac{M}{M_2}\right)^{1/3}\left(\frac{M_2}{M_\Theta}\right)R_\Theta q\right]^{1/2}$$

$$\Rightarrow\ J_{orb} = \left(\frac{GR_\Theta}{M_\Theta}\right)^{1/2}\frac{M_1M_2^{4/3}}{M^{1/3}}q^{1/2}10^{1/6}. \tag{2.60}$$

This allows the determination of $\dot{J}_{mb}/J_{orb}$ for various inferred dynamo models responsible for the generation of the stellar field. The expressions for mass loss rate by the secondary star for various dynamo laws can now be derive. For consistency, $|\dot{M}_w| << |\dot{M}_2|$ and thermal equilibrium holds for $\tau_{th} << M_2/|\dot{M}_2|$. Therefore the effect of stellar wind mass loss rate and thermal adjustment timescale will first be discussed.

2.2.2 Stellar wind mass loss rate

The Virial theorem gives an approximate scaling for characteristic temperature and densities in a star according to (e.g. Campbell 1997, p.271)

$$T \propto \frac{M_2}{R_2} \text{ and } \rho \propto \frac{M_2}{R_2^3}.$$

If the stellar corona also follows these scaling, then the sound speed c_d in the dead zone can be written as

$$c_d = \left(\frac{P}{\rho}\right)^{1/2}$$

$$\Rightarrow \quad c_d = \left(\frac{kT}{\mu m_H}\right)^{1/2},$$

where $P = \rho kT/\mu m_H$. Therefore this gives

$$c_d \propto T^{1/2} \propto \left(\frac{M_2}{R_2}\right)^{1/2}, \tag{2.61}$$

and from equation (2.58), for a lobe-filling secondary star the coronal base density $(\rho_0)_d$ in the dead zone scales as

$$(\rho_0)_d \propto \frac{M_2}{R_2^3} \propto \Omega_2^2. \tag{2.62}$$

If the magnetic field is assumed to be dynamo generated, the pole strength value B_0 is related to Ω_2 by the dynamo law (e.g. Campbell 1997, p.274)

$$B_0 = B_\Theta \left(\frac{\Omega_2}{\Omega_\Theta}\right)^n, \tag{2.63}$$

with $1 \le n \le 2$, and the magnetic flux in the dead zone is given by

$$\xi_d = \frac{B_0^2}{2\mu_0 (\rho_0)_d c_d^2}. \tag{2.64}$$

From equations (2.62), (2.63), and (2.64) it can be shown that

$$\xi_d^{1/6} = \left(\frac{B_0^2}{2\mu(\rho_0)_d c_d^2} \right)^{1/6} \propto \Omega_2^{\frac{2n-3}{6}},$$

and it is noted that $\xi_d^{1/6}$ is weakly dependent on Ω_2. Since the radial field region begins at $r = \bar{r}$ (outside the dead zone), the wind mass loss rate is given by

$$\dot{M}_w = -4\pi \bar{r}^2 \bar{\rho} \bar{v}. \tag{2.65}$$

Conservation of mass and flux along a poloidal flux tube yields

$$\frac{mass\ flux}{magnetic\ flux} = \frac{\rho v}{B} = \text{constant}.$$

Conservation of mass flux between surface (near surface) and dead zone gives

$$\frac{\rho_0 v_0}{B_0} = \frac{\bar{\rho} \bar{v}}{\bar{B}}$$

$$\Rightarrow \quad \bar{\rho} \bar{v} = \rho_0 v_0 \left(\frac{\bar{B}}{B_0} \right).$$

Since

$$\bar{B} = \frac{1}{2} B_0 \left(\frac{R_2}{\bar{r}} \right)^3,$$

the average mass flux is

$$\bar{\rho} \bar{v} = \frac{\rho_0 v_0}{2} \left(\frac{R_2}{\bar{r}} \right)^3, \tag{2.66}$$

where v_0 is the coronal base flow speed and ρ_0 the wind density at the coronal base. Substituting equation (2.66) into equation (2.65) gives

$$\dot{M}_w = -4\pi \bar{r}^2 \frac{\rho_0 v_0}{2} \left(\frac{R_2}{\bar{r}} \right)^3$$

$$\dot{M}_w = -2\pi \rho_0 v_0 \left(\frac{R_2}{\bar{r}} \right) R_2^2. \tag{2.67}$$

The wind speed at the coronal base is taken as (e.g. Campbell 1997, p.272)

$$v_0 = 0.15 c_w, \tag{2.68}$$

where c_w is the sound speed in the wind zone.

For $(R_2/\bar{r}) \approx$ constant, an expression for the wind mass loss rate can be obtained as follows:

From equations (2.61) and (2.68) it follows that,

$$v_0 \propto c_w \propto \left(\frac{M_2}{R_2}\right)^{1/2} \text{ and } \rho_0 \propto \left(\frac{M_2}{R_2^3}\right)\Omega_2 .$$

Therefore, from equation (2.67), for $(R_2/\bar{r}) \approx$ constant, it is seen that

$$|\dot{M}_w| \propto \rho_0 v_0 R_2^2$$

$$|\dot{M}_w| \propto \left(\frac{M_2}{R_2^3}\right)\Omega_2 \left(\frac{M_2}{R_2}\right)^{1/2} R_2^2$$

$$\Rightarrow \quad |\dot{M}_w| \propto \left(\frac{M_2}{R_2}\right)^{3/2} \Omega_2 . \tag{2.69}$$

Since the ratio $(M_2/R_2) = (M_\Theta/R_\Theta)$ = a constant, $\dot{M}_w$ evolves with the orbit as $\dot{M}_w = Z\Omega_2$ and also $\dot{M}_\Theta = Z\Omega_\Theta$, where Z is a constant.

Hence

$$\frac{\dot{M}_w}{\dot{M}_\Theta} = \frac{Z\Omega_2}{Z\Omega_\Theta} = \frac{\Omega_2}{\Omega_\Theta} . \tag{2.70}$$

From equation (2.64), the wind zone equivalent of ξ_d is given as

$$\xi_w = \frac{B_0^2}{2\mu_0 (\rho_0)_w c_w^2} . \tag{2.71}$$

This represents the ratio of the magnetic energy density to the thermal wind pressure at the coronal base. From equation (2.71)

$$c_w = \frac{B_0^2}{2\mu_0 (\rho_0)_w \xi_w c_w} . \tag{2.72}$$

From equation (2.67), an equivalent for $\dot{M}_\Theta$ is given as

$$\dot{M}_\Theta = -2\pi (\rho_0)_{w,\Theta} v_{0,\Theta} \left(\frac{R_2}{\bar{r}}\right) R_\Theta^2 . \tag{2.73}$$

Substituting equations (2.68) and (2.72) in equation (2.73), gives

$$\dot{M}_{\Theta} = -2\pi(\rho_0)_{w,\Theta}(0.15c_{w,\Theta})\left(\frac{R_2}{\bar{r}}\right)R_{\Theta}^2$$

$$\dot{M}_{\Theta} = -2\pi\left(\frac{R_2}{r}\right)R_{\Theta}^2(\rho_0)_{w,\Theta}(0.15)\frac{B_{\Theta}^2}{2\mu_0(\rho_0)_{w,\Theta}\xi_{w,\Theta}c_{w,\Theta}}$$

$$\Rightarrow \quad \dot{M}_{\Theta} = \left(-\frac{0.15\pi}{\mu_0}\right)\left(\frac{R_{\Theta}^2 B_{\Theta}^2}{c_{w,\Theta}\xi_{w,\Theta}}\right)\left(\frac{R_2}{\bar{r}}\right). \tag{2.74)}$$

Substituting for $\dot{M}_{\Theta}$ from equation (2.74) into (2.70) gives

$$\dot{M}_w = \left(\frac{\Omega_2}{\Omega_{\Theta}}\right)\dot{M}_{\Theta}$$

$$\Rightarrow \quad \dot{M}_w = \left(\frac{\Omega_2}{\Omega_{\Theta}}\right)\left(-\frac{0.15\pi}{\mu_0}\right)\left(\frac{R_{\Theta}^2 B_{\Theta}^2}{c_{w,\Theta}\xi_{w,\Theta}}\right)\left(\frac{R_2}{\bar{r}}\right). \tag{2.75}$$

Using equations (2.15) and (2.47), Ω_2 can be expressed in the form

$$\Omega_2 = \left(\frac{GM}{a^3}\right)^{1/2}$$

$$\Omega_2 = \left[\left(\frac{G}{a^3}\right)\left(\frac{M}{M_{\Theta}}\right)M_{\Theta}\right]^{1/2}$$

$$\Omega_2 = \left[\frac{0.1G(M_2/M_{\Theta})M_{\Theta}}{R_2^3}\right]^{1/2}$$

$$\Rightarrow \quad \Omega_2 = \left[\left(\frac{0.1G}{R_2^3}\right)\left(\frac{M_2}{M_{\Theta}}\right)M_{\Theta}\right]^{1/2}. \tag{2.76}$$

Substituting for R_2 from equation (2.46) into equation (2.76) gives

$$\Omega_2 = \frac{(0.1)^{1/2}}{q^{3/2}}\frac{G^{1/2}R_{\Theta}^{-3/2}M_{\Theta}^{1/2}}{(M_2/M_{\Theta})}$$

$$\Omega_2 = \frac{(0.1)^{1/2}}{q^{3/2}}G^{1/2}\frac{(M/M_{\Theta})}{(M_2/M_{\Theta})}\frac{(R_{\Theta}^{3/2}M_{\Theta}^{1/2})}{(M/M_{\Theta})}$$

$$\Omega_2 = \frac{(0.1)^{1/2}}{q^{3/2}}G^{1/2}\left(\frac{M}{M_2}\right)\left(\frac{M_{\Theta}}{M}\right)R_{\Theta}^{-3/2}M_{\Theta}^{1/2}$$

$$\Rightarrow \quad \Omega_2 = \frac{(0.1)^{1/2}}{q^{3/2}} G^{1/2} \left(\frac{1}{\mu}\right)\left(\frac{M_\Theta}{M}\right) R_\Theta^{-3/2} M_\Theta^{1/2}, \tag{2.77}$$

where $\mu = M_2/M$. From equation (2.76), it follows that

$$\Omega_\Theta = \left(\frac{0.1GM_\Theta}{R_\Theta^3}\right)^{1/2}. \tag{2.78}$$

Using equations (2.77) and (2.78) gives

$$\frac{\Omega_2}{\Omega_\Theta} = \frac{\left((0.1)^{1/2}/q^{3/2}\right) G^{1/2} (1/\mu)(M_\Theta/M) R_\Theta^{-3/2} M_\Theta^{1/2}}{\left(0.1GM_\Theta/R_\Theta^2\right)^{1/2}}$$

$$\Rightarrow \quad \frac{\Omega_2}{\Omega_\Theta} = \frac{1}{q^{3/2}} \frac{1}{\mu}\left(\frac{M_\Theta}{M}\right). \tag{2.79}$$

Substituting equation (2.79) into equation (2.75), it can be shown that

$$\dot{M}_w = \left(-\frac{0.15\pi}{\mu_0}\right)\left(\frac{R_\Theta^2 B_\Theta^2}{c_{w,\Theta}\xi_{w,\Theta}}\right)\left(\frac{R_2}{\bar{r}}\right)\frac{1}{q^{3/2}}\frac{1}{\mu}\left(\frac{M_\Theta}{M}\right) \text{ kg s}^{-1}.$$

The solar constants are approximately given by (e.g. Campbell 1997, p.274)

$\Omega_\Theta = 2.5\times10^{-6}$ s^{-1}, $B_\Theta = 2$ Gauss, $R_\Theta = 6.96\times10^{10}$ cm, $G = 6.67\times10^{-8}$ cm^3 g^{-1} s^{-1}

$c_w = 1.2\times10^7$ cm s^{-1}, $M_\Theta = 2\times10^{33}$ g and $c_{w,\Theta} \approx 10^6$ cm s^{-1}

Substituting for these constants gives

$$\dot{M}_w \cong -\frac{2\times10^{-11}}{q^{3/2}} \frac{1}{\xi_{w,\Theta}}\left(\frac{B_\Theta}{Gauss}\right)^2\left(\frac{R_2}{\bar{r}}\right)\left(\frac{1}{\mu}\right)\left(\frac{M_\Theta}{M}\right) M_\Theta \, yr^{-1} \tag{2.80}$$

$$\Rightarrow \quad \dot{M}_w \cong -\frac{1.3\times10^{15}}{q^{3/2}} \frac{1}{\xi_{w,\Theta}}\left(\frac{B_\Theta}{Gauss}\right)^2\left(\frac{R_2}{\bar{r}}\right)\left(\frac{1}{\mu}\right)\left(\frac{M_\Theta}{M}\right) g\, s^{-1}. \tag{2.81}$$

2.2.3 Thermal timescale

The Kelvin timescale for thermal adjustment of the secondary star is given by

$$\tau_{th} = \frac{E_{th}}{L_2} \tag{2.82}$$

where E_{th} is the total thermal energy and L_2 the surface luminosity of the secondary star. From the Virial theorem, the condition for hydrostatic equilibrium requires

$$E_{th} = -\frac{1}{2} E_g ,$$

where E_g is the gravitational potential energy. The gravitational potential energy of a polytrope of index n is given by (Kippenhahn & Weigert 1990)

$$E_g = \left(\frac{3}{5-n}\right)\left(\frac{M^2 G}{R}\right).$$

For ordinary main sequence star, $n = 3$ (King 1988) and therefore

$$E_g = \left(\frac{3}{2}\right)\left(\frac{M^2 G}{R}\right). \tag{2.83}$$

Since the contributions of rotational and magnetic energies are negligible E_{th} can be expressed as

$$E_{th} = \left(-\frac{3}{4}\right)\left(\frac{GM_2^2}{R_2}\right). \tag{2.84}$$

From the approximate main-sequence mass-luminosity relation (e.g. Campbell 1997, p.274)

$$L_2 = \left(\frac{M_2}{M_\Theta}\right)^5 L_\Theta . \tag{2.85}$$

Using equations (2.46) and (2.85), equation (2.82) can be expressed after simplification as

$$\tau_{th} = \frac{3}{4q}\frac{GM_\Theta^2}{L_\Theta R_\Theta}\left(\frac{M_\Theta}{M_2}\right)^4$$

$$\tau_{th} = \frac{3}{4q}\frac{GM_\Theta^2}{L_\Theta R_\Theta}\left(\frac{M_\Theta}{M}\right)^4\left(\frac{M}{M_2}\right)^4$$

$$\Rightarrow \quad \tau_{th} = \frac{3}{4q}\frac{GM_\Theta^2}{L_\Theta R_\Theta}\left(\frac{M_\Theta}{M}\right)^4\left(\frac{1}{\mu}\right)^4 .$$

Substituting for the constants and taking, $L_\Theta = 3.86\times10^{33}$ erg s^{-1}, $M_\Theta = 2\times10^{33}$ g gives

$$\tau_{th} = \frac{7.45\times10^{14}}{q}\left(\frac{M_\Theta}{M}\right)^4\left(\frac{1}{\mu}\right)^4 s$$

$$\Rightarrow \quad \tau_{th} = \frac{2.3\times10^{7}}{q}\left(\frac{M_{\Theta}}{M}\right)^{4}\left(\frac{1}{\mu}\right)^{4} \text{ yr.} \tag{2.86}$$

This discussion has been included aiming at illustrating the preservation of the condition $\tau_{th} << M_2 \Big/ \dot{M}_2$, $\tau_{\frac{\cdot}{M_2}} \sim 10^{16}\, s$ (e.g. p.37) required to keep the star in thermal equilibrium during the mass transfer process. A brief discussion of the inferred dynamo laws responsible for stellar magnetic field production in stars, and their influence on mass transfer via magnetic braking, will now be presented.

2.3 Mass transfer rates via magnetic braking

2.3.1 Linear dynamo law

From equation (2.63), the linear dynamo law (n = 1) is given by

$$\frac{B_0}{B_{\Theta}} = \frac{\Omega_2}{\Omega_{\Theta}}. \tag{2.87}$$

Using equations (2.87) and (2.70) in equation (2.57) gives

$$\dot{J}_{mb} = -\frac{2}{3}\left(\frac{2\pi}{\mu_0}\right)^{2/3} B_{\Theta}^{4/3}\, \dot{M}_{\Theta}^{1/3}\left(\frac{\Omega_2}{\Omega_{\Theta}}\right)^{5/3}\left(\frac{R_2}{\bar{r}}\right)^{4/3} \Omega_2^{1/3} R_2^{8/3}$$

$$\Rightarrow \quad \dot{J}_{mb} = -\frac{2}{3}\left(\frac{2\pi}{\mu_0}\right)^{2/3}\left(\frac{R_2}{\bar{r}}\right)^{4/3} \frac{B_{\Theta}^{4/3}\, \dot{M}_{\Theta}^{1/3}\, \Omega_2^2 R_2^{8/3}}{\Omega_{\Theta}^{5/3}}. \tag{2.88}$$

From equations (2.20) and (2.60) the rate of loss of orbital angular momentum can be expressed as

$$\dot{J}_{orb} = \left(\frac{4}{3} - \frac{M_2}{M_1}\right)\left(\frac{\dot{M}_2}{M_2}\right)\left[\left(\frac{GR_{\Theta}}{M_{\Theta}}\right)^{1/2} \frac{M_1 M_2^{4/3}}{M^{1/3}} q^{1/2} 10^{1/6}\right]. \tag{2.89}$$

Since it has been assumed that the secondary star is kept close to orbital corotation by tidal forces, then $\dot{J}_{orb} = \dot{J}_{mb}$ and from equations (2.88) and (2.89) the following expression is obtained

$$-\frac{2}{3}\left(\frac{2\pi}{\mu_0}\right)^{2/3}\left(\frac{R_2}{\bar{r}}\right)^{4/3}\frac{B_\Theta^{4/3}\,\dot{M}_\Theta^{1/3}\,\Omega_2^2 R_2^{8/3}}{\Omega_\Theta^{5/3}}=\left(\frac{4}{3}-\frac{M_2}{M_1}\right)\left(\frac{\dot{M}_2}{M_2}\right)\left(\frac{GR_\Theta}{M_\Theta}\right)\frac{M_1 M_2^{4/3}}{M^{1/3}}q^{1/2}10^{1/6}$$

$$\Rightarrow\quad \frac{\dot{M}_2}{M_2}=\frac{(-3/2)(2\pi/\mu_0)^{2/3}(R_2/\bar{r})^{4/3}\left(\dot{M}_\Theta^{1/3}\,B_\Theta^{4/3}\Omega_2^2 R_2^{8/3}\Big/\Omega_\Theta^{5/3}\right)}{(4/3-M_2/M_1)(GR_\Theta/M_\Theta)^{1/2}(M_1 M_2^{4/3}/M^{1/3})q^{1/2}10^{1/6}}.$$

Substituting for R_2, Ω_2 and $\dot{M}_\Theta$ from equations (2.46), (2.58) and (2.74) respectively gives the equation

$$\dot{M}_2=\frac{(-3/2)(2\pi/\mu_0)^{2/3}(0.15\pi/\mu_0)^{1/3}(R_2/\bar{r})^{5/3}(0.1)G^{1/2}M_\Theta^{5/6}R_\Theta^{-1/6}B_\Theta^2 M_2^{1/3}M^{1/3}}{(4/3-M_2/M_1)M_1 q^{5/6}10^{1/6}c_{w,\Theta}^{1/3}\xi_{w,\Theta}^{1/3}\Omega_\Theta^{5/3}}.$$

But since

$$\left(\frac{4}{3}-\frac{M_2}{M_1}\right)M_1=\frac{M}{3}\left(4-\frac{7M_2}{M}\right)$$

$$\left(\frac{4}{3}-\frac{M_2}{M_1}\right)M_1=\frac{M}{3}(4-7\mu),$$

it reduces to

$$\dot{M}_2=-\frac{3(2/3)(2\pi/\mu_0)^{2/3}(0.15\pi/\mu_0)^{1/3}(0.1)G^{1/2}}{10^{1/6}c_{w,\Theta}^{1/3}\xi_{w,\Theta}^{1/3}\Omega_\Theta^{5/3}}\left(\frac{M_\Theta}{M}\right)^{1/3}\left(\frac{M_2}{M}\right)^{1/3}\left(\frac{R_2}{\bar{r}}\right)^{5/3}\frac{B_\Theta^2 M_\Theta^{1/2}R_\Theta^{-1/6}}{q^{5/6}(4-7\mu)}.$$

Substituting for the constants gives

$$\dot{M}_2=-\frac{7.8\times10^{-10}}{q^{5/6}\xi_{w,\Theta}^{1/3}}\left(\frac{R_2}{\bar{r}}\right)^{5/3}\left(\frac{B_\Theta}{Gauss}\right)^2\left(\frac{M_\Theta}{M}\right)^{1/3}\left(\frac{\mu^{1/3}}{4-7\mu}\right)M_\Theta\ \mathrm{yr}^{-1}. \qquad (2.90)$$

But M_Θ yr^{-1} = 6.3376 × 10^{25} g s^{-1}, and therefore

$$\dot{M}_2=-\frac{4.94\times10^{16}}{q^{5/6}\xi_{w,\Theta}^{1/3}}\left(\frac{R_2}{\bar{r}}\right)^{5/3}\left(\frac{B_\Theta}{Gauss}\right)^2\left(\frac{M_\Theta}{M}\right)^{1/3}\left(\frac{\mu^{1/3}}{4-7\mu}\right)\ \mathrm{g\ s^{-1}}.$$

Taking $\xi_{w,\Theta}=2\xi_{d,\Theta}$ for $\xi_{d,\Theta}=8$ and $\bar{r}/R_2=4$ (for a fast rotator) and $q=1.1$ (e.g. Campbell 1997, p.274 - 275) gives the expression

$$\dot{M}_2=-7.19\times10^{15}\left(\frac{M_\Theta}{M}\right)^{1/3}\left(\frac{M_2}{M}\right)^{1/3}\left(4-7\frac{M_2}{M}\right)^{-1}\ \mathrm{g\ s^{-1}}. \qquad (2.91)$$

The ratio of the wind mass loss rate to the mass transfer rate of the secondary can be estimated by taking the ratio of equation (2.80) to (2.90) which gives

$$\left|\frac{\dot{M}_w}{\dot{M}_2}\right| = \frac{2.56\times10^{-2}}{q^{2/3}\xi_{w,\Theta}^{2/3}}\left(\frac{R_2}{\bar{r}}\right)^{-2/3}\left(\frac{M_\Theta}{M}\right)^{2/3}\frac{(4-7\mu)}{\mu^{4/3}}. \tag{2.92}$$

The ratio of mass transfer timescale to the thermal timescale follows from equations (2.44), (2.86) and (2.90), i.e.

$$\frac{\tau_{\dot{M}_2}}{\tau_{th}} = \frac{M_2}{\frac{2.3\times10^7}{q}\left(\frac{M_\Theta}{M}\right)^4\left(\frac{1}{\mu}\right)^4\left|\dot{M}_2\right|} \tag{2.93}$$

$$\frac{\tau_{\dot{M}_2}}{\tau_{th}} = 55.7q^{11/6}\xi_{w,\Theta}^{1/3}\left(\frac{B_\Theta}{Gauss}\right)^{-2}\left(\frac{R_2}{\bar{r}}\right)^{-5/2}\left(\frac{M_\Theta}{M}\right)^{-16/3}\left(\frac{M_2}{M}\right)\frac{\mu^{11/3}}{(4-7\mu)^{-1}}$$

$$\Rightarrow \frac{\tau_{\dot{M}_2}}{\tau_{th}} = 55.7q^{11/6}\xi_{w,\Theta}^{1/3}\left(\frac{B_\Theta}{Gauss}\right)^{-2}\left(\frac{R_2}{\bar{r}}\right)^{-5/2}\left(\frac{M_\Theta}{M}\right)^{-16/3}(4-7\mu)\mu^{14/3}. \tag{2.94}$$

Taking $\xi_{w,\Theta} = 16$ (e.g. Campbell 1997, p.274 - 275) gives

$$\frac{\tau_{\dot{M}_2}}{\tau_{th}} = 140q^{11/6}\left(\frac{B_\Theta}{Gauss}\right)^{-2}\left(\frac{R_2}{\bar{r}}\right)^{-5/2}\left(\frac{M_\Theta}{M}\right)^{-16/3}(4-7\mu)\mu^{14/3}. \tag{2.95}$$

2.3.2 Inverse Rossby number law

The depth of a star's convective envelope increases as its mass decreases towards $\sim 0.3M_\Theta$ (e.g. Campbell 1997, p.276). At this mass, i.e. $0.3M_\Theta$, a star will be fully convective. This change may influence the value of B_0 in addition to the effect of a change in Ω_2. There is observational evidence that B_0 scales according to the inverse turbulent Rossby number (e.g. Campbell 1997, p.276)

$$R_T^{-1} \propto \tau_T\Omega_2,$$

where τ_T is the convective turnover timescale and is given by

$$\tau_T \propto \left(\frac{R_2^2M_2}{L_2}\right)^{1/3}.$$

In this case the following scaling is obtained

$$\frac{B_0}{B_\Theta} = \frac{\tau_T \Omega_2}{\tau_{T,\Theta} \Omega_\Theta}.$$

The main-sequence mass-luminosity relation, equation (2.85), therefore leads to

$$\frac{B_0}{B_\Theta} = \left(\frac{M_\Theta^4}{R_\Theta^2}\right)^{1/3} \left(\frac{R_2^2}{M_2^4}\right)^{1/3} \left(\frac{\Omega_2}{\Omega_\Theta}\right). \tag{2.96}$$

The rate of orbital angular momentum loss is obtained by substituting equations (2.70) and (2.96) into equation (2.57), which gives

$$\dot{J}_{mb} = -\frac{2}{3}\left(\frac{2\pi}{\mu_\Theta}\right)^{2/3} B_\Theta^{4/3} \dot{M}_\Theta^{1/3} \left(\frac{R_2}{\bar{r}}\right)^{4/3} \left[\left(\frac{M_\Theta^4}{R_\Theta^2}\right)^{1/3} \left(\frac{R_2^2}{M_2^4}\right)^{1/3} \left(\frac{\Omega_2}{\Omega_\Theta}\right)\right]^{4/3} \left(\frac{\Omega_2}{\Omega_\Theta}\right)^{1/3} R_2^{8/3} \Omega_2^{1/3}$$

$$\Rightarrow \quad \dot{J}_{mb} = -\frac{2}{3}\left(\frac{2\pi}{\mu_\Theta}\right)^{2/3} B_\Theta^{4/3} \dot{M}_\Theta^{1/3} \left(\frac{R_2}{\bar{r}}\right)^{4/3} \left(\frac{\Omega_2^2}{\Omega_\Theta^{5/3}}\right) \left(\frac{M_2}{M_\Theta}\right)^{-16/6} \left(\frac{R_2}{R_\Theta}\right)^{16/9} R_2^{16/9} R_\Theta^{8/9}.$$

Substituting for R_2/R_Θ from equation (2.46) gives

$$\dot{J}_{mb} = -\frac{2}{3}\left(\frac{2\pi}{\mu_\Theta}\right)^{2/3} B_\Theta^{4/3} \dot{M}_\Theta^{1/3} \left(\frac{R_2}{\bar{r}}\right)^{4/3} \left(\frac{\Omega_2^2}{\Omega_\Theta^{5/3}}\right) \left(\frac{M_2}{M_\Theta}\right)^{-16/9} \left[q\left(\frac{M_2}{M_\Theta}\right)\right]^{16/9} R_2^{16/9} R_\Theta^{8/9}$$

$$\Rightarrow \quad \dot{J}_{mb} = -\frac{2}{3}\left(\frac{2\pi}{\mu_\Theta}\right)^{2/3} B_\Theta^{4/3} \dot{M}_\Theta^{1/3} \left(\frac{R_2}{\bar{r}}\right)^{4/3} \left(\frac{\Omega_2^2}{\Omega_\Theta^{5/3}}\right) q^{16/9} R_2^{16/9} R_\Theta^{8/9}. \tag{2.97}$$

Substituting for $\dot{J}_{mb}$ and J_{orb} from equations (2.97) and (2.60) respectively into equation (2.20) gives

$$\dot{M}_2 = \frac{M_2}{\left(\frac{4}{3} - \frac{M_2}{M_1}\right)} \left[\frac{-\left(\frac{2}{3}\right)\left(\frac{2\pi}{\mu_\Theta}\right)^{2/3} B_\Theta^{4/3} \dot{M}_\Theta^{1/3} \left(\frac{R_2}{\bar{r}}\right)^{4/3} \left(\frac{\Omega_2^2}{\Omega_\Theta^{5/3}}\right) q^{16/9} R_2^{19/9} R_\Theta^{8/9}}{\left(\frac{GR_\Theta}{M_\Theta}\right)^{1/2} \frac{M_1 M_2^{4/3}}{M^{1/3}} 10^{1/6} q^{1/2}}\right].$$

Substituting for R_2 from equation (2.46) and Ω_2^2 from equation (2.58), for $R_{L,2} = R_2$, it can be shown that

$$\dot{M}_2 = -\frac{7.7 \times 10^{-10}}{\xi_{w,\Theta}^{1/3} q^{-1/8}} \left(\frac{B_\Theta}{Gauss}\right)^2 \left(\frac{R_2}{\bar{r}}\right)^{5/3} \left(\frac{M_\Theta}{M}\right)^{11/9} \frac{1}{(4 - 7\mu)\mu^{5/9}} \; M_\Theta \, \mathrm{yr}^{-1} \tag{2.98}$$

$$\Rightarrow \quad \dot{M}_2 = -4.88\times10^{16}\left(\frac{q^{1/18}}{\xi_{w,\Theta}^{1/3}}\right)\left(\frac{B_\Theta}{Gauss}\right)^2\left(\frac{R_2}{\bar{r}}\right)^{5/3}\left(\frac{M_\Theta}{M}\right)^{11/9}\frac{1}{(4-7\mu)\mu^{5/9}}\ \text{g s}^{-1}.$$

Substituting for q, $\xi_{w,\Theta}$ and B_Θ, also taking $\bar{r}/R_2 = 4$ gives the expression

$$\dot{M}_2 = -7.73\times10^{15}\left(\frac{M}{M_\Theta}\right)^{-11/9}\left(\frac{M_2}{M}\right)^{-5/9}\left(4-7\frac{M_2}{M}\right)^{-1}\ \text{g s}^{-1}. \tag{2.99}$$

The ratio of the wind mass loss rate to the mass transfer rate from the secondary star is obtained by taking the ratio of equation (2.80) to equation (2.98) which gives

$$\left|\frac{\dot{M}_w}{\dot{M}_2}\right| = \frac{2.8\times10^{-2}}{q^{14/9}\xi_{w,\Theta}^{2/3}}\left(\frac{R_2}{\bar{r}}\right)^{-2/3}\left(\frac{M_\Theta}{M}\right)^{-2/9}\frac{(4-7\mu)}{\mu^{4/9}}, \tag{2.100}$$

and the timescale ratio is obtained by substituting equation (2.98) into (2.93) which gives

$$\frac{\tau_{\dot{M}_2}}{\tau_{th}} = \frac{55}{q^{17/18}\xi_{w,\Theta}^{1/3}}\left(\frac{B_\Theta}{Gauss}\right)^{-2}\left(\frac{R_2}{\bar{r}}\right)^{5/3}(4-7\mu)\mu^{50/9}. \tag{2.101}$$

2.3.3 Non-linear law

The non-linear law is given by (e.g. Campbell 1997, p.277)

$$\frac{B_0}{B_\Theta} = \left(\frac{\Omega_2}{\Omega_\Theta}\right)^{7/4}. \tag{2.102}$$

Substituting equations (2.70) and (2.102) in equation (2.57), it can be show that the rate of angular momentum loss is expressed as

$$\dot{J}_{mb} = -\frac{2}{3}\left(\frac{2\pi}{\mu_0}\right)^{2/3}B_\Theta^{4/3}\dot{M}_\Theta^{1/3}\left(\frac{\Omega_2}{\Omega_\Theta}\right)^{1/3}\left(\frac{\Omega_2}{\Omega_\Theta}\right)^{7/3}\left(\frac{R_2}{\bar{r}}\right)^{4/3}\Omega_2^{1/3}R_2^{8/3}$$

$$\Rightarrow \quad \dot{J}_{mb} = -\frac{2}{3}\left(\frac{2\pi}{\mu_0}\right)^{2/3}\frac{B_\Theta^{4/3}\dot{M}_\Theta^{1/3}}{\Omega_\Theta^{8/3}}\left(\frac{R_2}{\bar{r}}\right)^{4/3}R_2^{8/3}\Omega_2^3. \tag{2.103}$$

Substituting for Ω_2 from equation (2.58) into (2.103) gives

$$\dot{J}_{mb} = -\frac{2}{3}\left(\frac{2\pi}{\mu_0}\right)^{2/3}\frac{B_\Theta^{4/3}\dot{M}_\Theta^{1/3}}{\Omega_\Theta^{8/3}}\left(\frac{R_2}{\bar{r}}\right)^{4/3}\left(0.1\frac{GM_1}{R_2^3}\right)^{3/2}R_2^{8/3}. \tag{2.104}$$

Substituting for $\dot{J}_{mb}$ and J_{orb} from equations (2.104) and (2.60) respectively and for $\dot{M}_{\Theta}$ from equation (2.74) into equation (2.20), the mass transfer rate is obtained as

$$\dot{M}_2 = \frac{M_2}{\left(\frac{4}{3}-\frac{M_2}{M_1}\right)}\left[\frac{-\frac{2}{3}\left(\frac{2\pi}{\mu_0}\right)^{2/3}\frac{B_{\Theta}^{4/3}}{\Omega_{\Theta}^{8/3}}\left(\frac{0.15\pi R_{\Theta}^2 B_{\Theta}^2}{\mu_0 C_{w,\Theta}\xi_{w,\Theta}}\frac{R_2}{\bar{r}}\right)^{1/3}\left(\frac{R_2}{\bar{r}}\right)^{4/3}\left(\frac{0.1GM_1}{R_2^3}\right)R_2^{8/3}}{\left(\frac{GR_{\Theta}}{M_{\Theta}}\right)^{1/3}\frac{M_1 M_2^{4/3}}{M^{1/3}}10^{1/6}q^{1/2}}\right].$$

Substituting for the constants and re-arranging this equation gives

$$\dot{M}_2 = \frac{-6.2\times10^{-8}}{\xi_{w,\Theta}^{1/3}q^{7/3}}\left(\frac{B_{\Theta}}{Gauss}\right)^2\left(\frac{R_2}{\bar{r}}\right)^{5/3}\left(\frac{M_{\Theta}}{M}\right)^{4/3}\left(\frac{M_2}{M}\right)^{-2/3}\left(4-7\frac{M_2}{M}\right)^{-1} M_{\Theta}\,\mathrm{yr}^{-1} \quad (2.105)$$

$$\dot{M}_2 = -7.82\times10^{-9}\left(\frac{M}{M_{\Theta}}\right)^{-4/3}\left(\frac{M_2}{M}\right)^{-2/3}\left(4-7\frac{M_2}{M}\right)^{-1} M_{\Theta}\,\mathrm{yr}^{-1}$$

$$\Rightarrow \quad \dot{M}_2 = -4.96\times10^{17}\left(\frac{M}{M_{\Theta}}\right)^{-4/3}\left(\frac{M_2}{M}\right)^{-2/3}\left(4-7\frac{M_2}{M}\right)^{-1} \mathrm{g\ s}^{-1}. \quad (2.106)$$

Considering the case for field saturation at Ω_c, the mass transfer rate is given by (e.g. Campbell 1997, p.278 - 279)

$$\dot{M}_2 = -5.3\times10^{-13}\frac{q^{5/3}}{\xi_{w,\Theta}^{1/3}}\left(\frac{B_{\Theta}}{Gauss}\right)^2\left(\frac{R_2}{\bar{r}}\right)^{5/3}\left(\frac{\Omega_c}{\Omega_{\Theta}}\right)^{8/3}\left(\frac{M}{M_{\Theta}}\right)^{4/3}$$

$$\left(\frac{M_2}{M}\right)^2\left(4-7\frac{M_2}{M}\right)^{-1} M_{\Theta}\,\mathrm{yr}^{-1}. \quad (2.107)$$

Substituting for q, $\xi_{w,\Theta}$ and taking $\Omega_c = 80\Omega_{\Theta}$ for the field saturation case gives

$$\dot{M}_2 = -1.1626\times10^{-8}\left(\frac{M}{M_{\Theta}}\right)^{4/3}\left(\frac{M_2}{M}\right)^2\left(4-7\frac{M_2}{M}\right)^{-1} M_{\Theta}\,\mathrm{yr}^{-1}$$

$$\text{or} \quad \dot{M}_2 = -7.368\times10^{17}\left(\frac{M}{M_{\Theta}}\right)^{4/3}\left(\frac{M_2}{M}\right)^2\left(4-7\frac{M_2}{M}\right)^{-1} \mathrm{g\ s}^{-1}. \quad (2.108)$$

The ratio of the wind mass loss rate to the mass transfer rate, for unsaturated field, is obtained from equations (2.80) and (2.105), i.e.

$$\left|\frac{\dot{M}_w}{\dot{M}_2}\right| = 3\times10^{-4} q^{5/6} \xi_{w,\Theta}^{-2/3} \left(\frac{R_3}{\bar{r}}\right)^{-2/3} \left(\frac{M}{M_\Theta}\right)^{1/3} \left(\frac{M_2}{M}\right)^{-1/3} \left(4-7\frac{M_2}{M}\right) \qquad (2.109)$$

while the timescale ratio is obtained from equations (2.105) and (2.93), i.e.

$$\frac{\tau_{\dot{M}_2}}{\tau_{th}} = 0.7 q^{10/3} \xi_{w,\Theta}^{1/3} \left(\frac{B_\Theta}{Gauss}\right)^{-2} \left(\frac{R_2}{\bar{r}}\right)^{-5/3} \left(\frac{M_\Theta}{M}\right)^{-19/3} \left(\frac{M_2}{M}\right)^{17/3} \left(4-7\frac{M_2}{M}\right). \qquad (2.110)$$

For the case of saturated field the ratio of wind mass loss rate to the mass transfer rate is obtained from equations (2.80) and (2.107), i.e.

$$\left|\frac{\dot{M}_w}{\dot{M}_2}\right| = \frac{0.46}{q^{5/3} \xi_{w,\Theta}^{2/3}} \left(\frac{R_2}{\bar{r}}\right)^{-2/3} \left(\frac{M}{M_\Theta}\right)^{-4/3} \left(\frac{\Omega_\Theta}{\Omega_c}\right)^{5/3} (4-7\mu)\mu^{-2} \qquad (2.111)$$

and the timescale ratio is obtained from equations (2.93) and (2.107), i.e.

$$\frac{\tau_{\dot{M}_2}}{\tau_{th}} = \frac{8\times10^4}{q^{2/3} \xi_{w,\Theta}^{-1/3}} \left(\frac{B_\Theta}{Gauss}\right)^{-2} \left(\frac{R_2}{\bar{r}}\right)^{-5/3} \left(\frac{M}{M_\Theta}\right)^{1/3} \left(\frac{\Omega_\Theta}{\Omega_c}\right)^{8/3} (4-7\mu)\mu^3. \qquad (2.112)$$

In all the three scenarios that have been discussed it has been illustrated that all the three dynamo laws satisfy the condition $\tau_{th} << (M_2 / \dot{M}_2)$, $\tau_{\dot{M}_2} \sim 10^{16}\, s$ (e.g. p.37), the required condition for thermal equilibrium of the secondary star.

The detailed discussion presented in this chapter is aimed at providing a theoretical framework to evaluate the detailed calculations that will be presented in the next chapter.

Chapter Three

Calculations and investigations

3.1 Introduction

The majority of secondary stars in cataclysmic variables, especially MCVs have a convective envelope, implying a distinct possibility of the presence of significant surface magnetic fields generated through some internal dynamo mechanism. Since this study is aiming at investigating the influence of the secondary star magnetic field on the mass transfer process, the magnetic profile of the secondary star has to be determined. Using the stellar wind theory and the dynamo laws discussed in the previous chapter the surface polar magnetic field of the secondary stars can be determined for the various dynamo laws. This will be reviewed in the following section.

3.2 Model for estimating the surface polar magnetic fields of mass transferring secondary stars

Before developing the models for calculating the surface polar magnetic field of the secondary stars, the general expressions for orbital angular momentum and rate of loss of angular momentum via magnetic braking derived in the previous chapter have to be modified. Taking q = 1.1 (e.g. Campbell 1997, p.269) the orbital angular momentum, equation (2.60), can be expressed to take the form

$$J_{orb} = 1.54 G^{1/2} R_{\Theta}^{1/2} M_{\Theta}^{3/2} \left(\frac{M_1}{M_{\Theta}}\right)\left(\frac{M_2}{M_{\Theta}}\right)^{4/3}\left(\frac{M}{M_{\Theta}}\right)^{-1/3}. \qquad (3.1)$$

Using equations (2.70) and (2.63), the rate of loss of angular momentum via magnetic braking, i.e. equation (2.57), can be expressed in the form

$$\dot{J}_{mb} = -\frac{2}{3}\left(\frac{2\pi}{\mu_0}\right)^{2/3} B_{\Theta}^{4/3} \dot{M}_{\Theta}^{1/3}\left(\frac{\Omega_2}{\Omega_{\Theta}}\right)^{2/3}\left(\frac{B_0}{B_{\Theta}}\right)^{4/3}\left(\frac{R_2}{\bar{r}}\right)^{4/3}\left(\frac{R_2}{R_{\Theta}}\right)^{8/3} \Omega_{\Theta}^{1/3} R_{\Theta}^{8/3}. \qquad (3.2)$$

Equations (3.1) and (3.2) can be used to develop a suitable model for calculating the surface polar magnetic field of secondary stars in CVs using the different dynamo laws. This will be discussed for each dynamo law in the following sections. The general approach will be to develop basic equations for the surface polar magnetic field for the various dynamo laws, and then using these, the surface polar field for individual systems with known mass transfer rate and orbital period will be determined. These expressions are at first normalized with respect to the binary parameters of the nova-like variable AE Aqr for comparison.

3.2.1 Linear dynamo law

First an expression for the rate of loss of angular momentum via magnetic braking, using the linear dynamo law, has to be obtained. From the dynamo law, equation (2.63), i.e. $B_0/B_{\Theta} = (\Omega_2/\Omega_{\Theta})^n$, equation (3.2) can be expressed as

$$\dot{J}_{mb} = -\frac{2}{3}\left(\frac{2\pi}{\mu_0}\right)^{2/3} B_{\Theta}^{4/3} \dot{M}_{\Theta}^{1/3}\left(\frac{B_0}{B_{\Theta}}\right)^{\frac{4n+2}{3n}}\left(\frac{R_2}{\bar{r}}\right)^{4/3}\left(\frac{R_2}{R_{\Theta}}\right)^{8/3} R_{\Theta}^{8/3} \Omega_{\Theta}^{1/3}. \qquad (3.3)$$

The period-radius relation, for period in hours, is given by (e.g. Frank, King & Raine 1992, p.51)

$$R_2 = 7.9\times10^{9}\left(\frac{P_{orb}}{h}\right) \text{ cm}$$

$$R_2 = 7.8\times10^{10}\left(\frac{P_{orb}}{9.88h}\right) \text{ cm}$$

$$\frac{R_2}{R_\Theta} = \frac{7.8\times10^{10}}{6.96\times10^{10}}\left(\frac{P_{orb}}{9.88h}\right)$$

$$\Rightarrow \quad \frac{R_2}{R_\Theta} = 1.121\left(\frac{P_{orb}}{9.88h}\right). \tag{3.4}$$

Substituting equations (2.74) and (3.4) into equation (3.3), gives

$$\dot{J}_{mb} = \frac{2}{3}\left(\frac{2\pi}{\mu_0}\right)^{2/3} B_\Theta^{4/3}\left[\frac{0.15\pi R_\Theta^2 B_\Theta^2}{\mu_0 C_{w,\Theta}\xi_{w,\Theta}}\frac{R_2}{\bar{r}}\right]^{1/3}\left(\frac{B_0}{B_\Theta}\right)^{\frac{4n+2}{3n}}\left(\frac{R_2}{\bar{r}}\right)^{4/3}\left(1.121\frac{P_{orb}}{9.88h}\right)^{8/3} R_\Theta^{8/3}\Omega_\Theta^{1/3}$$

$$\Rightarrow \dot{J}_{mb} = \frac{2}{3}(1.121)^{8/3}\left(\frac{2\pi}{\mu_0}\right)^{2/3}\left(\frac{0.15\pi}{\mu_0}\right)^{1/3}\frac{R_\Theta^{10/3}\Omega_\Theta^{1/3}B_\Theta^2}{\left(C_{w,\Theta}\xi_{w,\Theta}\right)^{1/3}}\left(\frac{B_0}{B_\Theta}\right)^{\frac{4n+2}{3n}}\left(\frac{R_2}{\bar{r}}\right)^{5/3}\left(\frac{P_{orb}}{9.88h}\right)^{8/3}. \tag{3.5}$$

Using equations (3.1) and (3.5) an expression for the rate of loss of angular momentum through magnetic braking can be expressed as

$$\frac{\dot{J}_{mb}}{J_{orb}} = \frac{\frac{2}{3}(1.121)^{8/3}\left(\frac{2\pi}{\mu_0}\right)^{2/3}\left(\frac{0.15\pi}{\mu_0}\right)^{1/3}\frac{R_\Theta^{10/3}\Omega_\Theta^{1/3}B_\Theta^2}{\left(C_{w,\Theta}\xi_{w,\Theta}\right)^{1/3}}\left(\frac{R_2}{\bar{r}}\right)^{5/3}\left(\frac{B_0}{B_\Theta}\right)^{\frac{4n+2}{3n}}\left(\frac{P_{orb}}{9.88h}\right)^{8/3}}{1.54G^{1/2}R_\Theta^{1/2}M_\Theta^{3/2}\left(\frac{M_1}{M_\Theta}\right)\left(\frac{M_2}{M_\Theta}\right)^{4/3}\left(\frac{M}{M_\Theta}\right)^{-1/3}}.$$

Substituting for the constants into this equation and taking $B_\Theta = 2$ Gauss (solar value for polar field) gives

$$\frac{\dot{J}_{mb}}{J_{orb}} = 2.656\times10^{-21}\left(\frac{B_0}{B_\Theta}\right)^{\frac{4n+2}{3n}}\left(\frac{R_2}{\bar{r}}\right)^{5/3}\left(\frac{P_{orb}}{9.88h}\right)^{8/3}\left(\frac{M_1}{M_\Theta}\right)^{-1}\left(\frac{M_2}{M_\Theta}\right)^{-4/3}\left(\frac{M}{M_\Theta}\right)^{1/3}$$

$$\Rightarrow \frac{\dot{J}_{mb}}{J_{orb}} = 6.675\times10^{-21}\left(\frac{B_0}{B_\Theta}\right)^{\frac{4n+2}{3n}}\left(\frac{R_2}{\bar{r}}\right)^{5/3}\left(\frac{P_{orb}}{9.88h}\right)^{8/3}$$

$$\left(\frac{M_1}{0.9M_\Theta}\right)^{-1}\left(\frac{M_2}{0.6M_\Theta}\right)^{-4/3}\left(\frac{M}{1.5M_\Theta}\right)^{1/3} \text{ s}^{-1}. \tag{3.6}$$

From equations (2.42) and (3.6) an expression for the surface polar magnetic field of the secondary star scaled according to the corresponding solar value is obtained as

$$\left(\frac{B_0}{B_\Theta}\right)^{\frac{4n+2}{3n}} \geq \frac{5.24\times10^{-16}\left(\dot{M}_2\big/2\times10^{18}\,gs^{-1}\right)\left(M_2/0.6M_\Theta\right)^{-1}}{6.675\times10^{-21}\left(\frac{R_2}{\bar{r}}\right)^{5/3}\left(\frac{p_{orb}}{9.88h}\right)^{8/3}\left(\frac{M_1}{0.9M_\Theta}\right)^{-1}\left(\frac{M_2}{0.6M_\Theta}\right)^{-4/3}\left(\frac{M}{1.5M_\Theta}\right)^{1/3}}$$

$$\left(\frac{B_0}{B_\Theta}\right)^{\frac{4n+2}{3n}} \geq 78501.87\left(\frac{R_2}{\bar{r}}\right)^{-5/3}\left(\frac{\dot{M}_2}{2\times10^{18}\,gs^{-1}}\right)\left(\frac{M_2}{0.6M_\Theta}\right)^{1/3}\left(\frac{P_{orb}}{9.88h}\right)^{-8/3}\left(\frac{M_1}{0.9M_\Theta}\right)\left(\frac{M}{1.5M_\Theta}\right)^{-1/3}$$

For the linear dynamo law $n=1$, and taking $\bar{r}/R_2=4$ (for a fast rotator) and $B_\Theta=2$ Gauss an expression for B_0 can be obtained as

$$\left(\frac{B_0}{B_\Theta}\right)^{2} \geq 791249.28\left(\frac{\dot{M}_2}{2\times10^{18}\,gs^{-1}}\right)\left(\frac{M_2}{0.6M_\Theta}\right)^{1/3}\left(\frac{P_{orb}}{9.88h}\right)^{-8/3}\left(\frac{M_1}{0.9M_\Theta}\right)\left(\frac{M}{1.5M_\Theta}\right)^{-1/3}$$

$$B_0 \geq 1779.04\left(\frac{\dot{M}_2}{2\times10^{18}\,gs^{-1}}\right)^{1/2}\left(\frac{M_2}{0.6M_\Theta}\right)^{1/6}\left(\frac{P_{orb}}{9.88h}\right)^{-8/6}$$

$$\left(\frac{M_1}{0.9M_\Theta}\right)^{1/2}\left(\frac{M}{1.5M_\Theta}\right)^{-1/6} \text{ Gauss.} \qquad (3.7)$$

3.2.2 Inverse Rossby number law

The inverse Rossby number law, equation (2.96), can be expressed in the form

$$\left(\frac{\Omega_2}{\Omega_\Theta}\right)=\left(\frac{M_\Theta^4}{R_\Theta^2}\right)^{-1/3}\left(\frac{R_2^2}{M_2^4}\right)^{-1/3}\left(\frac{B_0}{B_\Theta}\right). \qquad (3.8)$$

Substituting equation (3.8) into (3.2) gives

$$\dot{J}_{mb}=-\frac{2}{3}\left(\frac{2\pi}{\mu_0}\right)^{2/3}B_\Theta^{4/3}\dot{M}_\Theta^{1/3}\left[\left(\frac{M_\Theta^4}{R_\Theta^2}\right)^{-1/3}\left(\frac{R_2^2}{M_2^4}\right)^{-1/3}\left(\frac{B_0}{B_\Theta}\right)\right]^{2/3}\left(\frac{B_0}{B_\Theta}\right)^{4/3}\left(\frac{R_2}{\bar{r}}\right)^{4/3}\left(\frac{R_2}{R_\Theta}\right)^{8/3}\Omega_\Theta^{1/3}R_\Theta^{8/3}$$

$$\Rightarrow \dot{J}_{mb}=-\frac{2}{3}\left(\frac{2\pi}{\mu_0}\right)^{2/3}B_\Theta^{4/3}\dot{M}_\Theta^{1/3}\left(\frac{B_0}{B_\Theta}\right)^{2}\left(\frac{R_2}{\bar{r}}\right)^{4/3}\left(\frac{M_\Theta^4}{R_\Theta^2}\right)^{-2/9}$$

$$\left(\frac{R_2^2}{M_2^4}\right)^{-2/9}\left(\frac{R_2}{R_\Theta}\right)^{8/3}\Omega_\Theta^{1/3}R_\Theta^{8/3}. \qquad (3.9)$$

Substituting for $\dot{M}_\Theta$ from equation (2.74) into (3.9) gives

$$\dot{J}_{mb} = \frac{2}{3}\left(\frac{2\pi}{\mu_0}\right)^{2/3}\left(\frac{0.15\pi}{\mu_0}\right)^{1/3}\frac{B_\Theta^2 R_\Theta^{10/9}\Omega_\Theta^{1/3}}{\left(C_{w,\Theta}\xi_{w,\Theta}\right)^{1/3}}\left(\frac{B_0}{B_\Theta}\right)^2\left(\frac{R_2}{\bar{r}}\right)^{5/3}\left(\frac{M_2}{M_\Theta}\right)^{8/9}\left(\frac{R_2}{R_\Theta}\right)^{20/9}R_\Theta^{20/9}$$

$$\Rightarrow \dot{J}_{mb} = \frac{2}{3}\left(\frac{2\pi}{\mu_0}\right)^{2/3}\left(\frac{0.15\pi}{\mu_0}\right)^{1/3}\frac{B_\Theta^2 R_\Theta^{10/3}\Omega_\Theta^{1/3}}{\left(C_{w,\Theta}\xi_{w,\Theta}\right)^{1/3}}\left(\frac{B_0}{B_\Theta}\right)^2\left(\frac{R_2}{\bar{r}}\right)^{5/3}\left(\frac{M_2}{M_\Theta}\right)^{8/9}\left(\frac{R_2}{R_\Theta}\right)^{20/9}. \qquad (3.10)$$

Using equation (3.4) and substituting for the constants, equation (3.10) can be expressed in the form

$$\dot{J}_{mb} = \frac{2}{3}\left(\frac{2\pi}{\mu_0}\right)^{2/3}(1.121)^{20/9}\left(\frac{0.15\pi}{\mu_0}\right)^{1/3}\left[\frac{B_\Theta^2 R_\Theta^{10/3}\Omega_\Theta^{1/3}}{\left(C_{w,\Theta}\xi_{w,\Theta}\right)^{1/3}}\right]$$

$$\left(\frac{B_0}{B_\Theta}\right)^2\left(\frac{R_2}{\bar{r}}\right)^{5/3}\left(\frac{M_2}{M_\Theta}\right)^{8/9}\left(\frac{P_{orb}}{9.88h}\right)^{20/9}. \qquad (3.11)$$

From equations (3.1) and (3.11) the rate of loss of orbital angular momentum via magnetic braking can be expressed in the form

$$\frac{\dot{J}_{mb}}{J_{orb}} = 2.52\times10^{-21}\left(\frac{B_0}{B_\Theta}\right)^2\left(\frac{R_2}{\bar{r}}\right)^{5/3}\left(\frac{M_2}{M_\Theta}\right)^{-4/9}\left(\frac{P_{orb}}{9.88h}\right)^{20/9}\left(\frac{M_1}{M_\Theta}\right)^{-1}\left(\frac{M}{M_\Theta}\right)^{1/3} \text{ s}^{-1}. \qquad (3.12)$$

From equations (2.42) and (3.12) and taking $\bar{r}/R_2 = 4$ an expression for B_0 for the case of the inverse Rossby number law can be obtained, i.e.

$$\left(\frac{B_0}{B_\Theta}\right)^2 \geq \left(\frac{5.24\times10^{-16}}{2.52\times10^{-21}}\right)\left(\frac{\dot{M}_2}{2\times10^{18}\,gs^{-1}}\right)\left(\frac{R_2}{\bar{r}}\right)^{-5/3}\left(\frac{M_2}{0.6M_\Theta}\right)^{-1}$$

$$\left(\frac{M_2}{M_\Theta}\right)^{4/9}\left(\frac{P_{orb}}{9.88h}\right)^{-20/9}\left(\frac{M_1}{M_\Theta}\right)\left(\frac{M}{M_\Theta}\right)^{-1/3}$$

$$\frac{B_0}{B_\Theta} \geq 1145.92\left(\frac{\dot{M}_2}{2\times10^{18}\,gs^{-1}}\right)^{1/2}\left(\frac{M_2}{0.6M_\Theta}\right)^{-5/18}\left(\frac{P_{orb}}{9.88h}\right)^{-10/9}\left(\frac{M_1}{0.9M_\Theta}\right)^{1/2}\left(\frac{M}{M_\Theta}\right)^{-1/6}$$

$$B_0 \geq 2291.84\left(\frac{\dot{M}_2}{2\times10^{18}\,gs^{-1}}\right)^{1/2}\left(\frac{M_2}{0.6M_\Theta}\right)^{-5/18}\left(\frac{P_{orb}}{9.88h}\right)^{-10/9}\left(\frac{M_1}{0.9M_\Theta}\right)^{1/2}\left(\frac{M}{M_\Theta}\right)^{-1/6} \text{ Gauss.} \qquad (3.13)$$

3.2.3 Non-linear law

Using the non-linear law, equation (2.102), i.e. $B_0/B_\Theta = \left(\Omega_2/\Omega_\Theta\right)^{7/4}$, equation (3.2) can be expressed in the form

$$\dot{J}_{mb} = -\frac{2}{3}\left(\frac{2\pi}{\mu_0}\right)^{2/3} B_\Theta^{4/3}\,\dot{M}_\Theta^{1/3}\left[\left(\frac{B_0}{B_\Theta}\right)^{4/7}\right]^{2/3}\left(\frac{B_0}{B_\Theta}\right)^{4/3}\left(\frac{R_2}{\bar{r}}\right)^{4/3}\left(\frac{R_2}{R_\Theta}\right)^{8/3}\Omega_\Theta^{1/3}R_\Theta^{8/3}$$

$$\Rightarrow \dot{J}_{mb} = -\frac{2}{3}\left(\frac{2\pi}{\mu_0}\right)^{2/3} B_\Theta^{4/3}R_\Theta^{8/3}\Omega_\Theta^{1/3}\,\dot{M}_\Theta^{1/3}\left(\frac{B_0}{B_\Theta}\right)^{12/7}\left(\frac{R_2}{\bar{r}}\right)^{4/3}\left(\frac{R_2}{R_\Theta}\right)^{8/3}. \qquad (3.14)$$

Substituting equations (2.74) and (3.4) into (3.14) gives

$$\dot{J}_{mb} = \frac{2}{3}\left(\frac{2\pi}{\mu_0}\right)^{2/3} B_\Theta^{4/3}R_\Theta^{8/3}\Omega_\Theta^{1/3}\left(\frac{0.5\pi R_\Theta^2 B_\Theta^2}{\mu_0 C_{w,\Theta}\xi_{w,\Theta}}\frac{R_2}{\bar{r}}\right)^{1/3}\left(\frac{B_0}{B_\Theta}\right)^{12/7}\left(\frac{R_2}{\bar{r}}\right)^{4/3}\left(1.121\frac{P_{orb}}{9.88h}\right)^{8/3}$$

$$\Rightarrow \dot{J}_{mb} = \frac{2}{3}\left(1.121\right)^{8/3}\left(\frac{2\pi}{\mu_0}\right)^{2/3}\left(\frac{0.5\pi}{\mu_0}\right)^{1/3}\frac{B_\Theta^2 R_\Theta^{10/3}\Omega_\Theta^{1/3}}{\left(C_{w,\Theta}\xi_{w,\Theta}\right)^{1/3}}\left(\frac{B_0}{B_\Theta}\right)^{12/7}\left(\frac{R_2}{\bar{r}}\right)^{5/3}\left(\frac{P_{orb}}{9.88h}\right)^{8/3}. \qquad (3.15)$$

From equations (3.1) and (3.15) it can be shown that

$$\frac{\dot{J}_{mb}}{J_{orb}} = \frac{\frac{2}{3}\left(1.121\right)^{8/3}\left(\frac{2\pi}{\mu_0}\right)^{2/3}\left(\frac{0.5\pi}{\mu_0}\right)^{1/3}\frac{B_\Theta^2 R_\Theta^{10/3}\Omega_\Theta^{1/3}}{\left(C_{w,\Theta}\xi_{w,\Theta}\right)^{1/3}}\left(\frac{B_0}{B_\Theta}\right)^{12/7}\left(\frac{R_2}{\bar{r}}\right)^{5/3}\left(\frac{P_{orb}}{9.88h}\right)^{8/3}}{1.54G^{1/2}R_\Theta^{1/2}M_\Theta^{3/2}\left(\frac{M_1}{M_\Theta}\right)\left(\frac{M_2}{M_\Theta}\right)^{4/3}\left(\frac{M}{M_\Theta}\right)^{-1/3}}$$

$$\Rightarrow \frac{\dot{J}_{orb}}{J_{orb}} = 6.675\times10^{-21}\left(\frac{R_2}{\bar{r}}\right)^{5/3}\left(\frac{B_0}{B_\Theta}\right)^{12/7}\left(\frac{P_{orb}}{9.88h}\right)^{8/3}\left(\frac{M_1}{0.9M_\Theta}\right)^{-1}$$

$$\left(\frac{M_2}{0.6M_\Theta}\right)^{-4/3}\left(\frac{M}{1.5M_\Theta}\right)^{1/3}\ \mathrm{s}^{-1}. \qquad (3.16)$$

From equations (2.42) and (3.16) the following expression is obtained

$$\left(\frac{B_0}{B_\Theta}\right)^{12/7} \geq \frac{5.24\times10^{-16}\left(\dot{M}_2/2\times10^{18}\right)\left(M_2/0.6M_\Theta\right)^{-1}}{6.675\times10^{-21}\left(\frac{R_2}{\bar{r}}\right)^{5/3}\left(\frac{P_{orb}}{9.88h}\right)^{8/3}\left(\frac{M_1}{0.9M_\Theta}\right)^{-1}\left(\frac{M_2}{0.6M_\Theta}\right)^{-4/3}\left(\frac{M}{1.5M_\Theta}\right)^{1/3}}$$

$$\left(\frac{B_0}{B_\Theta}\right)^{12/7} \geq 78501.87\left(\frac{\dot{M}_2}{2\times10^{18}\,gs^{-1}}\right)\left(\frac{R_2}{\bar{r}}\right)^{-5/3}\left(\frac{P_{orb}}{9.88h}\right)^{-8/3}$$

$$\left(\frac{M_1}{0.9M_\Theta}\right)\left(\frac{M_2}{0.6M_\Theta}\right)^{1/3}\left(\frac{M}{1.5M_\Theta}\right)^{-1/3}.$$

Again taking $\bar{r}/R_2 = 4$, this equation can be expressed as

$$B_0 \geq 5517.12\left(\frac{\dot{M}_2}{2\times10^{18}\,gs^{-1}}\right)^{7/12}\left(\frac{P_{orb}}{9.88h}\right)^{-14/9}\left(\frac{M_1}{0.9M_\Theta}\right)^{7/12}$$

$$\left(\frac{M_2}{0.6M_\Theta}\right)^{7/36}\left(\frac{M}{1.5M_\Theta}\right)^{-7/36} \text{ Gauss.} \qquad (3.17)$$

The equations developed in this section can be used to estimate the surface polar magnetic field of the secondary stars. This is possible if the rate of mass transfer from the secondary star is known, and this will be calculated in the following section.

3.3 Mass transfer rates

Using an empirical relationship from observations, it is shown that the period-mass relationship for a lobe-filling secondary star close to the lower main-sequence is given by (King 1988; Frank, e.g. King & Raine 1992, p.51)

$$M_2 = 0.11P_{orb}(h). \qquad (3.18)$$

This can be used to calculate the mass of a lobe-filling secondary star whose orbital period is known. Using this relation, the mass transfer rates can be calculated using equations (2.91) and (2.99) for the linear dynamo law (LDL) and the inverse Rossby number law (IRNL) respectively; while for the non-linear law (NLL) equations (2.106) and (2.107) can be used for the case of unsaturated field (USF) and saturated field (SF) respectively. The orbital periods of some intermediate polars can be obtained (e.g. Warner 1995, p.370; Campbell 1997, p.264). The results obtained are shown in Table 1.

Name	$P_{orb}(h)$	$-\dot{M}_2$ (gs^{-1}) LDL ($\times 10^{15}$)	$-\dot{M}_2$ (gs^{-1}) IRNL ($\times 10^{15}$)	$-\dot{M}_2$ (gs^{-1}) NLL (USF) ($\times 10^{17}$)	$-\dot{M}_2$ (gs^{-1}) NLL (SF) ($\times 10^{17}$)
BG CMi	3.24	1.94	5.17	3.72	0.36
V_{1223} Sgr	3.37	1.98	5.16	3.70	0.39
AO Psc	3.59	2.07	5.14	3.66	0.44
YY Dra	3.91	2.26	5.14	3.60	0.57
DQ Her	4.65	2.67	5.22	3.60	0.89
FO Aqr	4.85	2.78	5.26	3.62	0.99
V_{533} Her	5.04	2.90	5.31	3.64	1.10
PQ Gem	5.18	3.05	5.36	3.66	1.21
TV Col	5.49	3.22	5.46	3.70	1.45
TX Col	5.72	3.44	5.57	3.76	1.63
XY Ari	6.06	3.75	5.76	3.86	1.97

Table 1. Showing mass transfer rates calculated using different dynamo laws.

In calculating the mass transfer rates above it is assumed that the average mass of the white dwarfs $M_1 \approx 1 M_\Theta$, i.e. it is assumed that the systems are so much evolved that the white dwarfs have accreted a substantial amount of material (e.g. Warner 1995, p.399). The period range $3 \le P_{orb}(h) \le 7$ (above the period gap) is of interest in close binaries, and this corresponds to the mass range $0.3 \le M_2/M_\Theta \le 0.7$. Over this mass range $|\dot{M}_w| / |\dot{M}_2| << 1$ for all the cases considered above, i.e. mass loss due to the secondary star's wind is negligible, and the total mass of the systems can therefore be taken to be conserved. The mass transfer rates (i.e. Table 1) for the various dynamo laws are plotted against orbital period, i.e. Figure 7 (a) for LDL and IRNL and Figure 7 (b) for NLL for the case of USF and SF.

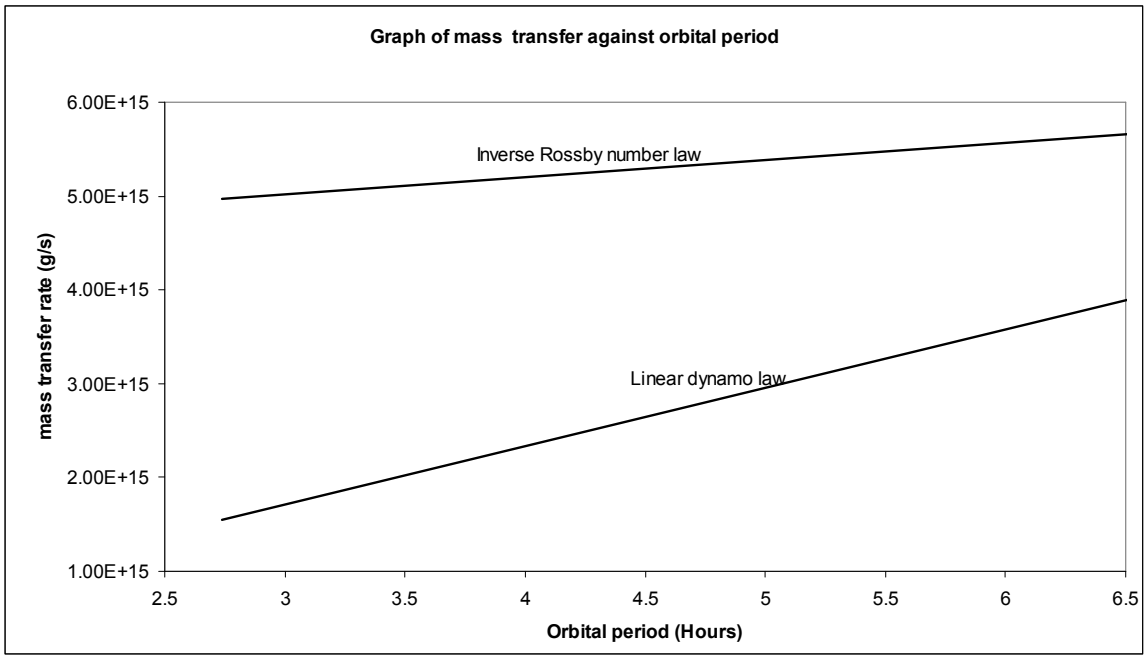

Figure 7 (a). Graph of mass transfer rate against orbital period for the linear dynamo law and the inverse Rossby number law.

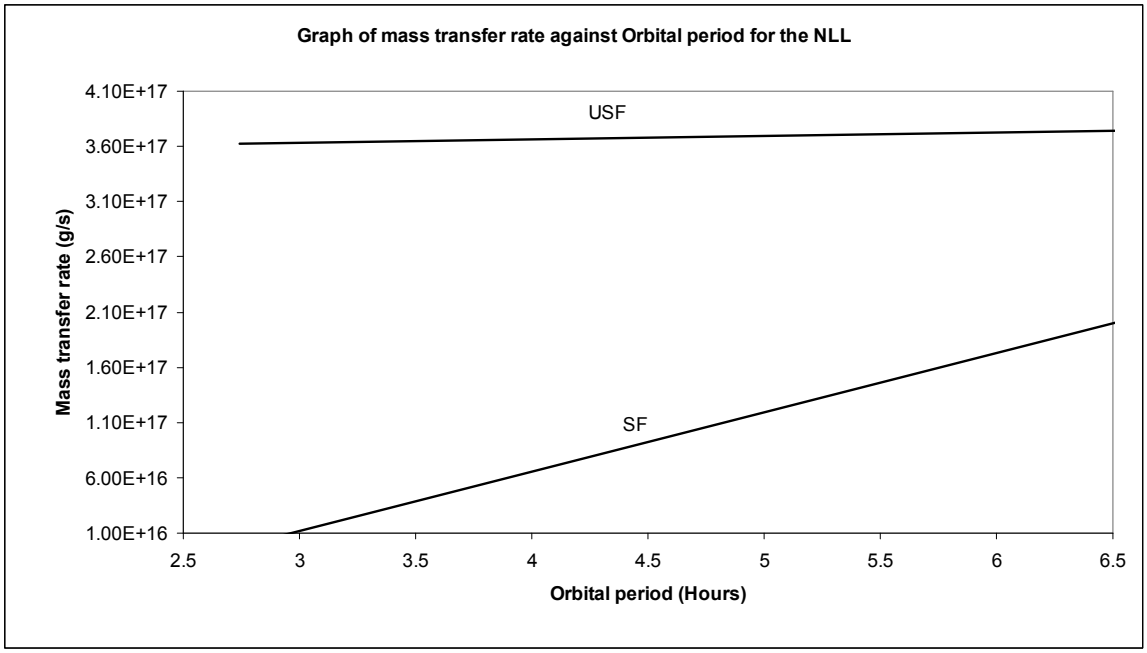

Figure 7 (b). Graph of mass transfer rate against orbital period for the non-linear law (NLL) for the case of unsaturated field (USF) and saturated field (SF).

A loss of orbital angular momentum caused by gravitational radiation losses leads to mass transfer rate, representative of systems in the period gap, given by (e.g. Campbell 1997, p.269)

$$\dot{M}_2 = -1.2 \times 10^{16} \frac{(1-\mu)^2}{(4-\mu)} \mu^{-2/3} \; g \; s^{-1}. \qquad (3.19)$$

where $\mu = M_2 / M$.

From equation (3.19) it is noted that the mass transfer rates obtained using the linear dynamo law are at most comparable to those driven by gravitational radiation; and thus cannot explain the observed high mass transfer rates above the period gap. The mass transfer rates obtained using the inverse Rossby number law exceed those driven by gravitational radiation, but are still not high enough to explain the inferred mass transfer rates above the period gap. The non-linear law, for the case of unsaturated field produces mass transfer rates which are rather high, while the case with field saturation produces mass transfer rates in best agreement with observation. The observed mass transfer rates above the period gap, i.e. for orbital periods in the range 3 hrs – 6 hrs, is $\sim 2 \times 10^{16}$ - 2×10^{17} g s^{-1} (e.g. Warner 1995, p.471; Campbell 1997, p.279; Hellier 2001, p.51). It is obvious from these model calculations that the mass transfer rates, driven by magnetic braking, decrease towards decreasing orbital period. Since there is an obvious relation between mass transfer rate and orbital period in systems where mass transfer is driven by magnetic braking, the corresponding relation between the inferred surface polar magnetic field and orbital period will determine any possible dependence. Using the mass transfer rates calculated in Table 1, the surface polar magnetic fields of the secondary stars can now be calculated.

3.4 Surface polar magnetic field

Using the results obtained in Table 1, the surface polar magnetic fields of the secondary stars can be calculated using equations (3.7), (3.13) and (3.17) for the linear dynamo law, inverse Rossby number law and the non-linear law respectively. The results are shown in Table 2.

It is believed that the surface polar magnetic field (B_0) of secondary stars in cataclysmic variables is of the order of 10^3 Gauss (Meyer-Hofmeister, Vogt & Meyer 1996; Meintjes 2004). From the results obtained in Table 2, it is noted that the surface polar magnetic field values obtained using the LDL and the IRNL are much lower than the expected values. However, in general, they decrease with increasing orbital period except for the non-linear law with field saturation. The lower values obtained for the LDL and the IRNL could be as a result of the low mass transfer rates obtained for these dynamo laws. The surface polar magnetic field (i.e. Table 2) for the various dynamo laws are plotted against orbital period, i.e. Figure 8 (a) for LDL and IRNL and Figure 8 (b) for NLL for the case of USF and SF.

Name	$P_{orb}(h)$	$B_0(Gauss)$ LDL	$B_0(Gauss)$ IRNL	B_0(Gauss) NLL (USF)	B_0(Gauss) NLL (SF)
BG CMi	3.24	241	497	11499	2954
V_{1223} Sgr	3.37	232	471	10824	2905
AO Psc	3.59	219	431	9821	2862
YY Dra	3.91	207	379	8632	2934
DQ Her	4.65	182	298	6743	2984
FO Aqr	4.85	176	282	6367	2989
V_{533} Her	5.04	172	268	6045	3008
PQ Gem	5.18	170	258	5837	3061
TV Col	5.49	162	240	5400	3076
TX Col	5.72	160	228	5144	3159
XY Ari	6.06	156	213	4810	3249

Table 2. Showing minimum surface polar magnetic field calculated using different dynamo laws.

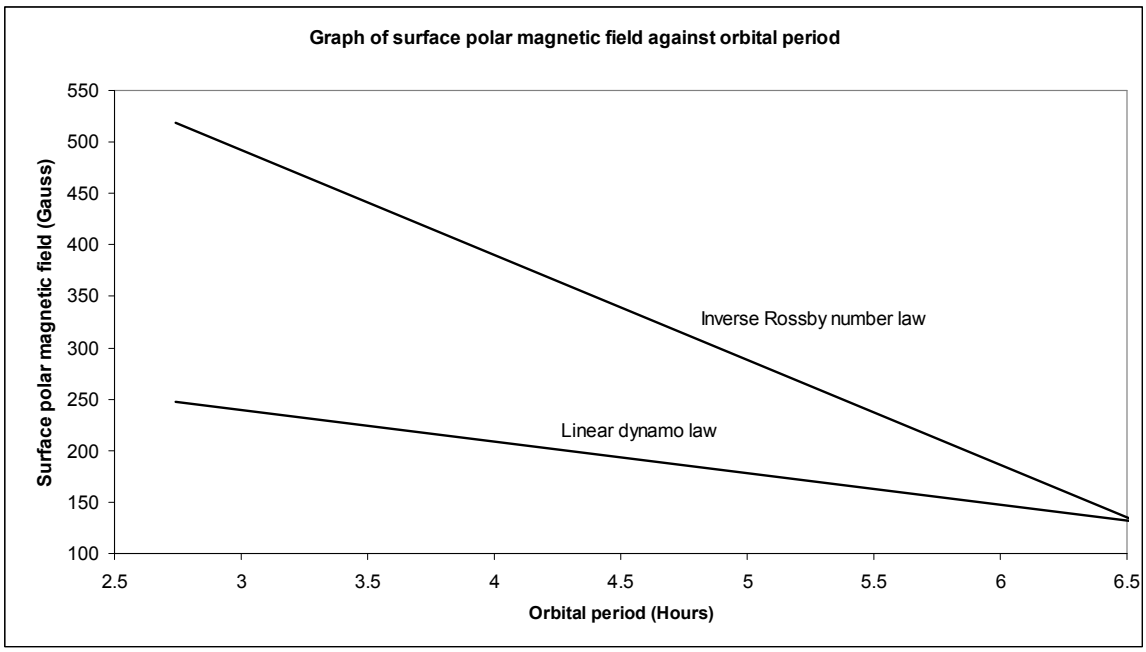

Figure 8 (a). Graph of surface polar magnetic field against orbital period for the linear dynamo law and the inverse Rossby number law.

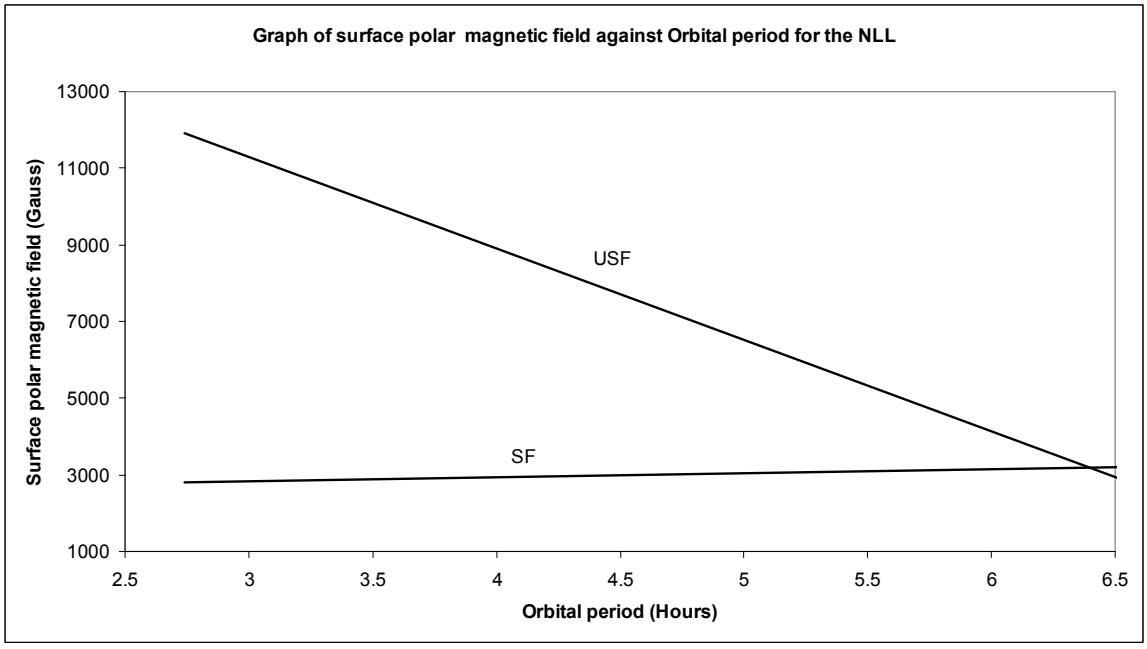

Figure 8 (b). Graph of surface polar magnetic field against orbital period for the NLL for the case of unsaturated field (USF) and saturated field (SF).

The following analysis and discussion will concentrate on the non-linear law for the case with field saturation since it gives mass transfer rates in best agreement with observation, consistently higher than the other dynamo laws, resulting in correspondingly higher surface polar magnetic fields for the secondary star. If it is assumed that the B_0-values obtained in this case are representative of tidally locked secondary stars in MCVs, then an average value of $B_0 \approx 3000$ Gauss can be assumed for all the systems considered. These fields are similar to the inferred fields on the secondary stars in magnetically locked polars (AM Her stars) which strengthens the conjecture that the intermediate polars evolve into polars if the binary loses the required angular momentum (Norton & Watson 1988; e.g. Hellier 2001, p.149). Although B_0 can be assumed to be constant for the systems considered, it is noted that there is a difference in mass transfer rates by a factor of approximately 10 between the most compact and least compact systems considered in this study. Secondary stars in some CVs may have magnetically active equatorial belts (Meintjes 2004) and this may apply to the systems considered here. The magnetic field lines close to the stellar surface may therefore influence the mass flow through the funnel. Therefore the mass transfer through the L_1 region and the possible influence of the surface magnetic field on the mass transfer rate has to be investigated.

3.5 Mass transfer through the L_1 region

Considering a funnel of cross-sectional area ΔS, the instantaneous mass transfer rate through the L_1 region for a fluid flowing at the local sound speed c_s can be estimated as

$$-\dot{M} \approx \rho_{L1} c_s \Delta S \tag{3.20}$$

where ρ_{L1} is the fluid density at the L_1 region. The funnel width H, can be approximated in terms of the orbital angular velocity Ω_{orb} (e.g. Frank, King & Raine 2002, p.352) as

$$H \approx \frac{c_s}{\Omega_{orb}}$$

$$H \approx \left(\frac{P_{orb}}{2\pi}\right) c_s$$

$$\Rightarrow \quad H \approx \frac{3600}{2\pi}\left[P_{orb}(h)\right]c_s \ \text{ cm.} \tag{3.21}$$

Approximating the funnel cross-section area as $\Delta S \approx \pi H^2$, equation (3.20) can be express in the form

$$-\dot{M}_2 \approx \rho_{L1} c_s \pi \left(\frac{P_{orb}}{2\pi} c_s\right)^2$$

$$-\dot{M}_2 \approx \frac{1}{4\pi}\rho_{L1} c_s^3 P_{orb}^2 . \tag{3.22}$$

It is obvious from this equation that the mass transfer rate from the secondary star depends on the fluid ram pressure ($\rho_{L1} c_s^2$), the temperature and the orbital period, i.e.

$$-\dot{M}_2 \propto \left(\rho_{L1} c_s^2\right)\left(P_{orb}\right)^2\left(c_s\right). \tag{3.23}$$

The orbital period is a measurable quantity but some knowledge of the general properties of stellar atmospheres is required to estimate the fluid density ρ_{L1}. It has been shown (Ritter 1988; e.g. Warner 1995, p.34-35) that atmospheric density of mass transferring stars at the L_1 region can be estimated as

$$\rho_{L1} \approx \frac{1}{\sqrt{e}}\rho_{phot} \exp\left[-\left(\frac{R_{2,L1} - R_{2,*}}{H_P}\right)\right] \tag{3.24}$$

where $\rho_{phot} \sim 10^{-6}$ g cm^{-3} (e.g. Frank, King & Raine 2002, p.352), and $R_{2,L1}$, $R_{2,*}$ and H_P represent respectively the Roche lobe radius of the secondary star at L_1, the photospheric radius of the secondary star and the pressure scale height

$$H_P \approx \frac{c_s^2 R_{2,*}^2}{GM_2} . \tag{3.25}$$

It has been shown (Meintjes 2004) that for AE Aqr the ratio

$$3 \le \frac{R_{2,L1} - R_{2,*}}{H_P} \le 4 ,$$

and this may be representative for most mass transferring stars in close binaries. Then the density of the secondary star's atmosphere at the L_1 region, i.e.

$$\rho_{L1} \approx 2\times 10^{-8}\left(\frac{\rho_{phot}}{10^{-6}\ g\,cm^{-3}}\right) \text{ g cm}^{-3} \tag{3.26}$$

may be a representative value for most secondary stars in MCVs. The ram pressure of the flow through the L_1 region is then basically determined by the photospheric temperature of the secondary star. Using equation (3.22) the density of a fluid flowing through the L_1 region for any orbital period and appropriate mass transfer rate above the period gap can be estimated. Since the secondary stars in the systems considered in this study are magnetized, this may have an effect on the mass transfer inflow and hence the difference in the mass transfer rates obtained, which is now investigated.

For a magnetically controlled mass transfer through the L_1 region, the magnetic pressure in the nozzle must dominate the ram pressure of the fluid. If the flow speed through the nozzle is of the order of local sound speed, the resulting ram pressure is given by

$$P_{ram} = \rho_{L1} c_s^2 . \tag{3.27}$$

The minimum magnetic field required to influence the fluid flow through the L_1 region is given by (Ritter 1988)

$$B_{L1} = \left(8\pi P_{ram}\right)^{1/2} . \tag{3.28}$$

If it is assumed that the region of the atmosphere of the secondary star close to the L_1 region is isothermal, then the isothermal sound speed in this region is given by (Ritter 1988; e.g. Campbell 1997, p. 64)

$$c_s = \left(\frac{P}{\rho}\right)^{1/2}$$

$$\Rightarrow \quad c_s = \left(\frac{\Re}{\gamma} T\right)^{1/2} \tag{3.29}$$

where $\Re$ is the gas constant, T the effective temperature and γ the mean molecular weight. Since the secondary stars in CVs are mainly cool late-type main-sequence stars, it can be assumed that $T \approx 3000\,K$ for these systems. Taking $\gamma \approx 0.6$ (e.g. Campbell 1997, p.64) and $\Re = 8.314 \times 10^7$ cm^2 s^{-2} K^{-1}, it can be shown that $c_s \approx 6.447 \times 10^5$ cm s^{-1}. The values of H, ρ_{L1}, P_{ram} and B_{L1} can then be calculated using equations (3.21), (3.22), (3.27) and (3.28) respectively. The results obtained are shown in Table 3.

Name	$P_{orb}(h)$	H (cm) ($\times 10^9$)	ρ_{L1}(g cm^{-3}) ($\times 10^{-8}$)	P_{ram}(erg cm^{-3}) ($\times 10^3$)	B_{L1}(Gauss)
BG CMi	3.24	1.197	1.248	5.187	361
V_{1223} Sgr	3.37	1.245	1.236	5.137	359
AO Psc	3.59	1.326	1.241	5.158	360
YY Dra	3.91	1.444	1.340	5.570	374
DQ Her	4.65	1.718	1.489	6.189	394
FO Aqr	4.85	1.792	1.523	6.330	398
V_{533} Her	5.04	1.862	1.567	6.513	404
PQ Gem	5.18	1.913	1.632	6.782	412
TV Col	5.49	2.028	1.741	7.236	426
TX Col	5.72	2.113	1.803	7.494	433
XY Ari	6.06	2.238	1.941	8.068	450

Table 3. Showing calculated values of the funnel width (H), density at L_1 (ρ_{L1}), ram pressure (P_{ram}) and magnetic field at L_1 (B_{L1}).

If a secondary star has magnetic activity in the equatorial region, prominences drifting across the stellar surface to the L_1 region can result in strong magnetic fields influencing the mass flow through the L_1 region. From the results obtained in Table 3, the magnetic field at the L_1 region $B_{L1} \sim 400$ Gauss. The model calculations performed and illustrated in Table 2 show that the secondary stars in MCVs may have surface polar field ranging between $B_0 \sim 2900 - 3200$ Gauss for the non-linear law with field saturation. This demonstrates that there is a distinct possibility that the equatorial belt may also be magnetically active like the sun. This could mean that there may be some equatorial magnetic field structures (prominences or star spots) having $B_{eq} > 400$ Gauss. It is also noted that, for these systems, the funnel width for the widest system is approximately twice that of the most compact system. This could also mean that the field density in the funnel for the compact systems exceeds that of the wider systems resulting in a higher

magnetic viscosity experienced by the flow in the compact systems. This may in fact explain why the mass transfer rate decreases with decreasing orbital period, which is implicated by the results obtained earlier. Therefore the physical process resulting in the enhanced magnetic viscosity and decreasing mass transfer in the short period systems has to be investigated.

3.5.1 Magnetic viscosity

In a fluid magnetic fields act on both electrons and ionized atoms to produce dynamical effects which affect the bulk motion of the medium itself. For a conducting fluid flowing across magnetic field lines, the electromagnetic influence is driven by the magnetic component of the Lorentz force due to its dominance over the electric component (e.g. Jackson 1975, p.471). In the presence of electromagnetic fields, the behaviour of a conducting fluid is governed to a large extend by the magnitude of the conductivity whose effects are both electromagnetic and mechanical.

Considering, for simplicity, a non permeable fluid described by matter density $\rho(\vec{x},t)$, velocity $\vec{v}(\vec{x},t)$, pressure $P(\vec{x},t)$, and conductivity σ, the equation of motion of a fluid is given by (e.g. Jackson 1975, p.471)

$$\rho\frac{d\vec{v}}{dt} = -\vec{\nabla}P + \frac{1}{c}\left(\vec{J}\times\vec{B}\right) + \vec{f}_v + \rho\vec{g}\,, \tag{3.30}$$

which in addition to pressure and magnetic forces includes gravitational force, $\rho\vec{g}$ and the viscous force, $\vec{f}_v$ given by

$$\vec{f}_v = \mu_k\nabla^2\vec{v}\,, \tag{3.31}$$

in the case of an incompressible fluid, where μ_k represents the coefficient of kinematic viscosity. Neglecting the displacement current, the electromagnetic field in the fluid is described by the equations (e.g. Jackson 1975, p.471)

$$\vec{\nabla}\times\vec{E} + \frac{1}{c}\frac{\partial\vec{B}}{\partial t} = 0\,, \tag{3.32}$$

$$\vec{\nabla} \times \vec{B} = \frac{4\pi}{c} \vec{J} \,. \tag{3.33}$$

For a one-component conductivity, Ohm's law can assume the form

$$\vec{J} = \sigma\left(\vec{E} + \frac{\vec{v}}{c} \times \vec{B} \right). \tag{3.34}$$

Assuming that the conductivity of the fluid is effectively infinite, then under the action of the fields $\vec{E}$ and $\vec{B}$ the fluid flows in such a way that

$$\vec{E} + \frac{1}{c}\left(\vec{v} \times \vec{B}\right) = 0 \,. \tag{3.35}$$

From equations (3.32), (3.33), (3.34) and (3.35), the evolution of the magnetic field in the fluid is determined by

$$\frac{\partial \vec{B}}{\partial t} = \frac{c^2}{4\pi\sigma} \nabla^2 \vec{B} + \vec{\nabla} \times \left(\vec{v} \times \vec{B}\right)$$

$$\frac{\partial \vec{B}}{\partial t} = \eta \nabla^2 \vec{B} + \vec{\nabla} \times \left(\vec{v} \times \vec{B}\right), \tag{3.36}$$

where $$\eta = \frac{c^2}{4\pi\sigma} \tag{3.37}$$

represents the resistive diffusion coefficient of the fluid. For a fluid at rest, i.e. $v = 0$, equation (3.36) reduces to

$$\frac{\partial \vec{B}}{\partial t} = \eta \nabla^2 \vec{B} \,. \tag{3.38}$$

If L is a length-scale of the magnetic field, from equation (3.38), an initial configuration of the magnetic field will decay in a diffusion time

$$\tau \sim \frac{L^2}{\eta} \,. \tag{3.39}$$

The magnetic Reynolds number R_m is defined as

$$R_m = \frac{v\tau}{L} = \frac{Lv}{\eta} = \frac{4\pi\sigma}{c^2} Lv \,. \tag{3.40}$$

The magnetic Reynolds number R_m is useful in distinguishing between situations in which diffusion of field lines relative to the fluid occur and those in which the lines of force are frozen into the fluid. From equation (3.40), $R_m \to \infty$ as $\sigma \to \infty$, resulting in

the diffusion term being zero. In this case the magnetic field is frozen into the fluid, implying that the magnetic field cannot easily diffuse into or out of the fluid. This implies that a moving fluid will advect the field with it if the fluid ram pressure significantly exceeds the magnetic pressure.

In CVs the effective gravity at the L_1 region is zero. In this case the gravitational term in equation (3.30) can be neglected and for a steady state, i.e. $dv/dt = 0$, it takes the form

$$\vec{\nabla} P = \frac{1}{c}\left(\vec{J} \times \vec{B}\right) + \mu_k \nabla^2 \vec{v} \,. \tag{3.41}$$

In the following discussion, consider an incompressible, viscous conducting fluid flowing in the x-direction between two non conducting boundary surfaces at $z = 0$ and $z = L$, representing the edges of the funnel across L_1. Also assume a uniform magnetic field B_a in the z-direction, acting as a barrier for the flow along the x-direction. In this case the only non varnishing component of $\vec{J}$ is given by (e.g. Jackson 1975, p.476)

$$J_y(z) = \sigma\left(E_0 - \frac{1}{c} B_a v\right),$$

where E_o is the only component of the electric field and is in the y-direction, and must therefore be constant. In the expression above v is the flow velocity in the x-direction. The x-component of the equation of motion, equation (3.41), is therefore given by

$$\frac{\partial P}{\partial x} = \frac{\sigma B_a}{c}\left(E_0 - \frac{B_a}{c} v\right) + \mu \frac{\partial^2 v}{\partial z^2} \,. \tag{3.42}$$

Assuming that the pressure gradient in the x-direction, i.e. $\partial P/\partial x \to 0$ at a localized position (i.e. L_1, if it is significantly removed from the photosphere), equation (3.42) can be expressed in the form

$$\frac{\partial^2 v}{\partial z^2} - \frac{\sigma B_a^2}{\mu_k c^2} v = -\frac{\sigma B_a}{\mu_k c} E_0$$

$$\frac{\partial^2 v}{\partial z^2} - \frac{\sigma B_a^2 L^2}{\mu_k c^2 L^2} v = -\frac{\sigma B_a^2 L^2}{\mu_k c^2 L^2} \frac{c E_0}{B_a}$$

$$\frac{\partial^2 v}{\partial z^2} - \left(\frac{M_H}{L}\right)^2 v = -\left(\frac{M_H}{L}\right)^2 \frac{cE_0}{B_a}, \tag{3.43}$$

where $$M_H = \left(\frac{\sigma B_a^2 L^2}{\mu_k c^2}\right)^{1/2} \tag{3.44}$$

is the Hartmann number, i.e. the ratio of the magnetic viscosity to the fluid kinematic viscosity (μ_k). If $M_H >> 1$ the flow will ram into a rigid magnetic obstruction, resulting in the fluid experiencing severe effect of magnetic viscosity (e.g. Jackson 1975, p.477), forcing it to decelerate across the field lines.

The interaction of magnetic field with the fluid mainly occurs through the Lorentz interaction with the electron-ion population. It has been shown (Meintjes 2004) that the plasma population in the envelope of the secondary star may be weakly ionized, resulting in a large discrepancy between the electron-ion and neutral atom concentrations. This may result in ambipolar diffusion which occurs readily in low-density plasma with a low degree of ionization. In the solar photosphere ($T_{phot} = 6000\,K$) where the ratio of ions to neutrals is one part in 10^4 (e.g. Parker 1979, p.46) ambipolar diffusion across a magnetic field of magnitude $B \sim 10^4$ Gauss is negligible. This result should hold for the secondary stars considered here, where the ion-neutral ratio and magnetic fields may probably not be drastically different from the solar photospheric values mentioned above. The ambipolar diffusion timescale of the ion population with magnetic field tied to them, through the sea of neutral atoms, represents essentially the timescale of diffusion of the neutral population through the field. Meintjes (2004) showed that the ambipolar diffusion timescale for the secondary star in AE Aqr is of the order of

$$\tau_{AD} \geq 20\left(\frac{L}{H}\right)^2 \left(\frac{B_{L1}}{300\,Gauss}\right)^{-2} \text{ yr},$$

and this diffusion timescale is most probably representative for the secondary stars considered here. This timescale is significantly higher than the timescale of interest in this study. This result seems to confirm that for all practical purposes the flow across the fields is stopped by the strong magnetic viscosity. The flow can only slip through the grip of the magnetic field over the timescale of interest when the ram pressure across the

magnetic barrier is strong enough, exceeding the magnetic pressure. In the case of a decelerated fluid, the necessary momentum density to traverse the magnetic region may be supplied if the fluid density increases significantly.

The effect of magnetic viscosity on the fluid flow in the funnel critically depends on the presence of magnetic field in the funnel region. Drifting star spots in the equatorial belt may eventually come in contact with the funnel region at L_1. The rapid diffusion of magnetic field into the flow is however prevented unless the flow may be turbulent. It can be shown that the Reynolds number of the flow, i.e.

$$R_m = \frac{\rho_{L1} H v}{\mu_k}$$

$$R_m \approx 2\times 10^9 \left(\frac{\rho_{L1}}{10^{-8}\, g\, cm^{-3}}\right)\left(\frac{H}{10^9\, cm}\right)\left(\frac{v}{c_s}\right)\left(\frac{\mu_k}{3.5\times 10^{-3}}\right)^{-1}, \qquad (3.45)$$

where $\mu \approx 3.5\times 10^{-3}$ g cm^{-1} s^{-1} represents the coefficient of kinematic viscosity. Flows with such high Reynolds number may be highly turbulent at times (e.g. Tritton 1973) since laboratory experiments seem to suggest that turbulence may set in at $R_m \sim 1000 - 10^5$. The onset of turbulence may result in a rapid break down of standard MHD which prevents rapid diffusion as a result of high magnetic Reynolds number in the flow. The onset of turbulence results in ordinary resistive diffusion coefficient being replaced by turbulent diffusion coefficient which is defined as (e.g. Campbell 1997, p.42)

$$\eta_T = \frac{1}{3} c_s L\,. \qquad (3.46)$$

From equations (3.37) and (3.46) the conductivity in this case can be expressed as

$$\sigma = \frac{3c^2}{4\pi c_s L}. \qquad (3.47)$$

The turbulent viscosity ν_T can be expressed in the form (e.g. Campbell 1997, p.64)

$$\nu_T = (0.1)\, c_s\, L\,. \qquad (3.48)$$

Using the equations above, the values of σ, ν_T, μ_k, M_H and R_m can be calculated. The results obtained are shown in Table 4.

Name	$P_{orb}(h)$	σ (s^{-1}) ($\times 10^5$)	ν_T ($cm^2\ s^{-1}$) ($\times 10^{14}$)	μ_k ($g\ cm^{-1}s^{-1}$) ($\times 10^6$)	M_H	R_m
BG CMi	3.24	2.784	0.772	0.963	7.74	3.00
V_{1223} Sgr	3.37	2.677	0.803	0.992	7.74	3.00
AO Psc	3.59	2.513	0.855	1.061	7.74	3.00
YY Dra	3.91	2.308	0.931	1.247	7.74	3.00
DQ Her	4.65	1.940	1.108	1.650	7.73	3.00
FO Aqr	4.85	1.860	1.155	1.759	7.74	3.00
V_{533} Her	5.04	1.790	1.200	1.880	7.73	3.00
PQ Gem	5.18	1.742	1.233	2.012	7.74	3.00
TV Col	5.49	1.643	1.307	2.275	7.74	3.00
TX Col	5.72	1.577	1.362	2.456	7.73	3.00
XY Ari	6.06	1.489	1.443	2.801	7.74	3.00

Table 4. Showing calculated values of conductivity (σ), turbulent viscosity (ν_T) kinematic viscosity (μ_k), Hartmann number (M_H) and magnetic Reynolds number (R_m).

From the results obtained in Table 4, $M_H \sim 7.74$ and $R_m \sim 3.00$. As mentioned earlier, the effect of magnetic viscosity is severe if $M_H >> 1$ and fast diffusion of magnetic field is possible when $R_m \to 1$. The results are promising since the presence of turbulence in the flow results in $R_m \to 1$, facilitating the fast diffusion of magnetic field into the funnel from the photospheric region surrounding it. The presence of turbulence results in the Hartmann number, i.e. the ratio of magnetic to particle viscosity $M_H \sim 1 - 10$, which opens-up the possibility of magnetic advection and accompanying magnetic reconnection in the funnel. The advection of flux along the funnel will have a significant influence on the mass transfer from the secondary star, and will be discussed briefly in the following section.

3.5.2 Magnetic advection with the fluid flow

In an earlier analysis (section 3.5), it was noted that there was variation in mass transfer in the systems considered in this study, which could be as a result of magnetic viscosity in the funnel. If magnetic field is advected with the fluid flow into the funnel, it may have severe effect on the mass flow through the funnel, and this could explain the mass transfer variation obtained in the systems considered in this study. In this section it will therefore be investigated if the results obtained in the previous discussions can account for magnetic field advection along the flow. As mentioned in the previous section, the condition for advection of magnetic flux with the fluid flowing across a magnetic field can be determined by the ratio of magnetic Reynolds number and Hartmann number which is now discussed in more detail.

The solution to equation (3.43), assuming boundary conditions $v(0) = v_1$ and $v(L) = v_2$ is readily found to be (e.g. Jackson 1975, p.477)

$$v(z) = \frac{v_1}{\sinh M_H}\left[M_H\left(\frac{L-z}{L}\right)\right] + \frac{v_2}{\sinh M_H}\sinh\left(\frac{M_H z}{L}\right) + \frac{cE_0}{B_a}\left[1 - \frac{\sinh\left[M_H\left(L-z\right)/L\right] + \sinh\left(M_H z/L\right)}{\sinh M_H}\right]. \tag{3.49}$$

Since the condition for magnetic viscosity to dominate the flow is $M_H >> 1$, and also from the calculation it is found that $M_H > 1$, the limit of $M_H >> 1$ will therefore be considered, in which case it is expected for the magnetic viscosity to dominate and the flow to be determined almost entirely by the $\vec{E} \times \vec{B}$ drift. Since the flow is considered to be in the x-direction, the magnetic field in the x-direction $B_x(z)$ can be determined from equations (3.33) and (3.34), i.e.

$$\frac{\partial B_x}{\partial z} = \frac{4\pi\sigma}{c}\left(E_0 - \frac{B_a v}{c}\right). \tag{3.50}$$

Substituting equation (3.49) for velocity into equation (3.50), it can be shown (e.g. Jackson 1975, p.478) that

$$B_x(z) = B_a\left[\left(\frac{4\pi\sigma L^2}{c^2}\right)\left(\frac{v_2 - v_1}{2L}\right)\right]\left(\frac{\cosh(M_H/2) - \cosh(M_H/2 - M_H z/L)}{M_H \sinh(M_H/2)}\right). \quad (3.51)$$

From equation (3.51) the term $(v_2 - v_1)/2$ is a typical velocity and L is a typical length. The dimensionless quantity in the square brackets can therefore be identified as the magnetic Reynolds number R_m. Therefore in the limit of $M_H >> 1$ equation (3.51) reduces to

$$\frac{B_x(r)}{B_a} = \frac{R_M}{M_H}\left[1 - \left(\exp\left(-\frac{M_H r}{L}\right) + \exp\left(-M_H\left[\frac{L - r}{L}\right]\right)\right)\right], \quad (3.52)$$

where the radial distance $r = z$. Expressing r as a fraction of the funnel width, i.e. r/L where $L = H$, values of $B_x(r)/B_a$ can be calculated, from which values of the magnetic field at the various radial distances advected into the funnel with the fluid flow can be determined. A graph of $B_x(r)/B_a$ against r/L is shown in Figure 9.

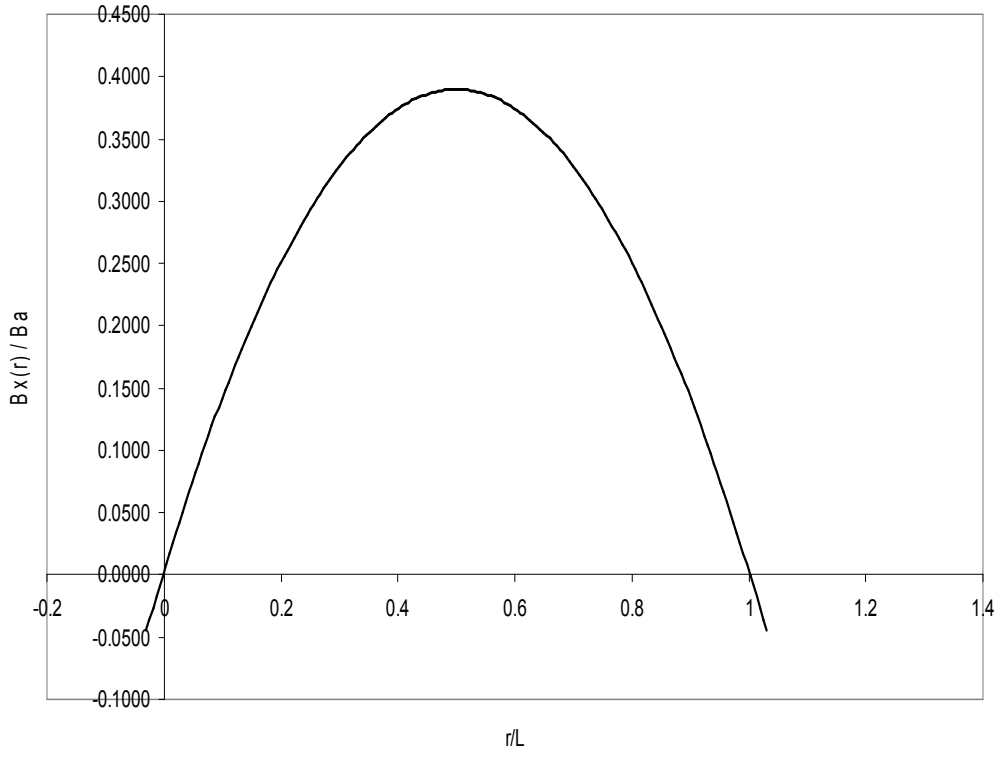

Figure 9. Radial component of magnetic field advected into the funnel (for Hartmann number, M_H = 7.74 and magnetic Reynolds number, R_m = 3.00).

From the graph above (Figure 9), it is noted that there is appreciable advection of magnetic field into the funnel which results in the flow having to cross a magnetic barrier. This forms the basis of magnetic viscosity in the funnel. This could be the cause for the mass transfer variation obtained for the systems considered. The tension in the advected field in the funnel will provide a resistance in the opposite direction to the fluid flow and this will break the flow of fluid across L_1. For the fluid to be able to flow freely across the L_1 region, the ram pressure, P_{ram} must significantly exceed the magnetic pressure in the L_1 region, i.e. $P_{ram} > P_{mag}$. The ratio $B_x(r)/B_a$ is representative of the ratio B_{L1}/B_{eq}, where B_{eq} represents the value of magnetic structures in the equatorial belt close to the stellar surface. Therefore B_{eq} is representative of the average limiting field strength of magnetic prominences which can allow mass transfer to proceed. From the ratio B_{L1}/B_{eq} the values of B_{eq} can be determined and is shown in Table 5. It can be seen from the results that an average field strength $B_{eq} \approx 1000$ Gauss is required for mass transfer to proceed in these systems.

Name	P_{orb} (hours)	B_{eq} (Gauss)
BG CMi	3.24	972
V_{1223} Sgr	3.37	967
AO Psc	3.59	969
YY Dra	3.91	1007
DQ Her	4.65	1061
FO Aqr	4.85	1072
V_{533} Her	5.04	1088
PQ Gem	5.18	1109
TV Col	5.49	1147
TX Col	5.72	1166
XY Ari	6.06	1212

Table 5. Showing calculated values of B_{eq}.

To conclude this study, the influence of the advected magnetic field into the funnel on the nature of mass transfer through the L_1 region will be investigated. The equation of motion of a fluid parallel and perpendicular to a magnetic field, grouping all the non-electromagnetic forces under $\vec{f}$, are given by (Meintjes 2004)

$$\rho\frac{dv_{\parallel}}{dt} = f_{\parallel} \tag{3.53}$$

$$\rho\frac{dv_{\perp}}{dt} = f_{\perp} - \frac{\sigma B^2}{c^2}\left(v_{\perp} - w\right), \tag{3.54}$$

where $v_{\perp}$ represents the flow speed across the magnetic field, and $\vec{w} = \left(c/B^2\right)\left(\vec{E}\times\vec{B}\right)$ is the drift velocity of the individual particle guiding centre in the presence of combined electric and magnetic field across the funnel. From equations (3.53) and (3.54), it is noted that only non-electromagnetic forces can drive the fluid parallel to the magnetic field, while a combination of both non-electromagnetic and electromagnetic forces have to drive the fluid across the magnetic field. As mentioned earlier, the magnetic field in the funnel will provide a barrier to the flow, i.e. magnetic viscosity, forcing the fluid to decelerate across the field lines. The viscosity component which provides the deceleration of the fluid across the magnetic field is manifested in the second term in equation (3.54), and therefore it can be taken as

$$\rho\frac{dv_{\perp}}{dt} = -\frac{\sigma B^2}{c^2}\left(v_{\perp} - w\right)$$

$$\rho\frac{dv_{\perp}}{dt} = -\frac{\sigma B^2 c_s}{c^2}\left(1 - \frac{w}{c_s}\right)$$

$$\Rightarrow \frac{dv_{\perp}}{dt} = -\frac{\sigma B^2 c_s}{\rho c^2}\left(1-\alpha\right), \tag{3.55}$$

where $v_{\perp} = c_s$ and $\alpha = w/c_s$. The speed of a particle at time t can be expressed as

$$v(t) = v(t=0) + \frac{dv}{dt}\Delta t\,. \tag{3.56}$$

Using equation (3.55), equation (3.56) can be expressed in the form

$$v(t) = c_s - \frac{\sigma \mathrm{B}^2 c_s}{\rho \mathrm{c}^2}\left(1-\alpha\right)\Delta t$$

$$\Rightarrow \quad v(t) = c_s\left[1 - \frac{\sigma \mathrm{B}^2 L}{\rho \mathrm{c}^2 c_s}(1-\alpha)\right], \tag{3.57}$$

where $v(t=0) = c_s$ and $\Delta t = L/c_s$. The rate of mass flow across the barrier (i.e. the L_1 region) for a fluid flowing at a speed given by equation (3.57) can be calculated from

$$-\dot{M}_2 = \rho A v(t), \tag{3.58}$$

where A is the cross-sectional area of the funnel at the L_1 region. Using equation (3.58) and approximating $A \approx \pi L^2$ and taking $\rho = \rho_{L1}$, the mass transfer rate for a fluid flowing at a speed given by equation (3.57) can be calculate. The results obtained are shown in Table 6.

Name	P_{orb} (hours)	$-\dot{M}_2 (g\,s^{-1})$ $(\times 10^{16})$
BG CMi	3.24	1.45
V_{1223} Sgr	3.37	1.56
AO Psc	3.59	1.77
YY Dra	3.91	2.27
DQ Her	4.65	3.57
FO Aqr	4.85	3.99
V_{533} Her	5.04	4.42
PQ Gem	5.18	4.87
TV Col	5.49	5.82
TX Col	5.72	6.57
XY Ari	6.06	7.89

Table 6. Showing mass transfer rates calculated in a case where there is magnetic viscosity.

From the results obtained in Table 6, it is noted that the mass transfer rates obtained in this case are approximately 40% of the observationally confirmed mass transfer rates

calculated earlier for these systems using the non-linear dynamo law for the case with field saturation (see Table 1). This is due to the magnetic viscosity at the L_1 region, resulting in a low fluid flow rate across the magnetic barrier, i.e. the effect of magnetic viscosity. The fluid pressure required to drive the fluid at the rates obtained using the non-linear dynamo law for the case with field saturation can be calculated from the results above. The required condition that has to be satisfied is given by

$$\rho_{L1} v^2(t) > \frac{B_{eq}^2}{8\pi}$$

$$\Rightarrow \quad \rho_{L1} > \frac{B_{eq}^2}{8\pi v^2(t)}.$$

The results are shown in Table 7.

Name	P_{orb} (hours)	ρ (g cm^{-3}) ($\times 10^{-8}$)
BG CMi	3.24	3.116
V_{1223} Sgr	3.37	3.082
AO Psc	3.59	3.101
YY Dra	3.91	3.347
DQ Her	4.65	3.711
FO Aqr	4.85	3.781
V_{533} Her	5.04	3.900
PQ Gem	5.18	4.054
TV Col	5.49	4.336
TX Col	5.72	4.475
XY Ari	6.06	4.845

Table 7. Showing the fluid density required for the mass transfer rates calculated in Table 1 for the non-linear dynamo law with field saturation, for fluid flowing with speed given by equation (3.57).

From the results obtained in Table 7, it is also noted that the required fluid density is appreciably higher compared to the density of the fluid at L_1 calculated earlier, which is approximately 40% of the required fluid density. This would mean that the pressure required for the fluid to flow freely though the magnetic barrier has to significantly exceed the magnetic pressure, i.e. $P_{ram} > P_{mag}$ (e.g. Davidson & Ostriker 1973). Thus for the mass to flow at the rate determined by the non-linear law with field saturation (see Table 1), the fluid pressure must build up in order to break through the magnetic barrier. This would therefore mean that the mass flow in these systems is not continuous but probably fragmented in the form of blobs. This blob accretion at the L_1 point therefore gives an alternative to blob accretion due to Rayleigh-Taylor instability at the threading point between the magnetic field of the white dwarf and the accretion stream (Kuijper & Pringle 1982). The result obtained is however consistent with the inferred mode of mass transfer in MCVs (King & Lasota 1991; King 1993; Wynn & King 1995). It has been pointed by these authors that the spin-up relation observed in the intermediate polars, i.e.

$$P_{spin} \sim 0.1 P_{orb},$$

and the shot noise observed in ASCA X-ray data of AM Her may be the direct result of a blob-like fragmented mass transfer and accretion in MCVs. This may be the direct result of mass transfer from a magnetized secondary star, resulting in magnetic viscosity to fragmentize (break-up) the flow through the funnel at L_1. The result above is consistent with the fact that the more compact systems are more affected by magnetic viscosity in the funnel, as a result of a more significant portion of the funnel being occupied by magnetic flux from star spots that diffused in as a result of turbulent flow.

Chapter Four

Conclusions

This study aimed to investigate the influence of the secondary star magnetic field on mass transfer in cataclysmic variables, particularly the intermediate polars whose orbital periods are known. The mass transfer rates and surface polar magnetic fields of these systems were calculated using the stellar wind theory and the inferred dynamo laws responsible for the stellar magnetic field production in stars. For all the dynamo laws considered, it was found that the mass loss rate of the secondary star due to its stellar wind is negligible over the lifetime of the system, and therefore the total mass of these systems can be considered to be conserved. All the three dynamo laws also satisfy the condition for thermal equilibrium of the secondary star.

The mass transfer rates obtained using the linear dynamo law are at most comparable to the mass transfer rates driven by gravitational radiation, while the inverse Rossby number law gives mass transfer rates slightly higher than those driven by gravitational radiation. In both cases the mass transfer rates obtained cannot explain the high mass transfer rates observed for these systems above the period gap. For the non-linear law, two cases were considered: the case with field saturation and unsaturated field. It is only the case with field saturation that gives mass transfer rates most consistent with the theories of the period gap. However, in general, the mass transfer rates driven by magnetic braking increase with increasing orbital period for all the three dynamo laws.

From the values of the surface polar magnetic field of the secondary stars determined for the three dynamo laws, both the linear dynamo law and the inverse Rossby number law produce values of the surface polar magnetic field which are lower than the expected values, while the non-linear law, with saturated field, gives values in the correct order of magnitude. In the case of field saturation, the values obtained are representative of tidally locked secondary stars in MCVs, and therefore it can be assumed that these systems have an average value of surface polar magnetic field, $B_0 \sim 3000$ Gauss. This could mean that the intermediate polars may evolve into polars if the orbital separation has shrunk enough to be comparable to the magnetospheric radius. In general, for the other dynamo laws the surface polar magnetic field decreases with increasing orbital period.

Based on the results for the non-linear law for the case with field saturation, these systems have an average surface polar magnetic field of $B_0 \sim 3000$ Gauss, while the mass transfer rates increase with increasing orbital period. For these systems it is also shown that there is probably a magnetic field of ~ 1000 Gauss on the surface which can significantly influence the flow. Magnetic viscosity has a significant effect on the mass flow if the Hartmann number, $M_H >> 1$. But for the systems considered it is found that $M_H \to 1$, i.e. $M_H \sim 7.74$ meaning that it is possible for magnetic field to be advected with the flow into the funnel. This is also possible if the magnetic Reynolds number, $R_m \to 1$, which is confirmed by the result obtained, $R_m \sim 3.00$, i.e. a small magnetic Reynolds number results in a more effective advection of magnetic field with the flow. As a result of the advected field, the fluid will be trapped in a rigid magnetic obstruction, resulting in a severe magnetic viscosity that results in a significant deceleration of the fluid across the magnetic barrier. This therefore explains the low mass transfer rates in the more compact systems since they are more affected by magnetic viscosity at the L_1 region, as a result of the advected magnetic field into the funnel due to turbulent flow.

For the systems considered here the magnetic pressure at the L_1 region exceeds the fluid pressure, i.e. the advected magnetic field in the funnel results in the magnetic pressure at the L_1 region exceeding the ram pressure. In this case the fluid can not easily flow across

the magnetic barrier. For the fluid to flow across the magnetic barrier, the fluid pressure must build up until it is high enough to break through the barrier. Each time the fluid has broken through the barrier, the ram pressure decreases below the equipartition value, preventing continuous flow of the fluid. This therefore means that the mass transfer in these systems is fragmented in form of blobs, which is consistent with the inferred mode of mass transfer in MCVs. This blob accretion at the L_1 point provides an alternative to the blob accretion due to Rayleigh-Taylor instability at the threading point between the magnetic field of the white dwarf and the accretion stream.

The advection of magnetic field with the flow may also provide a seed for accretion disc magnetic field in cataclysmic variables. This magnetic field can be amplified by dynamo mechanisms in the accretion disc. The presence of magnetic fields in the accretion disc play a significant role on the flow of material through the disc, i.e. so-called magnetic viscosity, which influences the mass accretion rate onto the white dwarf.

The advent of the SALT[2] era opens-up possibility for observational Astronomy in South Africa and Africa in general. The availability of a 10 m class telescope with sensitive photometric (SALTICAM[3]) and spectrophotometric and spectropolarimetric (PFIS[4]) capabilities will allow detailed observations of MCVs to identify possible short timescale variability of the red component possibly related to magnetic activity. The polarimetric capabilities of PFIS may be used to constrain magnetic fields on the secondary star which will constrain the dynamo mechanism at work in these systems. High time resolution photometry may also result in the detection of time variability associated with fragmented magnetized mass transfer.

[2] Southern African Large Telescope
[3] SALT Optical Imaging Camera
[4] Prime Focus Imaging Spectrograph

References

Beardmore, A.P., Done, C., Osborne, J.P., Ishida, M., 1995, *Mon. Not. R. Astr. Soc.*, **233**, 759

Beuermann, K., 1988*, in Polarizes Radiation of circumstellar Origin*, eds. G.V. Coyne, S.J., A.A. Magalhães, Moffat, A.F.J., R.E. Schulte-Ladbeck, S.Tapia, .T.Wickramasinghe (Vatican Observatory-Vatican city), 125

Beuermann, K.1998, *High Energy Astronomy and Astrophysics*, India University Press

Beuermann, K., Burwitz, V., 1995 *ASP Conference series,* **85**, 99

Beuermann, K., Woelk, U*., 1996 IAU coll*, **158**, 199

Boris, T. Gansicke, 1998 *ASP conference series* **137**, 88

Campbell, C.G., 1997*, Magnetohydrodynamics in Binary Stars*, Kluwer

Chanmugam, G., Ray, A. 1984, *Astrophys. J.*, **285**, 252

Chanmugam, G., Frank, J., 1987, *Astrophys. J.*, **320**, 746

Collier A. Cameron, *ASP Conference series* 2002, **261**, 11

Davidson, K., Ostriker, J.P., 1973, *Astrophys. J.*, **179**, 585

Done, C., Osborne, J.P., Beardmore, A.P., 1995*, Mon. Not. R. Astr. Soc*., **276,** 483

Frank, J., King, A.R., Raine, D., 1992 *Accretion Powers in Astrophysics*, Cambridge University Press

Frank, J., King, A.R., Raine, D., 2002 *Accretion Powers in Astrophysics*, Third edition, Cambridge University Press

Gansicke, B.T., Beuermann, K., de Martino, D., 1995 *Asron. Astrophys*., **303**, 127

Hamuery, J.M., King, A.R., & Lasota, J.P., 1986, *Mon. Not. R. Astr. Soc*., **218**, 695

Hamuery, J.M., King, A.R., & Lasota, J.P., 1989, *Mon. Not. R. Astr. Soc*., **237**, 39

Hellier, C., 2001, *Cataclysmic Variables, How and why they Vary*, Springer-Praxis

Jackson, D. J., 1975, *Classical Electrodynamics*, Wiley & sons, New York

King, A.R., 1988, *Mon. Not. R. Astr. Soc*., **29**, 1

King, A.R., 1993, *Mon. Not. R. Astr. Soc*., **261**, 144

King, A.R., & Lasota, J.P., 1979, *Mon. Not. R. Astr. Soc*., **188**, 653

King, A.R., & Watson, M., 1987, *Mon. Not. R. Astr. Soc*., **227**, 205

King, A.R., & Lasota, J.P., 1991, *Astrophys. J*., **378**, 674

Kippenhahn. R., & A.Weigert, 1990, *Stellar Structure and Evolution*, Springer-Verlag, Berlin

Kraft, R.P., Mathews, J.L., 1962, *Astrophys. J*., **136**, 312

Kuijper, J., Pringle, J.E., 1982, *Atron. Astrophys*., **114,** L4

Lamb, D.Q., & Masters, A.R., 1979, *Astrophys. J*., **234**, L117

Livio, M., Pringle, J.E., 1994, *Astrophys. J*., **427**, 956

Lubow, S.H., Shu F.N., 1975, *Astrophys. J*., **198**,383

Meintjes, P.J., 2002a, African Skies No.7

Meintjes, P.J., 2002b, *Mon. Not. R. Astr. Soc*., **336**, 265

Meintjes, P.J., 2004, *Mon. Not. R. Astr. Soc*., **352**, 416

Meintjes, P.J., Venter, L.A., 2003, *Mon. Not. R. Astr. Soc*., **341**, 891

Mestel, L., 1968, *Mon. Not. R. Astr. Soc*., **138**, 359

Mestel, L., Spruit, H.C., 1987, *Mon. Not. R. Astr. Soc*., **226**, 57

Meyer-Hofmeister, E., Vogt, N., Meyer, F., 1996, *Atron. Astrophys*, **310**, 519

Norton, A.J., Watson, M.G., 1988, *Mon. Not. R. Astr. Soc*., **237**, 853

Pearson, K.J., Wynn, G.A., King, A.R., 1997, *Mon. Not. R. Astr. Soc*., **288**, 421

Paczyriski, B., 1967, *Atron. Astrophys*., **17**, 287

Parker, E.N., 1963, *Interplanetary Dynamical Processes*. Interscience, New York

Parker, E.G., 1979, *Cosmical Magnetic Fields*. Oxford University Press, Oxford

Ritter, H., 1988, *Atron. Astrophys*., **202**, 93

Schatzman, E., 1962, *Atron. Astrophys*., **25**, 18

Schmidt, G.D., 1999, *ASP Conference series*, **157**, 207

Tritton, D.J., 1977, *Physical Fluid Dynamics*, Van Nostrand Reinhold, England

Verbunt, F., Zwaan, C. 1981 *Atron. Astrophys*., **100**, L7

Wang, Y.M., 1987, *Atron. Astrophys*., **183**,257

Warner, B., 1983, *IAU Colloquium series 72*, 155

Warner, B. 1995, *Cataclysmic variable stars*, Cambridge University Press

Warner, B., 1996*, Asrophys. Space Science*, **241**, 263

Weber, E.J., Davis, L., 1967, *Astrophys. J*., **148**, 217

Warner, B., Winkramasinge, D.T. 1991, *Mon. Not. R. Astr. Soc*., **248**, 370

Wickramasinghe, D., Li, J., 1998, ASP Conference series, **137**, 198

Wynn, G. A., King, A. R., 1995, *Mon. Not. R. Astr. Soc*., **275**, 9